Särtryck och preliminära
rapporter nr 34

ON THE BEARING CAPACITY OF DRIVEN PILES

INGENIÖRSVETENSKAPSAKADEMIEN
PÅLKOMMISSIONEN

INGENJÖRSVETENSKAPSAKADEMIEN
Pålkommissionen

ROYAL SWEDISH ACADEMY OF ENGINEERING SCIENCES
Commission of Pile Research

Särtryck och preliminära
rapporter nr 34

ON THE BEARING CAPACITY OF DRIVEN PILES

1. Methods Used in Sweden to Evaluate the Bearing Capacity of End-Bearing Precast Concrete Piles.
   Bengt Broms & Lars Hellman
2. Discussions at the Conference Behaviour of Piles, London 1970.
   Bengt Fellenius, Bengt Broms & Gunnar Fjelkner
3. Bearing Capacity of Piles Driven into Rock. With Discussion.
   Sven-Erik Rehnman & Bengt Broms
4. Bearing Capacity of Cyclically Loaded Piles.
   Bengt Broms
5. Bearing Capacity of End-Bearing Piles Driven to Rock.
   Sven-Erik Rehnman & Bengt Broms

Stockholm 1972

Price Sw. crs. 30:-

The papers presented are reprinted from:

Paper 1 - 2	Proc. Conf. Inst. Civil Engrs. Behaviour of Piles. London 15 - 17 Sept. 1970.
Paper 3	Canad. Geot. J. 8(1971):2, 4.
Paper 4	Presented at the Int. Geot. Conf. Shiraz 26 - 30 Oct. 1970. Iran.
Paper 5	Proc. 2nd Congr. Int. Soc. Rock Mech. Vol. 2 Belgrade 21 - 26 Sept. 1970. Jugoslavia.

Also published by the Swedish Geotechnical Institute
(Reprints and preliminary reports No. 44)

Methods used in Sweden to evaluate the bearing capacity of end-bearing precast concrete piles

B. B. BROMS, Director, Swedish Geotechnical Institute, Stockholm, Sweden

L. HELLMAN, Scandiaconsult, Stockholm, Sweden

There exist a large number of methods to evaluate the ultimate bearing capacity and the settlement of single piles and pile groups. However, the accuracy of the different methods is to a large extent dependent on how accurately the properties of the soils in which the piles have been driven can be determined. Stones and boulders can, for example, affect appreciably the bearing capacity and the driving resistance. According to the new Swedish Building Code (Svensk Byggnorm 1967), the bearing capacity of end-bearing piles can be calculated by traditional pile driving formulae or by a formula based on the stress wave equation. Traditional pile driving formulae are used when the applied loads are low and the penetration per blow during the driving is relatively large (> 3–5 mm). The stress wave equation is used when the penetration is small (< 3–5 mm). In this Paper, the methods which are used at present (1970) in Sweden to evaluate the bearing capacity of end-bearing concrete piles, and to determine the soil conditions at a given site, are reviewed.

Il existe un grand nombre de méthodes pour évaluer la charge portante finale et l'enfoncement de pieux uniques et de groupes de pieux. La précision des méthodes différentes dépend toutefois dans une large mesure du degré de précision avec lequel les qualités des sols dans lesquels les pieux ont été battus peuvent être établies. Les pierres et les gros blocs peuvent, par exemple, influencer de façon appréciable la charge portante et la résistance au battage. D'après le nouveau Code de la Construction Suédois (Svensk Byggnorm 1967) la charge portante de pieux résistant par la pointe peut être calculée au moyen des formules traditionnelles relatives au battage des pieux ou bien au moyen d'une formule se basant sur l'équation de l'onde des contraintes. Les formules traditionnelles relatives au battage des pieux sont utilisées lorsque les charges appliquées sont faibles et que la pénétration par coup pendant le battage est relativement importante (> 3 à 5 mm). On utilise l'équation de l'onde des contraintes lorsque la pénétration est réduite (< 3 à 5 mm). Dans cet exposé, l'on passe en revue les méthodes qui sont employées à l'heure actuelle (1970) en Suède pour évaluer la charge portante de pieux en béton résistant par la pointe et pour établir l'état du sol à un emplacement donné.

In Sweden the length of end-bearing piles and the difficulties which may be encountered during driving are determined primarily by the Swedish ram sounding method. The ram penetrometer, which is provided with a 200 mm (8 in.) long square point with an area of 40 mm × 40 mm (1·57 in. × 1·57 in.) is generally driven to refusal, or to a depth where at least 150–200 blows are required to drive the penetrometer 20 cm (8 in.). The penetrometer is driven by a 63·5 kg (140 lb) weight with a fall of 60 cm (24 in.). Experience indicates, for example, that concrete piles with a cross-sectional area of 30 cm × 30 cm usually can be driven in cohesionless soils to a depth where the penetration resistance is 80–100 blows/20 cm, when the estimated pile length is about 20 m (60 ft). When the length is about 40 m (120 ft) a concrete pile usually can be driven to a depth where the penetration resistance is about 150–200 blows/20 cm.

2. Large stones and boulders are probably present in the soil if the penetrometer stops at different elevations. It is therefore important to record the results from all penetration tests during an investigation. Also the results from so-called 'unsuccessful' tests should be recorded. When there are reasons to suspect the existence of boulders and large stones in the soil the penetration tests should be supplemented by percussion or rotary drilling to a depth of at least 2 m (6 ft) into rock. In some cases geophones are placed in adjacent boreholes in order to detect when bedrock has been reached during the drilling.[1]

3. The relative density of cohesionless soil is generally estimated by the Swedish weight sounding method or the Swedish ram sounding method. Static penetration tests such as the Swedish weight sounding method often give a more accurate indication of the relative density than the ram sounding test. The main drawback with the weight sounding method is that the penetration depth is limited. It is frequently not possible to penetrate dense layers of sand, gravel and moraine with this method.

4. A site investigation generally includes some sampling in order to classify the different soil layers. Frequently only disturbed but representative samples are required. Samples of loose sand above the ground water table and of clay and silt are as a rule taken with the Swedish standard piston sampler.[2] In sand below the ground water table, side intake soil samplers are generally used.[3]

5. The angle of internal friction of cohesionless soil is generally determined by the direct shear test, while the Swedish fall cone and vane tests are used to determine the undrained shear strength of cohesive soils. The undrained shear strength is reduced[4] when the so-called fineness number (which is approximately equal to the liquid limit) is larger than 80. The compressibility is determined by oedometer tests in the usual way.

6. Often the pile length and the bearing capacity cannot be estimated with sufficient accuracy from a soil investigation alone. The investigation must in many cases be supplemented by pile driving tests or by pile load tests as now described.

TRADITIONAL PILE DRIVING FORMULAE

7. In Sweden the bearing capacity of end-bearing piles which have been driven through sand or gravel is often calculated by traditional pile driving formulae. Great care has, however, to be exercised when such formulae are applied on piles which have been driven through silt and fine sand because of the high negative pore pressures. These can develop in these materials during driving and cause large errors in the calculated bearing capacity. Traditional pile driving formulae are only used in Sweden when the allowable load is less than 15 Mp (33 kips). The allowable load is generally chosen in Sweden as one-third of the calculated ultimate bearing capacity from the Kreüger pile driving formula.[5]

8. There exist at present a large number of different pile driving formulae. They are generally based on the following general equation:

$$Qh_e = Rs + 0{\cdot}5\,Re_{cap} + 0{\cdot}5\,Re_{pile} + 0{\cdot}5\,Re_{soil} + \frac{Qh_e q(1-k^2)}{Q+q} \qquad (1)$$

where Q = mass of hammer, h_e = effective height of fall, R = penetration resistance of the pile, s = penetration per blow, $e = (e_{cap} + e_{pile} + e_{soil})$ = elastic compression of driving cap, pile and soil, q = mass of pile and k = coefficient of restitution.

9. In Eqn 1 the term Qh_e represents the energy of the hammer when it strikes the pile and Rs the energy which is consumed when the pile penetrates the underlying soil. The term $(0{\cdot}5\ Re_{cap}+0{\cdot}5\ Re_{pile}+0{\cdot}5\ Re_{soil})$ corresponds to the elastic compression of the driving cap, the pile and the soil, and $Qh_eq(1-k^2)/(Q+q)$ corresponds to the energy consumed during the impact of the hammer. The last term also includes, however, part of the energy which is consumed by the elastic compression of the driving cap and of the pile. In the calculation of the energy loss $Qh_eq(1-k^2)/(Q+q)$ it has been assumed that all forces during the impact except those at the pile head can be neglected as pointed out by Sahlin[6] and others. This requirement is not satisfied when relatively large hammers are used. As a consequence some energy losses in Eqn 1 are included twice.

10. If it is assumed that the driving resistance R corresponds to the static ultimate bearing capacity P_{ult} of the pile, the following equation is obtained:

$$P_{ult} = \frac{Qh_e}{s+0{\cdot}5(e_{cap}+e_{pile}+e_{soil})}\left(\frac{Q+k^2q}{Q+q}\right) \quad . \quad . \quad . \quad (2)$$

for $k=0{\cdot}5$ and $e=(e_{cap}+e_{pile}+e_{soil})$. Eqn 2 can be simplified to

$$P_{ult} = \frac{Qh_e}{(s+0{\cdot}5\,e)} \cdot \frac{(Q+0{\cdot}25\,q)}{Q+q} \quad . \quad (3)$$

This equation is known in Sweden as the Kreüger pile driving formula. The term e which represents the elastic compression of the pile cap, the pile and the soil, is generally measured in the field.

11. Hellman[7] has, however, pointed out that the damping as expressed by the term $(Q+0{\cdot}25\,q)/(Q+q)$ is too large when the mass of the pile exceeds the mass of the hammer. Hellman has therefore proposed that the factor $0{\cdot}8\ (1-0{\cdot}1\ Q/q)$ should be used instead of $(Q+0{\cdot}25\,q)/(Q+q)$ in accordance with the practice in the United States. If this term is inserted in Eqn 3 the following expression is obtained:

$$P_{ult} = \frac{0{\cdot}8\ Qh_e}{(s+0{\cdot}5\,e)} \cdot (1-0{\cdot}1\ Q/q) \quad . \quad (4)$$

This equation is included in the Swedish Building Code.[8] The energy Qh_e of the hammer at the moment it strikes the driving cap is dependent on the effective height of free fall h_e, which is equal to ηh, where η is an efficiency coefficient. Bergfelt[9] reported $\eta=0{\cdot}5$ for inclined concrete piles (1:8) which had been driven by a 3 ton drop hammer. For vertical piles Bergfelt obtained $\eta=0{\cdot}8$. Fredricson[10] measured for vertical piles $\eta=0{\cdot}3$, 0·55 and 0·69 when the weight of the drop hammer was 0·75, 1·75 and 3·0 tons, respectively.

12. The efficiency coefficient varied between 0·68 and 0·75 during the test carried out by Sahlin[6] with a 2·0 ton drop hammer. The Swedish Pile Committee[11] reported values which varied between 0·05 for an extremely light drop hammer (0·75 ton) and 0·6–0·7 for a 1·78 ton drop hammer. For piles inclined 1:7 the efficiency coefficient varied between 0·42 and 0·55 for a 2·8 ton drop hammer.

13. These measurements indicate that the efficiency coefficient decreases with decreasing hammer weight and with increasing inclination of the pile. The test results also show that the efficiency coefficient varies appreciably with different types of driving rig and that the energy loss with light drop hammers is mainly caused by inertia effects in wires, sheaves and machinery.[11] It is generally assumed in calculations that $\eta=0{\cdot}8$ when single line drop hammers are used.

14. In the calculation of the energy Rs (Eqn 1), which is consumed during the penetration of a pile, it is generally assumed that the resistance R is constant. It is also assumed that this penetration resistance corresponds to the static ultimate bearing capacity of the pile. However, the dynamic penetration resistance for fine sand or silt is often considerably larger than the static ultimate bearing capacity of the pile because of the large negative pore pressure which can develop in these materials when the relative density of the soil is high, as pointed out earlier.

15. Test results indicate that the skin friction resistance of piles in cohesionless soil is affected by the loading rate. The skin friction resistance during driving appears to be much smaller than that for a static load test. It is, however, possible that this difference is caused by the compaction of the soil during the driving of subsequent piles. Fellenius[12] takes this effect into account by increasing the allowable load when the driving resistance in a layer of sand does not increase with depth.

16. The energy $(0{\cdot}5\ Re_{soil}+0{\cdot}5\ Re_{cap})$ which is consumed by the elastic compression of the soil and of the driving cap is difficult to calculate or estimate. The energy $0{\cdot}5\ Re_{pile}$ which is consumed by the elastic compression of the pile is dependent on the modulus of elasticity of the pile material, the area of the pile and the pile length. It has also been assumed in the calculations that the total length of the pile is subjected to a constant load R and that the pile material has a constant modulus of elasticity. The maximum force in the pile is often much larger than the penetration resistance R, and the equivalent modulus of elasticity of the pile section varies with the load intensity. The modulus of elasticity is often assumed to be $0{\cdot}1\times10^6$ kp/cm² for wood, $0{\cdot}3\times10^6$ kp/cm² for concrete and to $2{\cdot}1\times10^6$ kp/cm² for steel. It is also assumed in the calculations that the shape of the stress wave is rectangular and that the length of the stress wave corresponds to at least the length of the pile. This requirement is not satisfied when light hammers are used. These limitations restrict severely the use of conventional pile driving formulae.

17. Conventional pile driving formulae should be used[7] for concrete piles only when the penetration of the pile at each blow is larger than 2 to 3 mm. Otherwise, the losses which are caused by factors other than the elastic compression of the pile cannot be neglected in the calculations. The mass of the hammers should, in addition, be of the same magnitude as the mass of the pile. If the mass of the hammer is much smaller than the mass of the pile ($Q<0{\cdot}75$ to $0{\cdot}5\,q$), as is the case when air hammers are used, one must consider the length of the stress wave and its shape. For light hammers Hellman[7] recommends that an equivalent pile length L_{eq} should be used instead of the total length L. This equivalent is equal to QL/q.

18. The bearing capacity as calculated by different pile driving formulae differs appreciably. The formulae proposed by Hiley,[13] by Janbu[14] and by Sørensen and Hansen[15] appear to give for cohesionless soil the best agreement between calculated and measured ultimate loads for the conditions mentioned earlier.

PILE DRIVING FORMULAE BASED ON THE STRESS WAVE EQUATION

19. The bearing capacity of point bearing piles can also be calculated from the stress wave equation.[7] A stress wave is generated during the driving of a pile. The stress wave travels with a velocity

$$c = \sqrt{\left(\frac{Eg}{\gamma_{pile}}\right)}$$

where E = equivalent modulus of elasticity of the pile cross section and γ_{pile} = density of the pile material. The intensity of the stress wave is mainly affected by the mass of the hammer, the height of fall and the cross-sectional area of the pile.

20. In the following calculations it is assumed that the stress wave can be approximated as shown in Fig. 1. The assumed shape is based on stress measurements on concrete piles which have been driven by drop hammers. It should, however, be pointed out that the number of observations is relatively small. It has furthermore been assumed that the intensity of the stress wave increases linearly to a maximum value σ^* when the length of the stress wave is $0{\cdot}5\ QL/q$. The total length of the stress wave is $3\ QL/q$. For a 30 cm × 30 cm concrete pile driven by a 3 ton drop hammer the total length of the stress wave is approximately 42 m.

Table 1. Relationship[7] between allowable load, penetration, height of fall, pile length and cross-sectional area

Allowable load	Penetration (mm/10 blows)		Height of fall (cm) at pile length and cross-sectional area (cm²) of precast concrete piles								
	3 ton drop hammer*	4 ton drop hammer*	10 m (30 ft)			25 m (75 ft)			50 m (150 ft)		
			400 cm² (62 in.²)	600 cm² (93 in.²)	900 cm² (140 in.²)	400 cm² (62 in.²)	600 cm² (93 in.²)	900 cm² (140 in.²)	400 cm² (62 in.²)	600 cm² (93 in.²)	900 cm² (140 in.²)
33 Mp (73 kips)	13	18	35 cm	20 cm	—	45 cm	20 cm	—	55 cm	30 cm	—
45 Mp (99 kips)	10	13	—	30 cm	20 cm	—	40 cm	20 cm	—	50 cm	30 cm
60 Mp	5	7	—	45 cm	25 cm	—	50 cm	30 cm	—	(65 cm)	40 cm

* In single line.

21. It has also been assumed in the calculations that the pile point does not move until the intensity of the stress wave at the pile point exceeds the dynamic bearing capacity of the soil (the penetration resistance R) and that R is constant during the penetration of the pile. The rebound of the soil is neglected. For this assumption the stress at the pile point varies as shown by the solid line in Fig. 2. When the pile point rests on an unyielding support the initial stress wave is reflected as a compression wave. The maximum stress will in this case be equal to twice the maximum intensity of the initial wave. When the stress corresponds to the penetration resistance σ_{ult}^{dyn} (R/A_{point}) it is assumed that the pile moves. If $\sigma_{ult}^{dyn} > 2\,\sigma^*$ the pile does not move and the initial stress wave is reflected as a compression wave.

22. If the rebound of the soil is neglected, the penetration of the pile during the time (t_2-t_1) can be calculated from the equation

$$s = \int_{t_1}^{t_2} v_{point}\, dt \quad . \quad . \quad . \quad (5)$$

where v_{point} is the velocity of the pile point at the time t. The velocity v_{point} is equal to the difference between the particle velocities of the initial stress wave and of the reflected stress wave. Eqn 5 can be rewritten as

$$s = \int_{t_1}^{t_2} (v_{point}^{initial} - v_{point}^{reflected})\, dt \quad . \quad (6)$$

The particle velocity for the initial stress wave at the pile point can be calculated from the equation

$$v_{point}^{initial} = \sigma_{point}^{initial} \cdot \frac{c}{E} \quad . \quad . \quad (7)$$

The particle velocity is thus dependent on the intensity of the initial stress wave $\sigma_{point}^{initial}$. In the same way the particle velocity of the reflected wave $v_{point}^{reflected}$ can be calculated from

$$v_{point}^{reflected} = \sigma_{point}^{reflected} \cdot \frac{c}{E} \quad . \quad . \quad (8)$$

where $\sigma_{point}^{reflected}$ is the intensity of reflected wave at the pile point. Eqn 6 can then be rewritten as

$$s = \frac{c}{E}\int_{t_1}^{t_2} (\sigma_{point}^{initial} - \sigma_{point}^{reflected}) \quad . \quad (9)$$

The total stress at the pile point (the sum of the stresses from the initial and the reflected waves) is shown in Fig. 2. (It has been assumed that the pile point does not move until the intensity of the stress wave at the pile point exceeds the point resistance of the soil σ_{ult}^{dyn}.)

23. The shape of the reflected wave can be calculated from Fig. 2 as shown in Fig. 3. It can be seen that the intensity of the reflected wave increases linearly until it reaches half the dynamic point resistance. Thereafter the intensity of the stress wave varies, so that the sum of the stresses from the initial and the reflected waves is equal to σ_{ult}^{dyn}.

24. The difference between the initial and reflected stress waves corresponds to the cross-hatched area in Fig. 3. The area can be calculated from

$$\int_{t_1}^{t_2} (\sigma_{point}^{initial} - \sigma_{point}^{reflected})\, dt \quad . \quad (10)$$

It can be seen from Fig. 3 that

$$\int_{t_1}^{t_2} (\sigma_{point}^{initial} - \sigma_{point}^{reflected})\, dt = \frac{2\sigma^* - \sigma_{ult}^{dyn}}{2}(t_2 - t_1) \quad . \quad . \quad . \quad (11)$$

Since the two triangles ABC and OBE in Fig. 3 have the same shape it follows that

$$\frac{t_2 - t_1}{t_0} = \frac{\sigma^* - \frac{1}{2}\sigma_{ult}^{dyn}}{\sigma^*} \quad . \quad . \quad (12)$$

If this relationship is substituted in Eqn 11 the following relationship is obtained:

$$s = \frac{ct_0}{E}\frac{(2\sigma^* - \sigma_{ult}^{dyn})^2}{4\sigma^*} \quad . \quad . \quad (13)$$

The time t_0 can be calculated from

$$t_0 c = \frac{1{\cdot}5\ Q}{q/L} \quad . \quad . \quad . \quad (14)$$

where c is the velocity of the stress wave. If the allowable point resistance σ_{stat}^{allow} is 1/3 σ_{ult}^{dyn}, Eqn 13 can be rewritten as

$$s = \frac{0{\cdot}375\ Q}{Eq/L}\frac{(2\sigma^* - 3\sigma_{stat}^{allow})^2}{\sigma^*} \quad . \quad (15)$$

25. The maximum intensity σ_{head}^* (in kp/cm²) of the initial stress wave can be estimated at the head of a concrete pile from the relationship $\sigma_{head}^* = 30\sqrt{h_e}$ where h_e (in cm) is the equivalent height of free fall. Measurements indicate, however, that the maximum intensity of the initial stress wave decreases with approximately 5% per m of the pile. If these values are substituted in Eqn 14 the relationships shown in Table 1 are obtained. It has also been assumed in the calculations that $\eta = 0{\cdot}8$. If the driving is done with a free falling drop hammer the values of the fall shown in Table 1 should be reduced by 20%. The relationships in Table 1 are included in the Swedish Building Code[8] as shown in Table 2.

PILE LOAD TESTS

26. The most accurate method of estimating the ultimate bearing capacity of a pile is by pile load tests. Such tests are, however, time consuming and expensive. The cost is in Sweden about $2000 to $4000 for each pile.

27. Some time must, however, elapse before a pile can be tested because of the excess pore pressures which develop during the driving. Floating wooden piles which

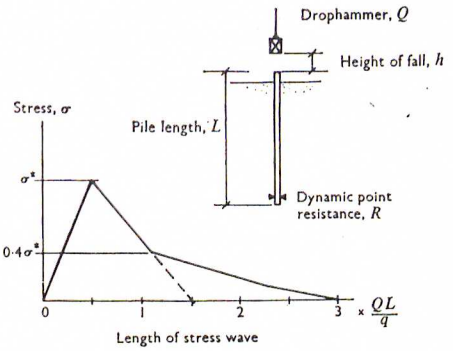

Fig. 1. Assumed shape of stress wave

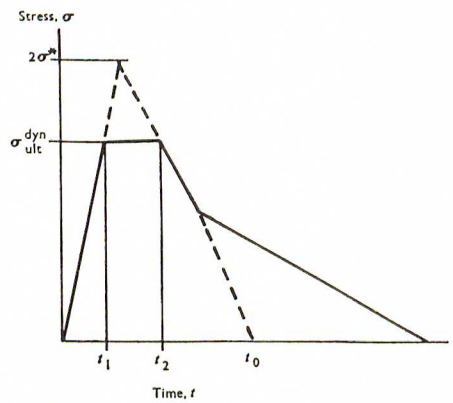

Fig. 2. Shape of stress wave at pile point

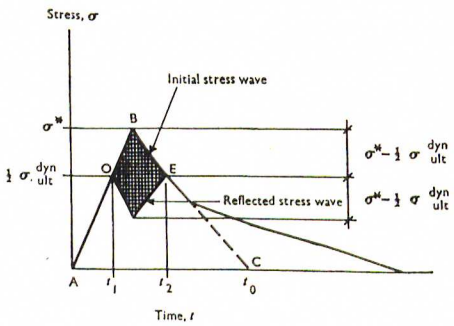

Fig. 3. (i) Comparison between initial and reflected stress waves; (ii) Reflected stress wave

Table 2. Required driving resistance of end-bearing precast concrete piles[8]

Allowable load	Penetration (mm/10 blows)			Height of fall† (cm) at the pile lengths		
	2 ton drop hammer*	3 ton drop hammer	4 ton drop hammer	10 m (30 ft)	25 m (75 ft)	50 m (150 ft)
33 Mp (73 kips) . .	7	13	18	30 cm	40 cm	—
45 Mp (99 kips) . .	5‡	10	13	40 cm	50 c	60 cm
60 Mp	—	5	7	50 cm	50 cm	60 cm

* Can only be used at pile lengths > 10 m.
† Single line drop hammer ($n = 0{\cdot}8$).
‡ Cannot be used when the cross-sectional area exceeds 700 cm².

have been driven through clay are generally loaded three weeks after the driving, while floating concrete or steel piles are not tested until 12 weeks after the driving. However, point bearing piles are tested as early as one week after the driving.[16]

28. Sheet piles are used as reaction piles when the intensity of the applied load is high, while wood, concrete or steel piles are generally used when the applied load is low. The distance between the test pile and the reaction piles should generally be larger for cohesionless soils than for cohesive soil, since the driving of the reaction piles can affect the relative density of cohesionless soils and thus also the ultimate bearing capacity of the test pile. The reaction piles can also affect the effective overburden pressure which is reduced appreciably if the spacing of the piles is small. In cohesive soils the remoulding of the soil caused by the driving of the reaction pile can also affect the bearing capacity of the test pile. The distance between the test piles and the reaction piles should be at least 1·5 m or five times the pile diameter.[16]

29. Test piles in Sweden are loaded by hydraulic jacks. A hydraulic pump is used when the piles are loaded at a constant deformation rate. The deformation is generally measured by dial indicators which are attached to a measuring beam. The distance from the supports of the measuring beam to the test pile or to the reaction pile should be at least 2 and 1 m, respectively.[16]

30. It is, however, frequently difficult to interpret the test results from load tests on end-bearing piles when the piles have been driven through a deep layer of clay. This is frequently the case in the south-western part of Sweden where very deep layers of normally consolidated clays are common. In this case a large part of the applied load is carried by skin friction, while only a small part is transferred to the underlying soil through the pile point. The displacement required to mobilize the full skin friction resistance is very small (a few millimetres). The elastic compression of the pile alone is generally sufficient. For example, the elastic compression of a 100 m long concrete pile is approximately 17 mm at an average axial stress of 50 kp/cm^2 and a modulus of elasticity of $0{\cdot}3 \times 10^6$ kp/cm^2. Test data[17] have shown for a 87 m (260 ft) long end-bearing precast concrete pile that 325 Mp (715 kips) was carried by skin friction of a total applied load of 405 Mp (890 kips). At 210 Mp (462 kips) the load at the pile point was equal to zero. Before 1967 test piles in Sweden were loaded in increments. At each load increment the pile was subjected to cyclic loading. Today (1970) the test piles are loaded at a constant deformation rate (approximately 0·5 mm/min) according to the procedure recommended by the Swedish Pile Committee. Piles in both cohesive and cohesionless soils are loaded to failure. End-bearing piles are loaded until the applied load reaches a maximum value or it corresponds to at least three times the design load. Load tests on floating piles which have been driven in clay are not terminated until the total deformation of the pile is at least 20 mm larger than that at the ultimate bearing capacity (the peak point of the load/deformation relationship). Floating piles in cohesionless soils are loaded until the total penetration of the pile is at least 60 mm. The rebound of the test pile is measured immediately after the unloading as well as 5, 15 and 30 min after the unloading.

31. In Denmark test piles are loaded in increments until the applied load reaches 95% of the calculated ultimate bearing capacity or until the penetration of the pile corresponds to 0·3 mm/min. Thereafter the pile is loaded at a constant deformation rate (0·3 mm/min) until the failure load has been reached.[18] The failure load is defined as the maximum point of the load/deflexion curve or the load which corresponds to a penetration equal to 10% of the diameter of the pile. In Norway[19] test piles are loaded at a constant penetration rate (1 mm/min).

REFERENCES

1. LUNDSTRÖM R. and STENBERG R. Soil–rock drilling and rock locating by rock indicator. *Proc. 6th Int. Conf. Soil Mech.*, 1965, **1**, 69–72.
2. Standard piston sampling, a report by the Swedish committee on piston sampling. *Proc. Swed. Geotechnical Instn* (Stockholm), 1961 (19) 45 pp.
3. KALLSTENIUS T. Some side-intake soil samplers for sand and gravel. *Proc. R. Swed. Geotechnical Instn* (Stockholm), 1953 (7) 35 pp.
4. KALLSTENIUS T. and HALLÉN A. Provtagning med standardkolvborr St 1. *Stat. Geot. Instn Meddr.* (Stockholm), 1963 (6) 53 pp.
5. KREÜGER H. Friktionspålars bärighet. *Avd. Väg-o. Vattenb. Tekn. Ts.*, 1915, **145** (1).
6. SAHLIN S. Pålkrafter vid slagning av betongpålar. *Väg-o. Vattenb.*, 1956 (5) 105–112.
7. HELLMAN L. Om stoppslagning av stödpålar. *Swed. Geot. Instn, Repr. o. Prel. Rep.* (Stockholm), 1967 (19) 6 pp.
8. Svensk Byggnorm. *Föreskrifter, råd och anvisningar till byggnadsstadgan.* Stat. Planverk, Stockholm, 1967, Publ. No. 1, 521 pp.
9. BERGFELT A. Nya hamnbyggen i Göteborg. *Nord. Betong*, 1957, **1** (2) 155–180.
10. FREDRICSON Å. Verkningsgraden hos fallhejare. *Väg-o. Vattenb.*, 1958 (13) 61–62.
11. Swedish Pile Committee. *Driving and test loading of long concrete piles, tests at Gubbero, Gothenburg.* Stat. Råd f. Byggnadsforskning, Rapp., 99, 230 pp, Stockholm, 1964.
12. FELLENIUS B. Aktuella pålningsproblem. *Nord. Järnbanets.*, 1964, **90** (6) 156–162.
13. HILEY A. Pile driving calculations with notes on driving forces and ground resistance. *Struct. Engr*, 1930 (8) 246–259 and 278–288.
14. JANBU N. Une analyse énergétique du battage des pieux à l'aide de paramètres sans dimension. *Annes Inst. tech. Bâtim.*, 1953, **6** (63–64) 352–360, Sér Sols et Fond. (13) Paris.
15. SØRENSEN T. and HANSEN B. Pile driving formulae—an investigation based on dimensional considerations and a statistical analysis. *Proc. 4th Int. Conf. Soil Mech.*, 1957, **2**, 61–65.
16. Swedish Pile Committee. *Förslag till anvisningar för provpålning och enkel provbelastning*, IVA: s Pålkomm, Repr. a. Prel. Rep. No. 11, 15 pp., Stockholm, 1968.
17. HELLSTRÖM O. Tillåtna laster på långa stödpålar av betong inom Östra Nordstaden, Göteborg. Slutrapport. *Swed. Pile Comm. Repr. o. Prel. Rep.*, 1968 (12) 112 pp., Stockholm.
18. DIF. *Vejledning til dansk ingeniørforenings normer for bygningskonstruktioner 6. Fundering.* Teknisk Forlag, 24 pp, Copenhagen, 1965.
19. HJELDNES E. *Utførelse og interpretering av prøvebelastning på peler.* Norges Tekniske Høgskole, Inst. Geotekn. og Fundamenteringslaere 85 pp., Trondheim, 1964.
20. KALLSTENIUS T. Studies on clay samples taken with standard piston sampler. *Proc. Swed. Geotechnical Inst.* (Stockholm), 1963 (21) 207 pp.

Discussions at the Conference
Behaviour of Piles, London 1970

Bengt Fellenius, Bengt Broms & Gunnar Fjelkner

Performance, instrumentation and interpretation of load tests on piles.

Dr B. H. Fellenius (Swedish Geotechnical Institute): The various load testing methods described in the Papers submitted to this Conference are based upon measurements of pile head settlement versus load in maintained load tests (ML tests). The methods used in Sweden differ from these methods and I therefore want to make a few points.

A106. In Sweden we normally employ a testing procedure recommended by the Swedish Pile Commission in which the CRP test is used. The tests are carried out to at least 60 mm settlement of the pile head or to a minimum of three times the design load (see Fig. A34). The load–settlement curve indicates whether the pile is an end-bearing pile or a friction pile in sand or in clay, or a combination of the two. The method is quick. With the standard rate of deformation of 0·5 mm/min the test requires only 2 hours and can thus be done within a day with a minimum of cost and delay to the contractor's operations.[20]

A107. The advantage of this method is not only the low cost; it means that one method is employed for all types of piles. Furthermore, all reports are drawn up in the same manner and thus various tests from various places can be compared.

A108. When for some reason the CRP method is not used, an incremental method is used. Then, however, the increments are small, 1/15–1/20 of the expected ultimate load, and kept only for 10–15 minutes. This testing method is quick, also. For example, with 20 ton increments applied every 15 min and with an ultimate load of 300 tons, the test is completed within 4 hours.

A109. The main difference between the CRP method and the incremental method on the one hand and the ML method on the other is that the first two tests are quick and there are no unloading cycles that can disturb the results of the test involved. Furthermore, the ML method includes both initial settlement and time-dependent settlement, and therefore it is sometimes difficult to interpret the results. The CRP method and the incremental method obviate this difficulty.

A110. When testing a pile longer than about 20 m, measurements of the pile head settlement only do not provide enough information on the pile behaviour to allow any detailed studies. When detailed studies are needed the movement of the pile tip is measured; there is a standard equipment for this.[21] This equipment also allows measurement of the deformation of the lower portion of the pile and makes it possible to evaluate an approximate load distribution in the pile and the load at the pile tip.

A111. Figs A35–A38 demonstrate the information which can be gained by measuring pile tip movement and pile deformation. (The Figs are selected from a paper by Fellenius.[22] The test results were originally reported by Tavenas.[23])

A112. Figure A35 shows load vs settlement from a test on a friction pile in sand where the two measurements were made. Only the head and tip movement are shown in the diagram.

A113. Figure A36 shows the evaluated load distribution in the pile for each load applied on the pile head. The evaluated tip loads are related to the measured tip movements and a load–settlement curve is obtained for the pile tip as shown in Fig. A37.

A114. From Fig. A36, also, the mean skin friction along the lower portion of the pile is obtained, and in the same manner as in Fig. A37, a diagram is obtained showing the skin friction versus the pile shaft movement (see Fig. A38).

A115. Measurements of tip movement and pile deformation can be obtained very simply and at low extra cost by using the standard equipment. The measurements add a considerable amount of valuable information to a test, and thus a more economical design of the contract pile is achieved.

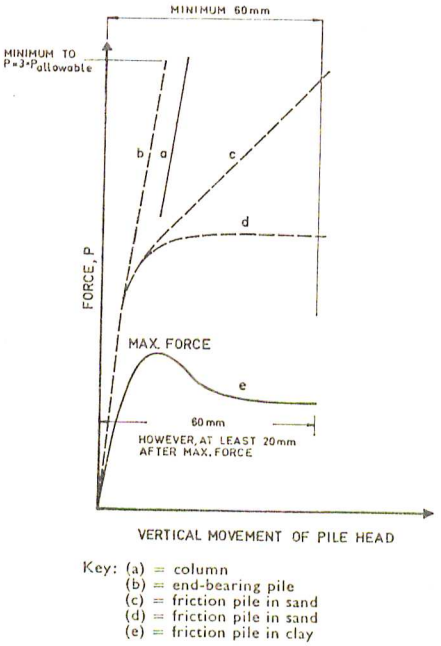

Fig. A34. Typical load testing curves obtained in a CRP test

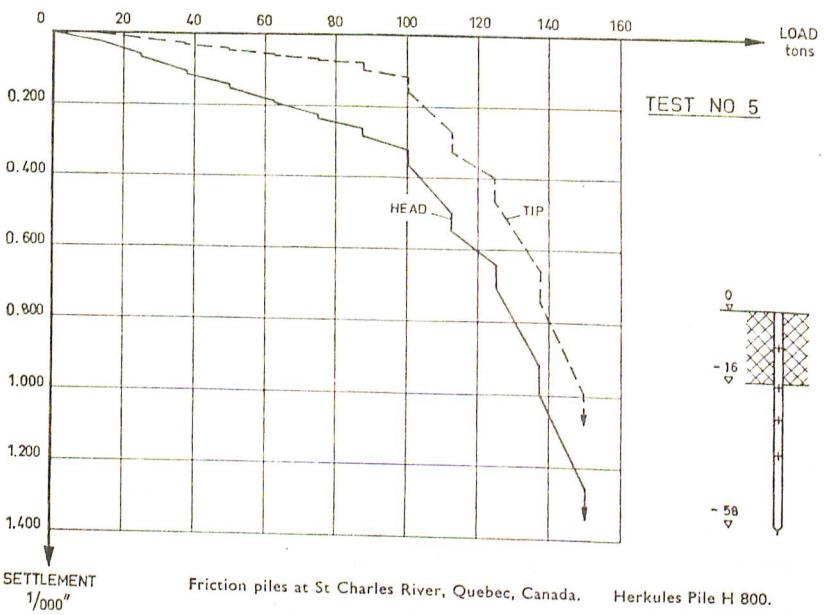

Fig. A35. Load–settlement diagram including settlement of the pile tip

Disturbance caused by the driving of piles.

Mr B. B. Broms (Author, Paper 4): Some long term load tests have been carried out at Skå-Edeby in Sweden which throw some light on the effects of pile driving on the total settlement and on the settlement rate. Fills with a height of 1·5–2·2 m and a diameter of 35–70 m were placed, in 1957, on an approximately 12 m thick deposit of very soft clay. The average shearing strength of the clay was about 0·7 t/m^2 below the approximately 1 m thick surface crust. The sensitivity was about 10.

B67. Sand drains with a diameter of 180 mm were driven at a spacing which varied between 0·9 and 1·5 m below three of the test fills. Sand drains were not used below the fourth fill. A closed-end drive pipe was used for the placement of the sand drains. The driving caused some remoulding of the clay, similar to that which occurs during the driving of timber or precast concrete piles. Settlement observations on the drained fills indicated that the remoulding by the driving did not appreciably increase the total settlements of the fills. The total settlement for the undrained area could be estimated by measuring the pore pressures which remained in the soil. These measurements indicated that the settlement caused by the remoulding pile driving is probably small.

B68. The second effect of the remoulding is on the settlement rate and on the pore pressure dissipation. Frequently the permeability of a soil is considerably larger in the horizontal than in the vertical direction. For the very soft clay at Skå-Edeby the average permeability in the horizontal direction was, for the undisturbed clay, approximately four times the average permeability in the vertical direction. The remoulding caused by the pile driving appeared to have appreciably affected the average permeability of the soil so that the settlement rate and the pore pressure dissipa-

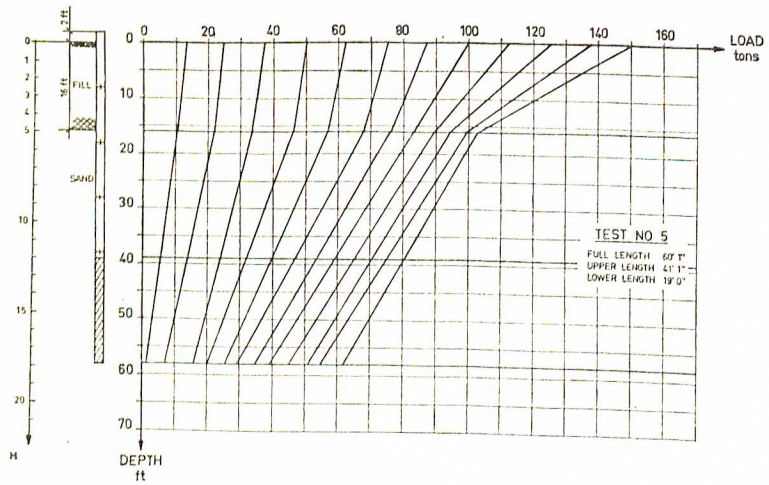

Friction piles at St Charles River, Quebec, Canada Herkules Pile H 800

Fig. A36. Load distribution *vs.* depth of pile

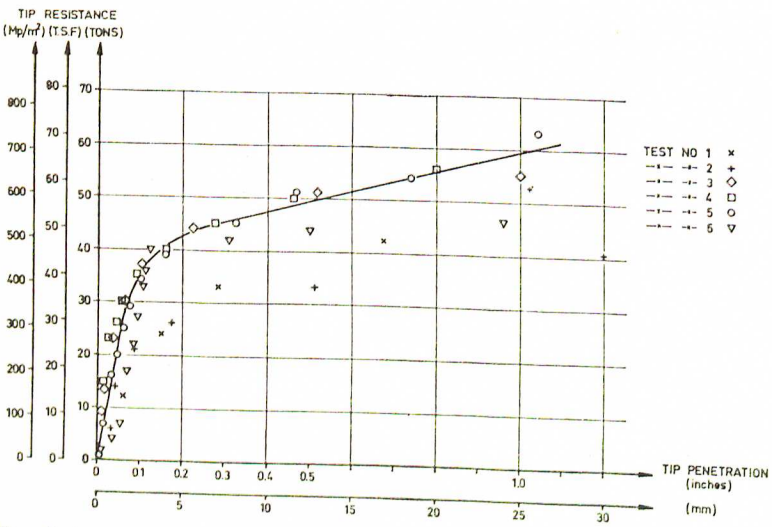

Friction piles at St Charles River, Quebec, Canada Herkules Pile H 800

Fig. A37. Pile tip load *vs.* tip penetration

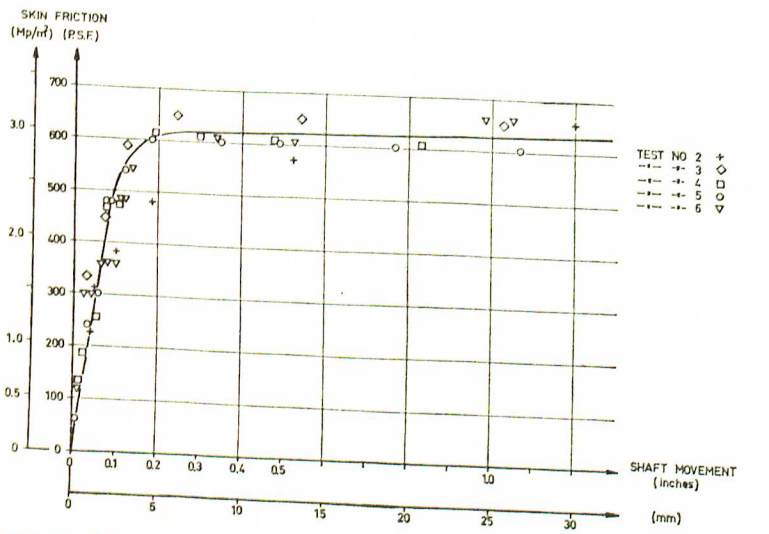

Friction piles at St Charles River, Quebec, Canada
Herkules Pile H 800

Mean skin friction along the lower 18 ft measured at various depths

Fig. A38. Mean skin friction along the lower portion of a pile *vs.* shaft movement

tion for the drained area corresponded to the average permeability as determined by oedometer test. Since the settlement rate for a fill with sand drains is governed primarily by the permeability of the soil in the horizontal direction, the remoulding caused by the driving of the sand drains appeared to have caused a reduction of the permeability to about one quarter of its initial value. The average permeability in the horizontal direction became approximately the same as the permeability in the vertical direction. These test results indicate that the remoulding caused by pile driving can have an appreciable effect on the average permeability of a clay and thus on the settlement rate.

Influence of pile driving on soil compaction, soil movement and bearing capacity of adjacent piles.

Dr B. H. Fellenius (Swedish Geotechnical Institute): My comments relate to the influence of pile driving on soil compaction, soil movement and bearing capacity of adjacent piles.

C27. Early in 1968 a large number of 33 cm dia. precast piles 25–30 m long were driven to form a foundation for a silo building. The piles were driven at a spacing of 1·3 m over an area of 20×50 m^2. The driving was carried out with a drophammer weighing 4 tons and the height of fall was 50 cm. The soil consisted of a top layer of soft clay 5–12 m thick followed by loose sand to about 30 m depth and then dense sand and gravel.

C28. The compaction effects of the pile driving were studied by means of the Swedish dynamic penetration test.* The number of blows/20 cm penetration were recorded before and after pile driving as shown in Fig. C5. The penetration resistance in the sand was low before the piles were driven, whereas the resistance increased considerably because of the pile driving. The variation of this increased resistance can be related to the gradation of the sand. The largest increase is obtained where the sand is poorly graded, i.e. not uniform.

C29. The magnitude of the compaction was studied very simply by installing two piles at their respective locations well ahead of the driving of adjacent piles. One of the two piles was driven to refusal according to the requirements of the contract. The other one was just driven through the clay layer. During the driving of the remaining piles, levels were taken on the heads of these two piles (Nos 314 and 327) and Fig. C6 shows the settlement–time curves which were obtained from these readings.

C30. The settlement curve for pile No. 327 shows that the sand settled 18 cm due to the driving of adjacent piles. The curve for pile No. 314 shows that no settlement occur-

* The dynamic penetration test consists of driving a 32 mm dia. rod provided with a 40 mm wide point by means of a free falling hammer of 63·5 kg. The height of fall is 50 cm and the number of blows/20 cm penetration is recorded.

red below the depth of its tip. Obviously the driving of piles further away than about 7 m had little effect.

C31. Figure C7 shows the same kind of curves for another pair of piles. The distance of 7 m also seems to be critical in this case. The conclusion is that the driving of a pile in this type of soil influences the soil within a circle of about the same diameter as the length of the pile in the soil.

C32. Figure C8 shows the results of inclinometer measurements of one of the long piles of the previously mentioned pairs. Inclinometer readings were made immediately after the driving of the pile and after the adjacent piles had been driven around the measured pile. The driving caused horizontal movements in the soil, displacing the pile by several centimetres.

C33. Figure C9 shows load test curves of tests on four piles of practically equal length driven near each other. For comparison purposes the parts of the load test curves after

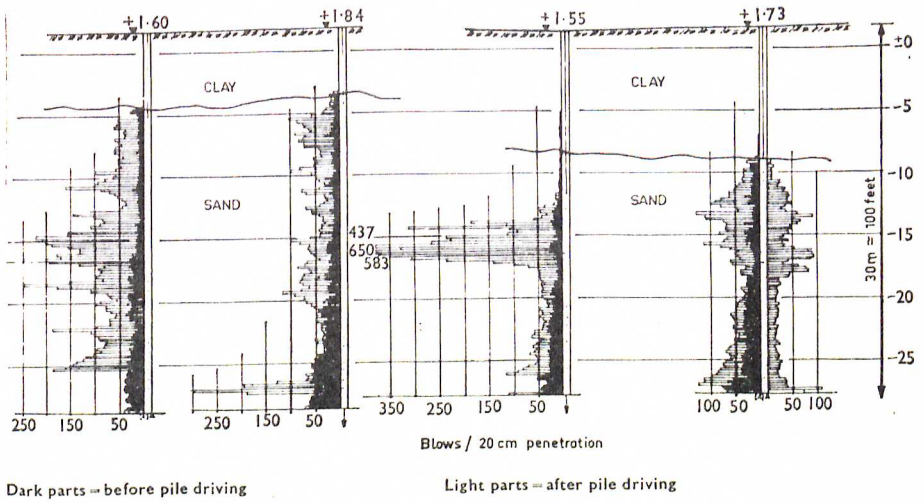

Fig. C5. Swedish dynamic penetration test diagrams obtained before and after pile driving

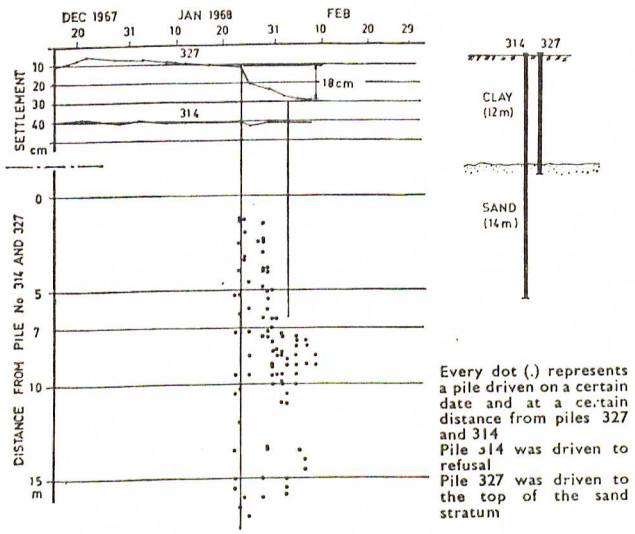

Fig. C6. Relative settlements of a sand stratum and of a pile driven into it, caused by driving additional piles

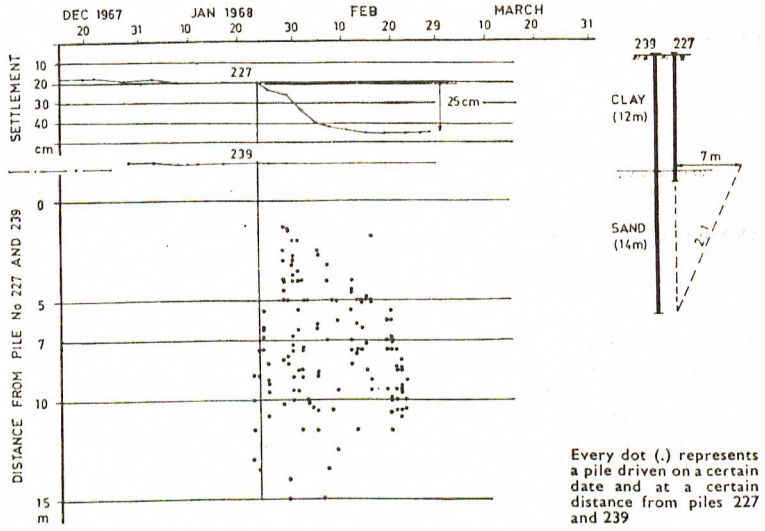

Fig. C7. Further relative settlement records of a sand stratum and of a pile driven into it, caused by driving additional piles

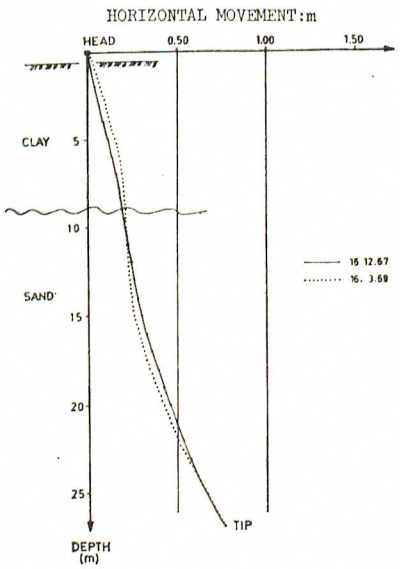

Fig. C8. Results of inclinometer measurements of a pile before and after driving adjacent piles

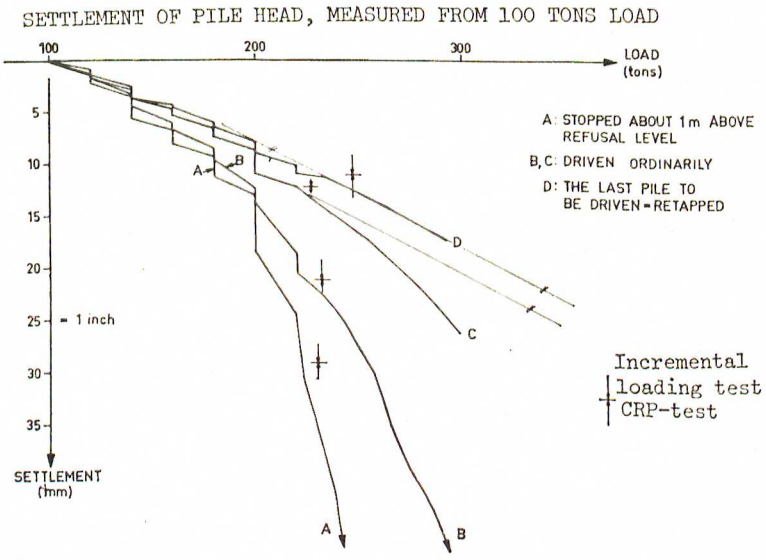

Fig. C9. Load test curves obtained from four piles of approximately equal length

100 tons load on the pile head have been extracted from the complete diagrams. The test equipment did not allow higher loads than 300 tons. The driving of one pile, A, was stopped about 1 m above the expected refusal depth. Piles B, C and D were driven according to the requirements of the contract. However, pile D was the last one to be driven in this part of the piling site. One might say that piles B and C would have been equal to this pile, had they been retapped.

C34. Pile D behaves as an end-bearing pile and piles A, B and C behave as friction piles. The curves for piles B and C show that the pile tips are being pressed down and pile A behaves as if the tip resistance is smaller than the skin friction resistance.

C35. The general conclusions of this brief account are that driving of piles in loose sand can cause settlements for a neighbouring building—that is, if this building is founded directly in the sand or on shorter piles than the ones that are being driven. Furthermore, to really ensure a sufficient bearing capacity of piles working as both friction and end-bearing piles in this type of soil, it is wise to redrive them.

Experience with steel piles in Sweden.

Mr G. Fjelkner (Swedish Geotechnical Institute, Stockholm): The Authors of Paper 14 ask for more research on pile driving in general. I would like to contribute some information on a method for predicting dynamic forces in steel piles driven with air-hammers. In Sweden about 5% of all piles are made of steel. Normally those steel piles are used for relatively small buildings where the load per unit area is low. Steel piles have many advantages; they have a relatively high bending strength and can thus withstand driving into hard ground with boulders, they can be obtained in thin sections for small loads, they can be welded, and they can be driven with light air-hammers, which means that the driving costs will be low. There are, however, three main problems concerning steel piles and they are, how to predict the bearing capacity, the buckling resistance, and the corrosion of the steel.

D52. The problem concerning buckling of slender steel piles, has been treated theoretically by a number of authors.[5–9] They have all found that buckling can just occur when the pile is surrounded by very soft materials, for example clay with a shearing strength lower than about 1 Mp/m² (1·4 lb/sq. in.). There are only a few load tests on slender steel piles in soft clay where buckling has been discovered. Two such load tests made by me have given buckling loads about twice as high as the calculated loads.

D53. In Sweden, the corrosion on steel piles which are surrounded by soil is normally slight. Some types of soils, especially sulphuric soils, have, however, a very high corrosion rate. To investigate this problem, the Swedish Pile Commission has set up a research group on corrosion.

Swedish pile splicing systems.

Dr B. B. Broms (Author, Paper 4): I would like to mention splicing systems in Sweden. There are extensive deposits of very soft clays in the southwestern part of Sweden and the depth of these deposits may exceed 100 m. In this area long precast end-bearing concrete piles are frequently used.

D60. When the estimated pile length exceeds 13–14 m the piles are generally spliced. The Swedish Building Code requires that the strength and deformation properties of a joint should be essentially the same as those of the pile itself. The spliced pile should be able to withstand the stresses which develop during driving as well as an unspliced pile.

D61. At present (1970) there are three makes of joints which satisfy these requirements, namely Herkules, ABB and JF.

D62. The Herkules joint which is used today in many parts of the world was developed about 20 years ago by Nya Asfalt AB. The joint consists of two parts (male and female) which can be connected by a bayonet type coupling as illustrated in Fig. D6. Each coupling is provided with short lengths of reinforcement. The splicing of two pile sections with the Herkules joint requires only a few minutes by twisting the upper pile section with a special handle. The protruding guide rod centres the two pile segments with respect to each other. The two sections are locked in place by two screws.

D63. The ABB joint consists of two parts identical with each other. Each joint segment is provided with two protruding studs which fit the joint segment in the next pile segment. The studs are locked in place by four locking pins as illustrated in Fig. D7. Only a few minutes are required to connect two pile segments. The locking pins force the two segments together with a force of approximately 10 tonnes. Different shapes of the joints are available which fit circular or rectangular pile cross sections.

D64. The JF joint which was developed during the last year consists also of two identical parts which are connected by four X-shaped pins as shown in Fig. D8. Each pin is provided with a nose which locks the pins in place when they are driven. With the JF joint also, the splicing of two pile segments can be carried out rapidly.

D65. The development of inexpensive and rapid splicing systems is one reason why long precast concrete piles are used extensively in Sweden. In 1968 over two-thirds of all piles driven in Sweden were precast concrete piles. A large part of these were spliced.

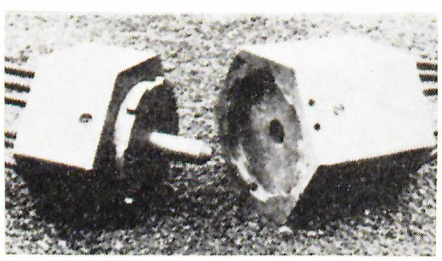

Fig. D6. Herkules joint

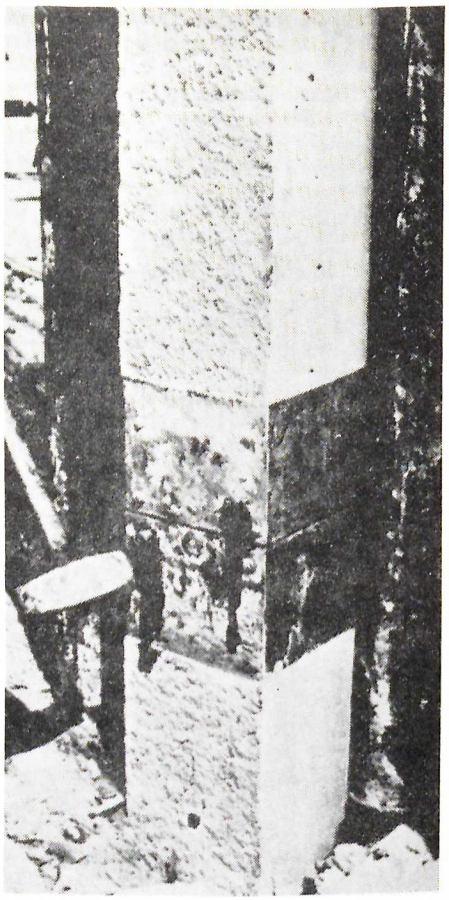

Fig. D7. ABB joint. Driving at locking pins

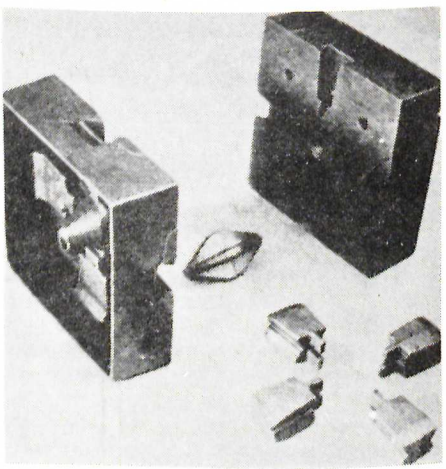

Fig. D8. JF joint

Inclinometer measurements and allowable bending of piles.

Dr B. H. Fellenius (Swedish Geotechnical Institute): Doubts have been cast on the accuracy of inclinometer measurements of piles. This is contrary to Swedish experience. We have more than 10 years of experience of

inclinometer measurements of piles and we are quite satisfied with the accuracy of our readings.

E19. The inclinometer used in Sweden is a strain gauge instrument developed by the Swedish Geotechnical Institute.[1] When measuring piles, the instrument is lowered down a central pipe and readings are taken at certain levels, normally at every metre, of the pile. Each reading gives the inclination of the pile and the direction of the inclination at the measuring level. The inclination is obtained within 0·01 of a degree and the horizontal direction of the inclination within 1 degree. This applies to each individual reading, but the actual accuracy is less when calculating, for instance, the location of a pile tip, where the errors are additive. However, the location of the pile tip can be obtained with a maximum error of 1–2 in., which is acceptable.

E20. There are two reasons for using the inclinometer. The first is to decide the exact location of a pile in a cluster, thinking for instance of the risk of two piles interfering with each other. The second is to investigate the bending of the pile.

E21. The second reason is the more important one. However, what is a bent pile or rather, when does a pile cease to be considered straight and when should it be considered bent and when is it bent too much? There is no general answer to this. In Sweden we employ the following guide rules.

E22. The rules are applied to the slender precast concrete pile, which is by far the most widely used pile in Sweden. The piles are driven in segments, normally 10–12 m in length, which are spliced in the field by means of rigid joint couplings. When studying pile bending by means of inclinometer measurements, we use a standard system for casting inclinometer pipes (42 mm) in the piles using special couplings with inclinometer holes.

E23. Normally, there is no bending problem for piles shorter than 15–20 m in length. With longer piles, the bending over the splices is studied separately from the bending over the pile segments.

E24. First, no sudden changes of inclination, called dog legs, should be allowed, as pointed out by Hanna.[2] Such dog legs can be caused by a joint coupling not being cast square to the pile. Therefore, the change of inclination measured 0·5 m above and 0·5 m below a splice should be less than 0·8°. The squareness may be satisfactory and yet bending of the pile over the splice can result from bad interaction between the coupling and the segment. This is checked by the change of inclination in terms of the bending radius between 1·0 m above and 1·0 m below the splice. The bending radius should be greater than 100 m.

E25. However, a pile can be subjected to a continuous bending without having any dog legs. Therefore, secondly, the bending of the pile is studied in terms of the bending radius over each pile segment. The bending radius is naturally related to the soil conditions. For example, in southwestern Sweden, where thick deposits of soft clay with a shear strength of 1–2 t/m² are common, a bending radius of 300–400 m may be considered bad for the pile, depending upon the intended loading of the pile and other factors. Should the same bending occur in a stiff soil, there would normally be no need for concern.

E26. Thirdly, the deviation from verticality is studied. However, it is recognized that it is the bending which is important and not the lack of verticality.

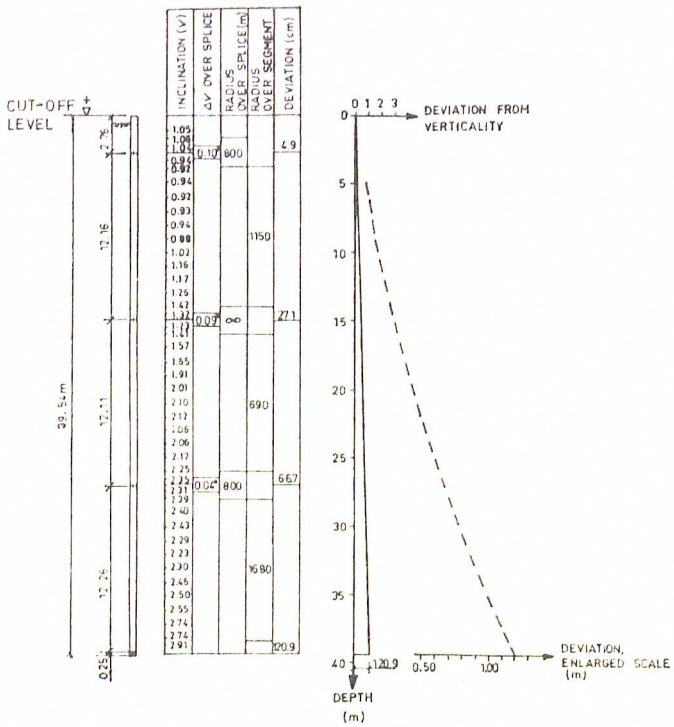

Fig. E1. Results of pile inclinometer measurements

E27. The results of inclinometer measurements are reported as shown in Fig. E1. The figure shows the pile and the location of the splices, and so on, and the measured inclinations. Furthermore, the results of all necessary calculations are presented in a table for examination by the engineer in charge. The vertical and plan view of the pile are also shown.

E28. Inspection of pile bending by means of inclinometer measurements is an accurate and reliable method. However, the inclinometer measurements can, for cost and time reasons, only be employed in special cases together with other investigations such as pile driving tests and load tests. It is not a very practical instrument for the inspection officer checking the contracting work. For this purpose more simple devices must be considered.

E29. One very simple way of checking a pile for bending is to use a long straight plumb bob which will get stuck in the centre pipe at the level of excessive bending. However, piles are not normally provided with a centre pipe.

E30. For other piles, the only thing to do is to observe the driving closely and to measure the rebound and set of the piles. Should the rebound for a pile be considerably larger than for other piles, this may be a sign of severe bending. Naturally, it could also be due to other causes, such as a very elastic soil at the pile tip. After all, at this point, as so often in foundation engineering, reliance has to be placed upon carefully calculated guesses. However, we have found in inclinometer investigations that even long piles are normally driven straight, provided that they are equipped with good quality joints and are driven by experienced and conscientious contractors.

Stresses in steel piles during the driving with air hammer.

Mr G. Fjelkner (Swedish Geotechnical Institute, Stockholm): One of the main problems concerning steel piles is how to predict the bearing capacity. There are three ways of predicting bearing capacity of a pile: loading tests, geostatic calculations and use of pile-driving formulae. It is not economically possible to make load tests on steel piles at every small working site, so either geostatic calculations or pile-driving formulae must be used. Steel piles in Sweden are usually driven into hard layers of moraine and are thus end-bearing. In moraine it is very difficult to take samples and make tests, so the use of a geostatic formula to predict the bearing capacity seems impossible. In this case, therefore, it is best to use pile-driving formulae.

E167. If the common dynamic formula, i.e. Hiley's formula, is used to predict the bearing capacity of a steel pile driven with a light air-hammer, a very small value of the force is obtained. If a loading test is performed on such a pile, an ultimate bearing capacity 10 or even 20 times larger than the calculated one might be found. There is obviously something wrong with pile-driving formulae, at least in this case.

E168. Because of this, I have investigated the forces which develop in steel piles driven with air hammers.[37] There are many parameters to deal with and therefore I have collected them into a dynamic formula. Here it must be pointed out that with this formula only the dynamic forces in steel piles can be calculated and from that a permissible static

force must be estimated. It is therefore a dynamic formula and not a pile-driving formula.

E169. The first question which must be asked is, why do the common pile-driving formulae give such low values of the force, when a pile is being driven with a light hammer? Putting strain-gauges on a steel pile can provide the answer to this question. When driving with a heavy hammer, the whole length of the pile is loaded with a nearly constant dynamic force. This is what Hiley assumed when deriving his formula, so these formulae give an over-estimate of the dynamic force in the pile: but when driving with a light hammer, only a part of the pile is dynamically loaded and the force is not constant, the force/depth relationship tending to be triangular. I have concentrated on attempting to predict the maximum force (the amplitude) of this quasi-triangular waveform.

E170. The best way to derive a dynamic formula is by means of the wave theory. There are several different methods of treating this theory and I have used the grapho-dynamical method,[38] which has been developed in Sweden for percussion drilling. The derivation of the formula is given in a paper published by the Swedish Pile Commission.[37] It contains symbols and figure-texts in English.

E171. Calculations made with this dynamic formula have shown that the force in the pile can be high even when driven with a light hammer. It is mainly dependent on the striking velocity of the ram and to a lesser extent on the weight of the ram and the energy of the blow.

Canadian Geotechnical Journal

Published by THE NATIONAL RESEARCH COUNCIL OF CANADA

VOLUME 8 MAY 1971 NUMBER 2

Bearing Capacity of Piles Driven into Rock

SVEN–ERIK REHNMAN AND BENGT B. BROMS
Swedish Geotechnical Institute, Stockholm, Sweden

Received May 22, 1970

An experimental study is presented on the point bearing capacity of piles in rock. The bearing capacity for granite, limestone, and sandstone was found to be approximately four to six times the unconfined compressive strength of the rock material when the load was applied perpendicular to the rock surface. The ultimate bearing capacity was affected by the inclination of the applied load and by the penetration depth. The ultimate strength decreased rapidly when the inclination exceeded 45°. The strength increased with increasing penetration depth. The increase for granite and sandstone was 25 to 50% when the depth increased from 0 to 1.0 times the point diameter. The corresponding increase for limestone was 60 to 70%.

The point bearing capacity was calculated by the Coulomb–Mohr and by the Griffith failure theories. The test results indicated that the effect of the inclination of the rock surface and of the penetration depth for granite and sandstone was less than calculated. Satisfactory agreement was found for the limestone between measured and calculated values. Comparisons with the Griffith failure theory indicated that the measured failure loads were approximately twice the calculated failure loads.

Une étude expérimentale sur la force portante en pointe de pieux sur le roc est présentée. La résistance en pointe pour du granit, du calcaire et du grès a été trouvée égale à environ quatre à six fois la résistance à la compression de la roche lorsque la charge était appliquée perpendiculairement à la surface de la roche. La portance est influencée par l'inclinaison de la charge appliquée et par la profondeur de pénétration. La résistance limite diminuant rapidement pour une inclinaison supérieure à 45°. La résistance augmente avec la profondeur de pénétration. L'augmentation pour le granit et le grès étant de 25 à 50% quand la profondeur passe de 0 à 1.0 fois le diamètre de la pointe; l'augmentation correspondante pour la pierre calcaire est de 60 à 70%.

La résistance en pointe a été calculée par les théories de rupture de Coulomb–Mohr et de Griffith. Les résultats d'essais indiquent que l'effet de l'inclinaison de la surface de la roche et de la profondeur de pénétration pour le granit et le grès est inférieur à celui calculé. Une concordance relativement bonne a été constatée pour le calcaire entre les valeurs mesurées et calculées. Des comparaisons avec la théorie de rupture de Griffith indiquent que les charges de rupture mesurées ont été approximativement doubles des charges de rupture calculées.

Introduction

Foundation piles in Sweden which have been driven into rock are provided with a high strength steel point as illustrated in Fig. 1. The diameter of the point is generally 60 mm. These point bearing piles are as a rule driven 60 to 120 mm into the underlaying rock with 300 to 500 light blows of a 3- to 4-metric-ton drop hammer. The height of fall varies between 20 and 30 cm. The driving is generally terminated by ten blows where the height of fall of the hammer has been increased in order to test the bearing capacity of the pile. The bearing capacity is considered satisfactory if the penetration of the pile for the ten blows is less than a certain amount. For example, at an allowable load of 60 metric tons (132 kips) and a pile length of 50 m the penetration after ten blows by a 3-ton hammer with a free fall of 35 cm should be less than 7 mm.

The points are generally hollow as indicated in Fig. 1 to prevent the piles from sliding along a sloping rock surface. Due to the small diameter of the rock point (60 mm) the contact pressure will be very high and can in some cases approach or even exceed the unconfined

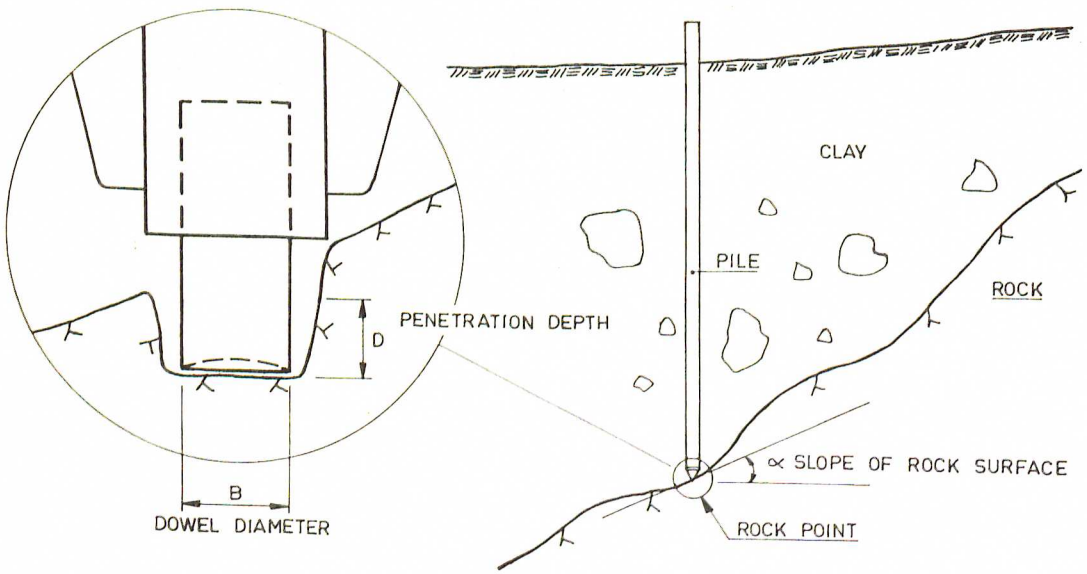

FIG. 1. Pile with rock point.

compressive strength of the rock material. Due to this reason an investigation of the factors which affect the ultimate point bearing capacity of rock was initiated at the Swedish Geotechnical Institute. The results from this investigation are reported in this article.

Outline of Test Program

The bearing capacity of three different rock materials (granite, limestone, and sandstone) has been investigated by laboratory load tests on rock samples which were encased in concrete. The penetration depth ($D/B = 0$ and 1.0) and the inclination of the rock surface ($\alpha = 0°$, 30°, 45°, and 60°) were varied (Fig. 1). Three tests were carried out for each set of parameters.

Rock Material

The granite used in this investigation was mined at Rixö in Bohuslän, Sweden, and is locally known as Rixö granite. The Rixö granite is massive with a particle size of 0.5 to 2 mm. The mineral particles are mainly composed of quartz, feldspar, mica and biotite. The granite probably also contains some ortite. The volume of ortite has probably increased due to radioactivity since the formation of the granite causing expansion cracks in adjacent mineral particles. It is believed that the expansion cracks have not affected appreciably the strength of the rock material.

The limestone, which is fossiliferous, was obtained from Borghamn at lake Vättern in Sweden. The limestone is banded and the band boundaries are diffuse. The average particle size is less than 0.001 mm. Some shell fragments have been found in the limestone. All observed cracks were healed.

The sandstone was obtained from Burgsvik on the Isle of Gotland, Sweden. The sandstone is cemented and banded. The particle size is approximately 0.1 mm. The particles which are mainly angular, are composed of quartz, mica, biotite, and feldspar. The cementing material is calcite.

The unconfined compressive strength of the rock was determined from cylinders of 50 mm diameter and 50 mm height. The test results are given in Table 1. It can be seen that the spread of the individual test values is small.

The shear strength τ_f of the rock material at different normal pressures σ_f was determined with the double shear apparatus shown in Fig. 2. Cylinders of 15 mm diameter and

TABLE 1. Unconfined compressive strength

Rock material	Unconfined compressive strength, q_u, kg/cm² (kips/m²)			
	Test 1	Test 2	Test 3	Average
Granite	2320 (32.0)	2300 (32.7)	2290 (32.6)	2300 (32.7)
Limestone	1470 (20.9)	1180 (16.8)	1055 (15.0)	1240 (17.6)
Sandstone	713 (10.2)	703 (10.0)	698 (9.9)	705 (10.1)

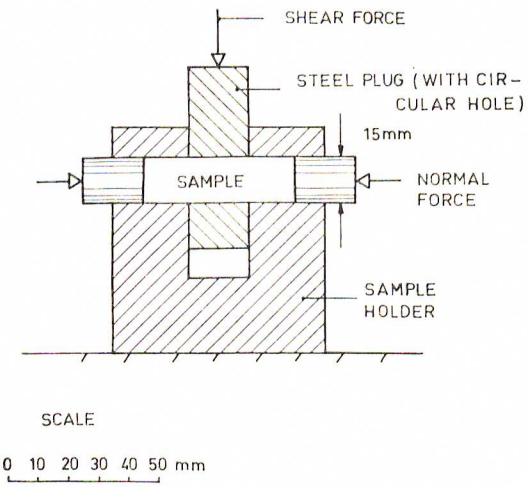

FIG. 2. Double shear test on rock (Lundborg 1966).

50 mm length were tested. The following equation was found to fit the test results (Lundborg 1966).

$$[1] \qquad \tau_f = \tau_0 + \frac{\mu\sigma_f}{1 + \frac{\mu\sigma_f}{\tau_i - \tau_0}}$$

where τ_0 and τ_i are the shear strength at $\sigma_f = 0$ and $\sigma_f = \infty$, respectively, and μ is the slope of the τ_f–σ_f relationship at $\sigma_f = 0$. The test results are shown in Fig. 3 and in Table 2. For comparison the unconfined compressive strength was determined on samples with the same diameter and height as those used at the double shear tests. The results from this test series are also shown in Fig. 3. It can be seen that the stress circles for the unconfined compression tests almost touch the τ_f–σ_f relationships determined from the double shear tests. It can also

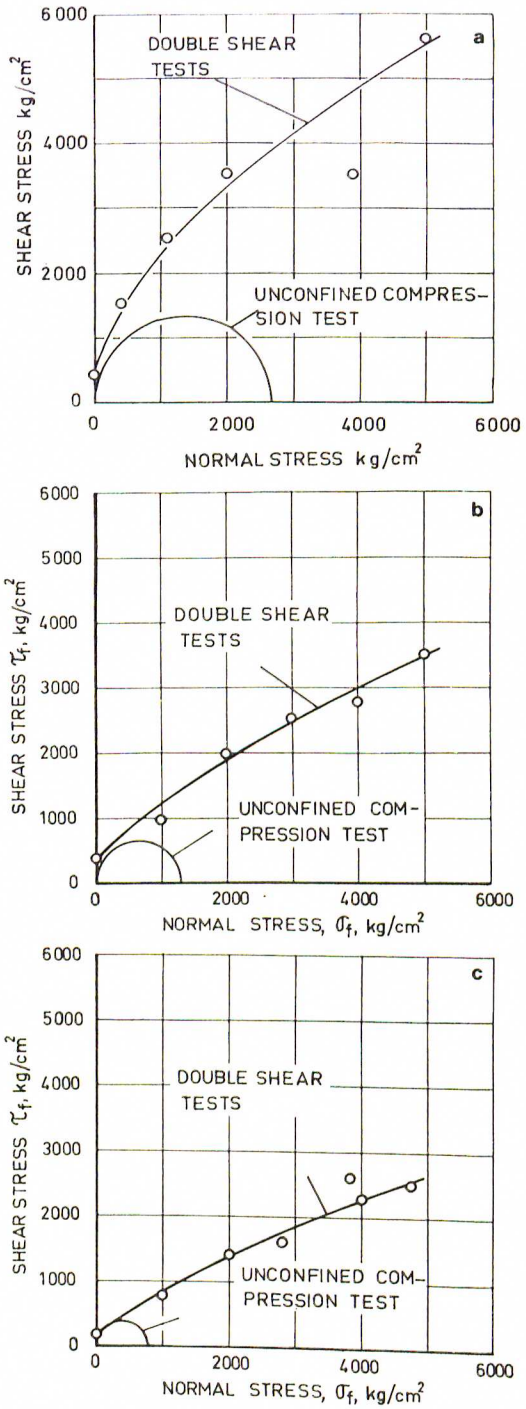

FIG. 3. Shear strength results for *a*) granite, *b*) limestone, *c*) sandstone.

TABLE 2. Test results from double shear tests

Rock material	τ_o kg/cm² (kips/in.²)	τ_t kg/cm² (kips/in.²)	μ	q_u* kg/cm² (kips/in.²)
Granite	300 (4.3)	11900 (16.9)	1.8	2700 (38.4)
Limestone	200 (2.8)	10200 (14.5)	1.0	1300 (18.5)
Sandstone	200 (2.8)	9000 (12.8)	0.7	800 (11.4)

*Unconfined compression tests on cylinders with 15 mm diameter and 50 mm height.

be seen that the slope of τ_f–σ_f relationships decreased with increasing pressure.

The tensile strength was determined by the indirect Brazilian tension test method on cylindrical samples of 40 mm diameter and 40 mm length. Only a few samples were tested. The average tensile strength was 148 kg/cm² (2100 lb/in.²) for the granite, 127 kg/cm² (1800 lb/in.²) for the limestone and 60 kg/cm² (850 lb/in.²) for sandstone.

The modulus of rupture was determined for the Rixö granite on rods with a cross-section of 2 × 5 cm. The length of the rods was 25 cm. The average modulus of rupture was 158 kg/cm² (2240 lb/in.²) at 0 °C and 133 kg/cm² (1890 lb/in.²) at +60 °C. The influence of temperature on the modulus of rupture was thus small.

Test Equipment and Test Procedure

The load tests were carried out on rock cubes (13 × 13 × 10 cm) which were cast in concrete in rigid steel cylinders as illustrated in Fig. 4. The steel cylinders were used to prevent the rock specimen from splitting during the load tests. The rock specimens were soaked in water for several hours before the casting of the concrete. A hole with 21 mm diameter was drilled with an air hammer in each rock specimen, after the concrete had hardened in order to simulate the penetration of the steel point into rock during the driving. The drill holes were finished by hand to obtain a plane bottom surface. A thin layer of crushed rock (rock flour) was left at the bottom of the drill hole to distribute the applied load evenly during the load test.

The point bearing capacity was investigated with steel dowels of 20 mm diameter. The

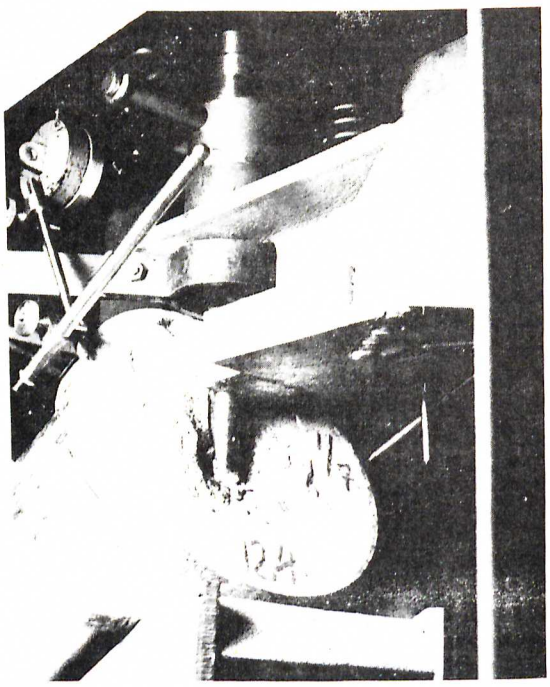

FIG. 4. Test arrangement. Load test on limestone ($\alpha = 60°$, $D/B = 0$).

bottom surface of the dowels was plane. The steel dowels were manufactured of high strength steel bars with 70 mm diameter. The length of the dowels was varied to fit the depth of the predrilled hole and the inclination of the rock surface. Load was applied in 2000 kg (4.4 kips) increments by a hydraulic jack. After every fifth load increment the dowel was unloaded to 4000 kg (8.8 kips) to simulate the unloading during a pile test. The time between each load increment was 2 min. The increments were decreased to 1000 kg (2.2 kips) during the load tests on sandstone when the slope of the rock surface was 45° and 60° because of the relatively low ultimate strength of the rock in this case.

The applied load was read on a calibrated manometer and the penetration by two dial indicators which were rigidly attached to the dowel. The steel dowel was guided by a steel arm which was attached to a rigid steel frame. The inclination of the rock samples could be varied with respect to the axis of the dowel through a specially designed sample holder.

The load tests were carried out to failure

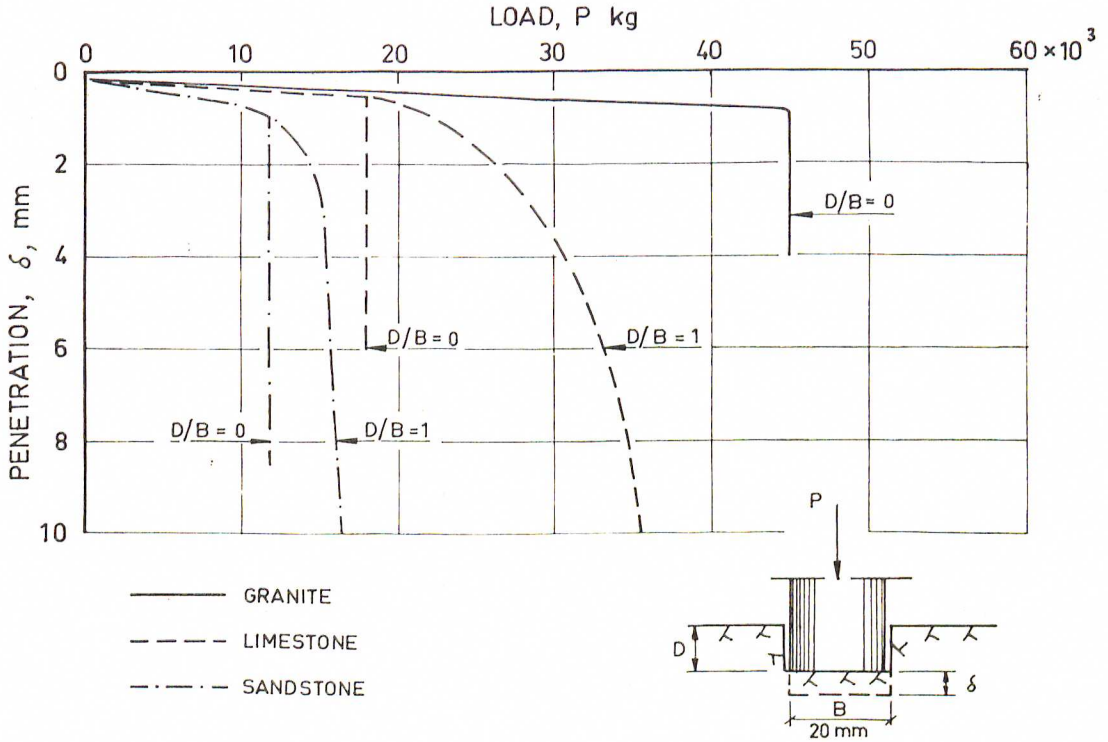

FIG. 5. Load–penetration relationships for granite, limestone, and sandstone.

which in most cases occurred suddenly without warning. In a few cases the penetration of the dowel increased slowly with increasing applied load. The failure load was in these cases defined as the load when the penetration was twice the penetration at 90% of the failure load. The dowel was unloaded after the failure load had been reached. Failure occurred in several cases when the rock sample was reloaded after the unloading to 4000 kg (8.8 kips).

A plaster cast was made of the rock surface after the crushed rock material had been removed below the dowel. The shape of the failure surface could be determined by cutting the plaster cast in sections.

Test Results

Load–Penetration Relationships

Typical load–penetration relationships at $D/B = 0$ and $D/B = 1.0$ for the three rock materials are shown in Fig. 5 when the load was perpendicular to the rock surface. When the load was applied at the rock surface ($D/B = 0$) the penetration of the dowel increased approximately linearly with increasing load up to failure which in this case occurred suddenly when the total penetration of the dowel was about 1 mm. The penetration at failure was thus small. However, the additional penetration after failure of the rock was relatively large. The total penetration was about 4 mm for the granite samples, about 6 mm for the limestone samples and about 8 mm for the sandstone samples. A crackling sound was heard in the granite when the failure load was approached. At each sound the penetration of the dowel increased a few hundredths of a millimeter. The intensity of the crackles increased rapidly just before failure. Similar sounds were not observed in the limestone or sandstone samples.

The penetration increased gradually with increasing load when the load was applied at some depths below the rock surface ($D/B = 1.0$). The penetration at the failure load was relatively large. Only the limestone and the sandstone samples could be loaded to failure

due to the limited load capacity of the testing machine.

Approximately the same behavior as that shown in Fig. 5 was observed when the load was inclined and the slope of the rock surface α was less than about 30°. When the slope exceeded 30° failure occurred suddenly without warning, even if the load was applied at the same depth below the free rock surface ($D/B = 1.0$).

The slope of the rock surface also affected the load–penetration relationship after failure. When the slope was less than about 30° the residual (remaining) bearing capacity of the rock after failure was relatively large. The residual bearing capacity was small when the slope exceeded 30°. A relatively large chip often broke loose below the dowel which left the dowel hanging free as illustrated in Fig. 4.

Ultimate Bearing Capacity

The influence on the bearing capacity of the slope of the free rock surface (α) and of the penetration depth (D/B) has been investigated. The test results for granite, limestone, and sandstone are shown in Fig. 6.

Failure occurred for the Rixö granite when the average contact stress below the dowel was 14 000 kg/cm² (20 kips/in.²) and the load was applied at and perpendicular to the free rock surface (Fig. 6*a*). This contact stress is

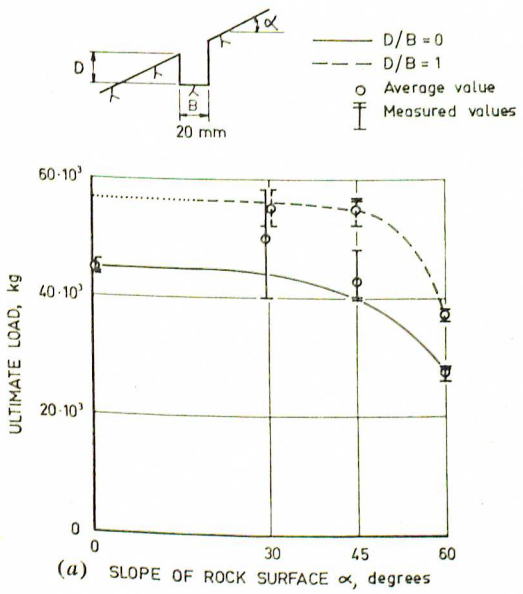

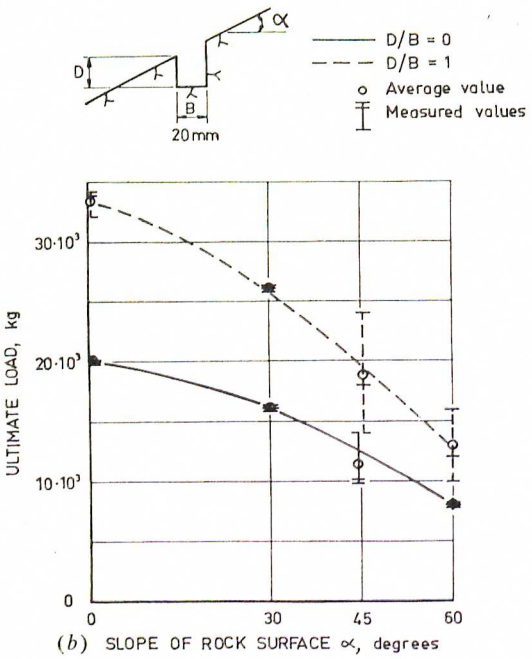

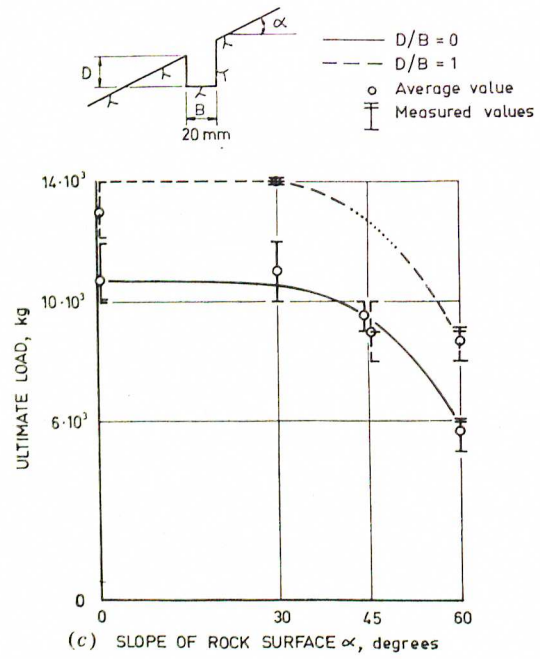

FIG. 6. Ultimate load of rock as affected by inclination and embedment of dowel: *a*) granite; *b*) limestone; *c*) sandstone.

considerably larger than the unconfined compressive strength of the rock mass (2300 kg/cm^2). It can also be seen from Fig. 6*a* that the failure load was not affected by the inclination of the rock surface as long as the inclination was less than about 30°. At an inclination of 60° the failure load was approximately 60% of the failure load at $\alpha = 0°$. The failure load increased by 25 to 35% when the relative penetration depth D/B increased from 0 to 1.0. The load increase was approximately independent of the inclination of the rock surface.

For the limestone, the inclination of the rock surface influenced appreciably the failure load as shown in Fig. 6*b*. At $D/B = 0$ the failure load decreased from 20 000 kg (44 kips) to 8000 kg (17.6 kips) when the inclination increased from 0° to 60°. The corresponding decrease at $D/B = 1.0$ was from 33 000 kg (72.6 kips) to 13 000 kg (28.6 kips) when the inclination increased from 0° to 60°. The relative penetration depth affected also appreciably the failure load. When relative penetration depth D/B increased from 0 to 1.0 the failure load increased by 60 to 70%.

As for granite the ultimate bearing capacity of the sandstone was found to be independent of the slope of the rock surface when the slope was less than 30°. The bearing capacity increased with increasing penetration D/B and it increased with 30 to 50% when the relative penetration D/B increased from 0 to 1.0.

Appearance of Failure Surface

Three principal failure modes were observed. The first failure mode, local crushing, occurred just below the loaded dowel and some chipping was observed around the dowel perimeter (Fig. 7). The diameter of the resulting crater was approximately 5 cm for the granite samples, about 10 cm for the limestone samples and about 11 cm for the sandstone samples.

The second failure mode occurred in limestone and sandstone when load was applied at some depth below and perpendicular to the rock surface. This type of failure developed gradually and the penetration of the dowel at failure was large. Radial cracks occurred in the rock specimen just before failure as shown in Fig. 8. The length of these radial cracks increased with increasing applied load. At failure the crack length was 3 to 5 cm. The cracks penetrated into the surrounding concrete in a few cases.

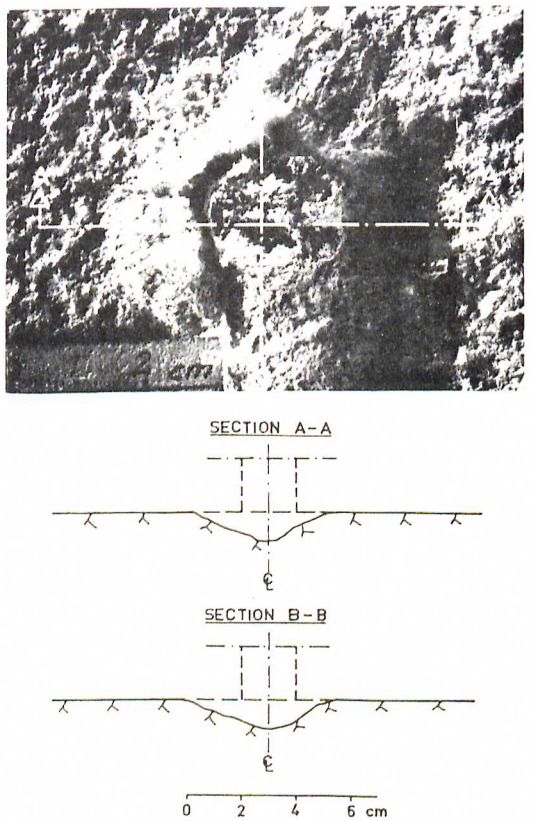

FIG. 7. Surface fracture in granite (Test No. 3, $\alpha = 0°$, $D/B = 0$).

The third failure mode was observed when the slope of the rock surface was equal to or exceeded 30°. In this failure type a cone of crushed rock formed below the dowel which displaced a large chip of rock in front of the dowel as shown in Fig. 4. This chip was in some cases larger than the surface area of the rock specimen and part of the surrounding concrete was torn loose. However, the failure load has probably not been affected by the concrete due to the brittle character of the failure.

Discussion of Test Results

Coulomb–Mohr's Failure Theory

The methods which are used to calculate the ultimate bearing capacity of soils are sometimes also applied to rocks. These methods are

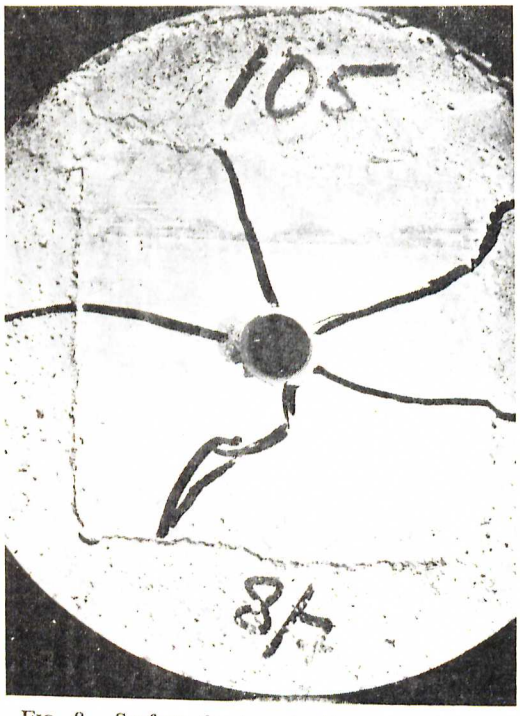

FIG. 8. Surface fracture in limestone (Test No. 105, $\alpha = 0°$, $D/B = 1$).

based on the theory of plasticity. It is assumed in these methods that yielding occurs when the stress in the soil or rock reaches a critical value. This critical value is generally calculated from the yield criterion proposed by Tresca, Coulomb–Mohr, or van Mises.

The ultimate bearing capacity q_{ult} of soils is generally calculated from the following general equation (Terzaghi 1943)

$$[2] \quad q_{ult} = K_c N_c c + K_q N_q \gamma_1 D + K_\gamma N_\gamma \gamma_2 B$$

where K_c, K_q, K_γ = shape factors which are dependent of the shape of the loaded area.

γ_1, γ_2 = unit weight of soil above and below the foundation level, respectively (Fig. 9).

N_c, N_q, N_γ = bearing capacity factors which are dependent of the angle of internal friction ϕ, the foundation level and the direction of the applied load.

B = width of loaded area (Fig. 9).

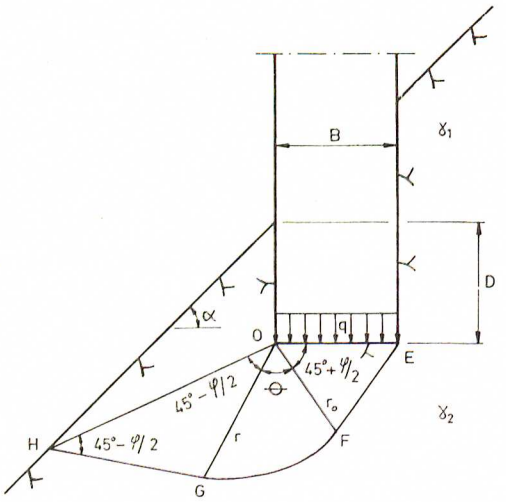

FIG. 9. Assumed rupture surface for a sloping rock surface. OEF = active Rankine zone; OFG = Prandtl zone; OGH = passive Rankine zone.

D = depth below surface (Fig. 9).

c = cohesive strength.

In the derivation of Eq. [2] it is assumed that soil behaves as an ideal plastic material with a constant cohesion c and a constant angle of internal friction ϕ and that the shear strength τ_f is governed by the Coulomb–Mohr failure theory

$$[3] \quad \tau_f = c + \sigma_f \operatorname{tg}\phi$$

where σ_f is the normal stress on the failure surface. If Eq. [2] can be used to predict the ultimate bearing capacity of rock the following equation can be derived

$$[4] \quad q_{ult} = K_c N_c c$$

In the derivation of this equation it is assumed that the terms $\gamma_1 D$ and $\gamma_2 B$ are small in comparison with the cohesion c of the material. (The numerical values of the bearing capacity factors N_c, N_q, and N_γ are approximately the same.)

The cohesion c_m which corresponds to the average angle of internal friction ϕ_m for the load interval, can be evaluated from the unconfined compressive strength $q_{compression}$. From geometrical considerations it can be shown that

$$[5] \quad \frac{c_m}{q_{compression}} = \frac{(1 - \sin \phi_m)}{2 \cos \phi_m}$$

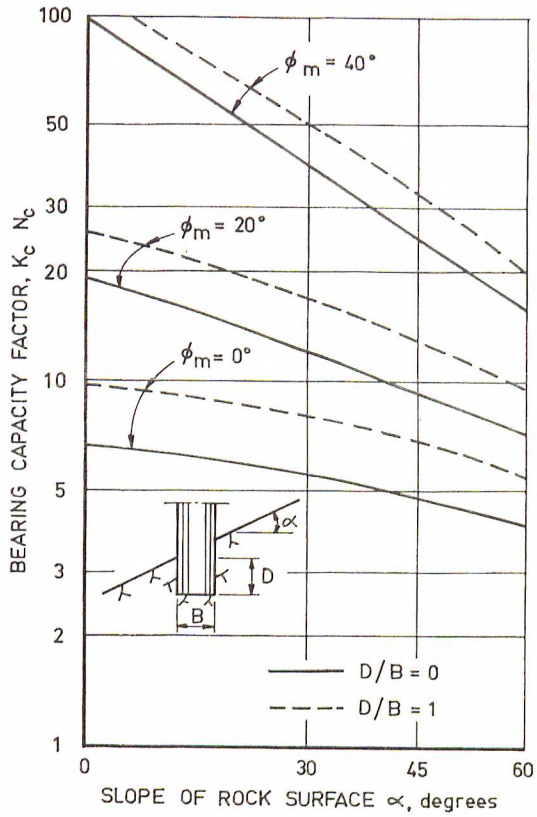

FIG. 10. Bearing capacity factor $K_c \cdot N_c$ in Eq. [4] as a function of slope α, depth of embedment D/B and mobilized angle of internal friction ϕ_m.

With this value of c_m Eq. [4] can be rewritten as

$$[6] \qquad \frac{2q_{ult}}{q_{compression}} = \frac{(1 - \sin \phi_m)}{\cos \phi_m} \cdot K_c N_c$$

The bearing capacity factor N_c can be evaluated from an assumed failure or rupture surface as shown in Fig. 9 as for example proposed by Meyerhof (1951). It has been assumed in the following calculations that the weight of the rock can be neglected and that the failure surface between G and F is spiral shaped according to the equation

$$[7] \qquad r = r_0 e^{\theta \operatorname{tg} \phi}$$

where r, r_0, and θ are defined in Fig. 9.

The calculated values of $K_c N_c$ in Eq. [4] are plotted in Fig. 10 as a function of the slope α of the free rock surface at different values of the angle of internal friction and of the penetration depth D/B. It has been assumed in Fig. 10 that the shape factor K is equal to 1.3.

The test results and the calculated relationship for granite, limestone, and sandstone are shown in Fig. 11 as a function of the slope α of the free rock surface. It can be seen that the test values correspond to a mobilized angle of internal friction of 10° to 20° at $\alpha = 0°$ which is considerably less than the measured angles of 30° to 45° from the double shear tests. Furthermore the influence on the ultimate bearing capacity of the inclination of the applied load was for granite and sandstone less than calculated as well as the increase of the bearing capacity with increasing penetration depth D/B. Relatively good agreement between measured and calculated values was obtained for the limestone.

Analysis of the test data indicates that the ultimate bearing capacity of ductile rock can be predicted relatively satisfactorily by the theory of plasticity. The test data also indicate that methods based on the theory of plasticity cannot be used for relatively brittle rocks such as granite and sandstone.

Griffith's Failure Theory

Griffith's failure theory presumes elliptical microcracks in the rock mass. Failure occurs when the maximum stress caused by the stress concentrations around the microcrack reaches the tensile strength of the material.

The ultimate bearing capacity for a point load acting on and perpendicular to the rock surface is, according to Griffith's failure theory, equal to (Coates 1965)

$$[8] \qquad q_{ult} = 24\sigma_{tension}$$

or

$$[9] \qquad q_{ult} = 3\sigma_{compression}$$

where $\sigma_{tension}$ is the tensile strength and $\sigma_{compression}$ the unconfined compressive strength of the rock material. The ratio $\sigma_{compression}/\sigma_{tension}$ is equal to 8.

In Table 3 is shown the experimentally determined values of the ratio $\sigma_{compression}/\sigma_{tension}$, $q_{ult}/\sigma_{compression}$ and $q_{ult}/\sigma_{tension}$. Average values

TABLE 3. Comparisons with Griffith's failure theory

Strength ratio	Granite	Limestone	Sandstone
$\sigma_{compression}/\sigma_{tension}$	16	10	12
$q_{ult}/\sigma_{compression}$	6.2	5.2	4.8
$q_{ult}/\sigma_{tension}$	96	50	52

have been used in the calculation. It can be seen from this table that the values of the ratios $q_{ult}/\sigma_{compression}$ and $q_{ult}/\sigma_{tension}$ were approximately twice those calculated by the Griffith's failure theory. This comparison thus indicates that the Griffith's failure theory underestimates the ultimate bearing capacity of brittle rocks.

Empirical Method

The results from the tests when the load was applied at and perpendicular to the rock surface ($\alpha = 0°$, $D/B = 0$) are plotted in Fig. 12 as a function of the unconfined compressive strength $\sigma_{compression}$ of the rock material.

These test data indicate that the ultimate strength q_{ult} can be calculated from the equation

[10] $$q_{ult} = 4 \text{ to } 6\sigma_{compression}$$

The compressive strength has been evaluated from tests on cylinders with 50 mm diameter and 50 mm height as mentioned previously. The test data indicate that the bearing capacity increases with increasing compressive strength. However, Eq. [10] can only be used to predict the bearing capacity when $\alpha = 0$ and $D/B = 0$. The calculated point bearing capacity must be corrected when the rock surface is sloping ($\alpha \neq 0$) or the load is applied at some depth below the surface ($D/B \neq 0$). It should be noted that Eq. [10] is based on data obtained from load tests with 20 mm steel dowels.

Previous Investigations

The bearing capacity of rock points has previously been investigated by Petterson (1941). Rock points of steel with 75 and 100 mm diameter were jacked against rock specimens which were cast in concrete. The load was applied perpendicular to the rock surface. The load tests could not be carried out to failure because the steel points cracked before the failure load of the rock was reached at an applied stress of 3080 kg/cm^2 (43.8 kips/in.^{2}).

Some load tests were also carried out on a sloping rock surface ($\alpha = 45°$). The penetra-

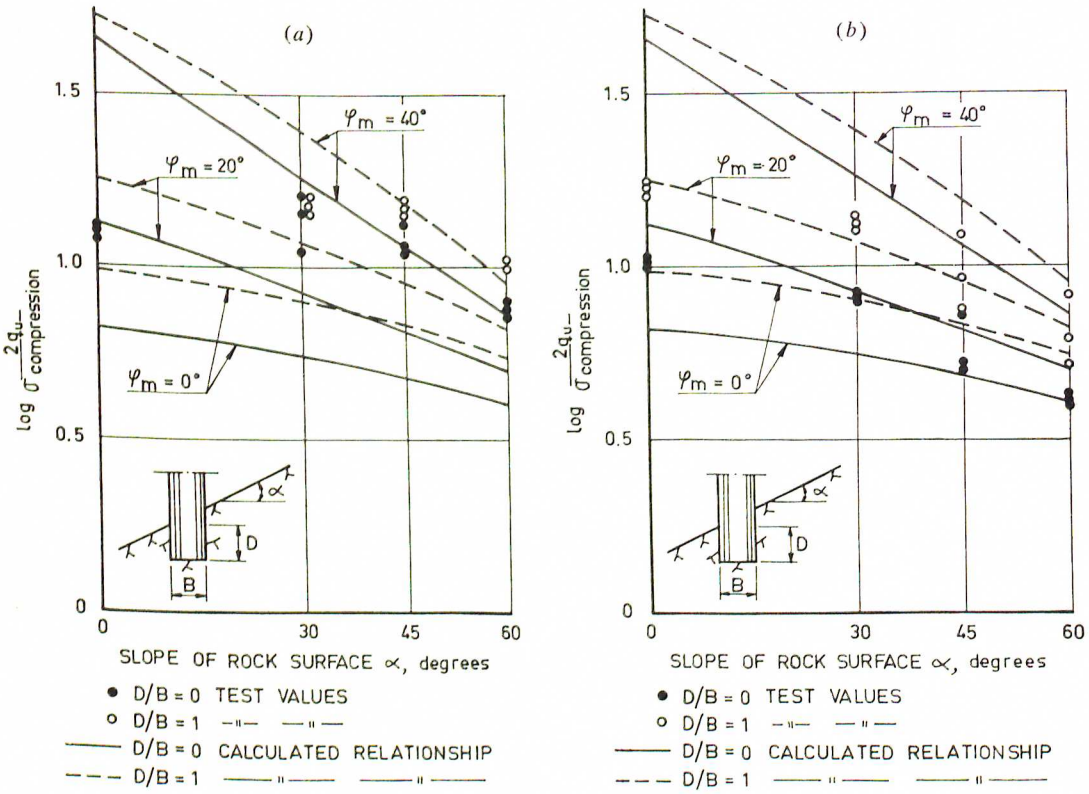

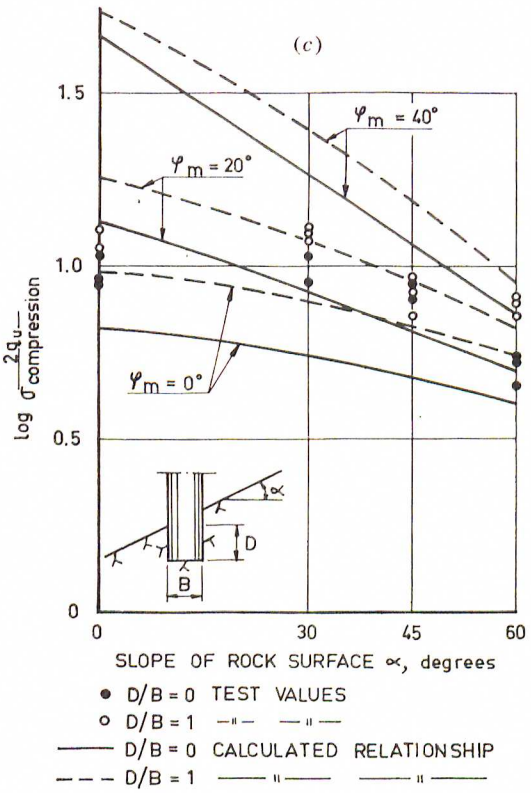

FIG. 11. Ultimate bearing capacity of rock. Comparison between measured and calculated values: *a*) granite; *b*) limestone; *c*) sandstone.

tion of the rock point during driving was studied during these tests.

Load tests on piles with rock points have also been reported by Bjerrum (1957). Steel H-piles provided with a so-called Oslo-point with 100 mm diameter were used for this investigation. The piles were driven into shale. The slope of the rock surface varied between 35° and 60°. One of the piles was loaded to failure after the soil around the pile had been excavated down to the rock. Failure occurred at a load which corresponded to an average contact stress of 300 to 500 kg/cm² (4.3 to 7.1 kips/in.²) below the rock point. The penetration of the point was at failure 3 to 5 cm. When the applied load was doubled the penetration increased by approximately 15 cm. The compressive strength of the rock material was not determined in this investigation.

The bearing capacity of rock points have also been investigated by Engström (1949). These load tests were carried out in an air shelter in rock. Rock points with 140 mm diameter were jacked against the unlined granite walls. The maximum applied load was 300 metric tons (660 kips) which corresponds to an average contact stress of 2000 kg/cm² (28.4 kips/in.²). The tests could not be carried out to failure. The rock crushed locally below the rock points.

Results from load tests on gneiss have been reported by Bergfelt (1955). These tests were carried out in gneiss with rock points of 118 mm diameter. The average slope of the rock surface was 45°. The maximum applied load was 150 to 160 metric tons (330 to 352 kips) which corresponds to a maximum stress of about 4000 kg/cm² (56.8 kips/in.²). The tests were not carried out to failure.

Additional tests by Bergfelt (1958) with 60 mm rock points gave a failure contact stress for gneiss of about 5300 kg/cm² (75.3 kips/in.²). The load was applied perpendicular to the rock surface. The compressive strength of the gneiss was approximately 1000 kg/cm² (14.2 kips/in.²). The ratio $q_{ult}/\sigma_{compression}$ was in this case about 5. This value agrees well with the results from the present investigation.

Granholm (1967) has reported results from three load tests on concrete piles which have been driven through soft clay into rock. The diameter of the rock points was 60 mm. The concrete piles failed at an applied load 320, 330, and 380 metric tons (704, 726, and 836 kips). At this load the compressive strength of the pile section was exceeded. The applied loads did not exceed the point bearing capacity of the rock. These loads correspond to a contact stress of 14 000 to 13 400 kg/cm² (198 to 191 kips/in.²) below the rock points if the total applied load is transferred to the pile tip. The unconfined compressive strength of the rock was not measured.

Thus previous load tests indicate that the ultimate point bearing capacity of rock is high and can exceed considerably the unconfined compressive strength of the rock. However, few of the load tests were carried out to failure.

Summary

The ultimate point bearing capacity of rock has been investigated. Load tests were carried out on three rock types (granite, limestone, and sandstone). The effects of penetration

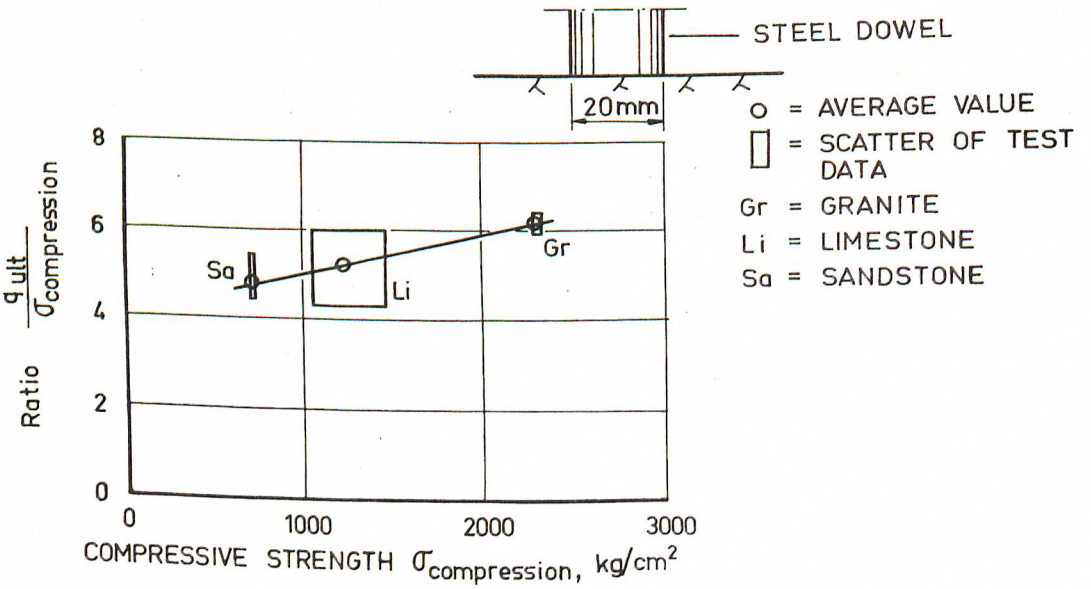

FIG. 12. Relationship between ultimate point bearing capacity q_{ult} and compressive strength $\sigma_{compression}$ of rock.

depth (D/B) and the slope (α) of the free rock surface were investigated. The diameter of the rock point was 20 mm.

The test results indicate that the ultimate bearing capacity corresponds to four to six times the unconfined compressive strength of the rock material when the load is applied at and perpendicular to the rock surface. The effects of the penetration depth (D/B) and the slope (α) of the free rock surface could be satisfactorily predicted for limestone which is relatively ductile by a bearing capacity formula based on the Coulomb–Mohr failure theory. The ultimate bearing capacity of granite and sandstone was less affected by the slope (α) of the rock surface and by the penetration depth (D/B) than the limestone. The ultimate strength was approximately twice that predicted by the Griffith failure criterion when the load was applied at and perpendicular to the rock surface.

Acknowledgments

The tests reported in this paper are part of an investigation by the first author for the degree 'teknologie licentiat' at the Royal Institute of Technology, Stockholm, Sweden (Rehnman 1968). The investigation has been supported financially by the Swedish Committee on Pile Research.

BERGFELT, A. 1955. Pålspetsar för anliggning mot berg. Tek. Tidskr. **85**:4, pp. 67–70.

——— 1958. Provtryckning av pålspetsar mot berg. Nya Asfalt AB, rapport nr 8, 12 p.

BJERRUM, L. 1957. Norwegian experiences with steel piles to rocks. Géotechnique, **7**:2, pp. 73–96.

COATES, D. F. 1965. Rock mechanics principles. Department of Mines and Technical Surveys, Mines Branch Monogr. 874, Ottawa, 327 p.

ENGSTRÖM, N. 1949. Hållfasthet hos betongpålspetsar (On the strength of concrete pile tips). Betong, **34**:1, pp. 30–49.

GRANHOLM, H. 1967. Bärförmågan hos armerade betongpålar slagna till fast bergbotten. IVA:s pålkommitté meddelande nr 10. 19 p. + 51 pl.

LUNDBORG, N. 1966. Triaxial shear strength of some Swedish rocks and ores. Proc. Congr. Int. Soc. Rock Mech. 1st. Lisbon. **1**, pp. 251–255.

MEYERHOF, G. G. 1951. The ultimate bearing capacity of foundations. Géotechnique, **2**:4, pp. 301–332.

——— 1953. The bearing capacity of concrete and rock. Mag. Concr. Res. No. 12.

PETTERSON, K. E. 1941. Grundläggning av specialtyp. Tek. Tidskr. V.o.V. **71**:4, pp. 45–52.

REHNMAN, S.-E. 1968. Bärförmåga hos sluntberg vid statisk belastning av bergspets. Resultat från modellförsök. Swedish Geotechnical Institute, Reprints and Preliminary Reports, No. 27, 74 pp.

TERZAGHI, K. 1943. Theoretical soil mechanics. London. 510 p.

Bearing Capacity of Piles Driven into Rock: Discussion

B. LADANYI
École Polytechnique, Montreal, Quebec
Received June 23, 1971

Rehnman and Broms (1971) have presented some interesting experimental data on bearing capacity of rock under flat-ended cylindrical dowels, obtained in a laboratory study that was carried out in connection with the problem of bearing capacity of piles in rock. As this writer has recently conducted two similar experimental investigations (Ladanyi 1968; Ladanyi and Roy 1971), it may be interesting to compare both sources of data and the conclusions drawn from the data. The discussion will concern only that part of the paper dealing with the bearing capacity of rock when the load is applied perpendicularly to the rock surface and either at or below the surface, in a predrilled hole.

For the particular test conditions, the authors' findings and conclusions may be summarized as follows:

(1) When the load is applied at and perpendicular to the rock surface, the bearing capacity corresponds to 4 to 6 times the unconfined compression strength of the rock material.

(2) When the depth of embedment of the dowel, D/B, increases from 0 to 1.0, the bearing capacity increases by 25 to 30% in granite, 30 to 50% in sandstone, and 60 to 70% in limestone.

(3) The Terzaghi (1943) bearing capacity formula predicts relatively well the bearing capacity of limestone but overestimates the bearing capacities of more brittle rocks such as granite and sandstone.

(4) The Coates (1965) bearing capacity formula, based on the Griffith failure theory,

underestimates the observed bearing capacities by a factor of at least 2.

As far as the ratio between the ultimate bearing capacity in surface indentation and the unconfined compression strength of rock is concerned, the writer's results obtained in both aforementioned studies, one of which (Ladanyi 1968) was carried out in the laboratory on solid rock blocks and the other (Ladanyi and Roy 1971) on a natural rock face in the field, show the values of the ratio varying between about 7 and 15. The difference is obviously most likely due to the different types of rocks used in the tests. However, in evaluating these ratios one should be careful to take into account the size effect on the value of $\sigma_{\text{compression}}$. It is not clear how that was done in the authors' paper.

As far as the effect of the depth of embedment is concerned, the depth factors obtained in the two mentioned investigations were on the average of the same order of magnitude as those noted by the authors. However, a large scatter of results was observed, particularly in the field tests, resulting in a large variation of the depth factors. As the authors have not given any statistical analysis of their data, it is difficult to see what are the confidence limits of the quoted depth factors.

The use of Prandtl–Terzaghi type bearing capacity formula for estimating the bearing capacity of rock under concentrated loads has been considered in the past by several investigators, in particular in connection with the rock failure under drilling bits (*e.g.* Cheatham 1958, 1964; Cheatham and Gnirk 1967) with reasonable success. It is obvious, however, that such a formula, based on the assumption of a shear failure, is only a crude approximation when applied to the brittle rock failure in indentation. Moreover, it was shown (Ladanyi and Roy 1971) that for brittle and nonhomogeneous materials such as rock, it actually gives an upper limit of the bearing capacity, which may be useful for designing the rock-drilling tools.

A theory based on the model of cavity expansion, which seems to come closer to the observed phenomenon in brittle rocks, has been proposed by the writer some time ago and compared with experimental data on several rocks and concrete (Ladanyi 1966, 1968).

However, from the point of view of practical evaluation of the bearing capacity of rock for foundation purposes, where safety against failure is a primary concern, the two mentioned theories can only be recommended if they are used with statistically valid rock strength parameters, enabling the probability of failure to be estimated. If, on the contrary, an overall factor of safety approach is used, a better alternative may be to select a very conservative lower bound bearing capacity theory in the design. The Coates (1965) formula mentioned by the authors is based on such a lower bound solution.

In comparing the experimental data with the latter formula, however, one should not be surprised to find that it underestimates the ultimate bearing capacity of rock. This is exactly what one should expect from the use of the Griffith theory, which gives conditions for fracture initiation and not for general failure. If, however, instead of the Griffith theory, the Mohr–Coulomb theory is used in the same lower bound solution, and if, moreover, the effect of the depth is estimated correspondingly, one finds (Ladanyi and Roy 1971) that

$$[1] \quad q_{\text{ult}}/\sigma_{\text{comp}} = (N_\Phi + 1)\left(1 + \frac{D}{2B}\cos\Phi\right)$$

where N_Φ is the flow value

$$[2] \quad N_\Phi = (1 + \sin\Phi)/(1 - \sin\Phi)$$

For example, for the values of Φ quoted by the authors, Eq. [1] would give

$$\text{For } \Phi = 30^\circ\text{: } q_{\text{ult}}/\sigma_{\text{comp}} = 4 \quad \text{at } D/B = 0$$

$$= 5.72 \text{ at } D/B = 1$$

$$\text{For } \Phi = 45^\circ\text{: } q_{\text{ult}}/\sigma_{\text{comp}} = 5.83 \text{ at } D/B = 0$$

$$= 7.90 \text{ at } D/B = 1$$

which are conservative lower bounds to the observed ratios at failure.

Finally, it is interesting to mention that the same lower bound solution enables easily taking into account the effect on the bearing capacity of one or two systems of rock joints.

CHEATHAM, J. B., JR. 1958. An analytical study of penetration by a single bit tooth. 8th Annu. Drilling and Blasting Symp. Univ. Minn., Minneapolis, Minn.

——— 1964. Indentation analysis for rock having a parabolic yield envelope. Int. J. Rock. Mech. Min. Sci. **1**, pp. 431–440.

CHEATHAM, J. B., JR., and GNIRK, P. F. 1967. The mechanics of rock failure associated with drilling at depth. *In* Failure and breakage of rock (*Edited by* Fairhurst), AIME, New York, pp. 410–439.

COATES, D. F. 1965. Rock mechanics principles. Dep. Min. Tech. Surv., Min. Br. Monogr. 874.

LADANYI, B. 1966. Failure mechanism of rock under a plate load. Proc. 1st Congr. Int. Soc. Rock Mech., Lisbon, **1**, pp. 415–420.

——— 1968. Rock failure under concentrated loading. 10th Symp. on Rock Mech., Austin, Texas.

LADANYI, B., and ROY, A. 1971. Some aspects of bearing capacity of rock mass. Proc. 7th Can. Symp. on Rock Mech., Edmonton, Alberta.

REHNMAN, S.-E., and BROMS, B. B. 1971. Bearing capacity of piles driven into rock. Can. Geotech. J. **8**, pp. 151–162.

TERZAGHI, K. 1943. Theoretical soil mechanics. Wiley and Sons Inc., New York.

BEARING CAPACITY OF CYCLICALLY LOADED PILES

Bengt B Broms
Swedish Geotechnical Institute, Stockholm, Sweden

SYNOPSIS

The bearing capacity of driven precast concrete and timber piles has been investigated at four different test sites in Sweden (Uppsala I, Uppsala II, Björktorp and Gullbergsmotet). The piles were driven into a deep layer of normally consolidated clay and subjected to cyclic loads at successively higher load levels. The test was terminated at the load level when the deflection increment from each load cycles started to increase. This load level is defined herein as the critical load. It is considered that a pile can resist an indefinite number of load cycles without failure if the intensity of the cyclic loading is less than the critical load. The measured critical loads have been compared with calculated values.

INTRODUCTION

Piles which support such structures as bridges, oil tanks and water towers are often subjected to high variable loads (live loads). The live loads are for bridges often of the same magnitude as the dead load, while the live loads for buildings are generally small. Often the question comes up about the effects of cyclic loading on the ultimate bearing capacity of a pile and how one can determine a critical load level below which cyclic loads will not cause failure.

Results from cyclic load tests on piles which have been driven into normally consolidated clays are described in this article. The load tests at Uppsala I, Uppsala II and Björktorp, Sweden were carried out during the years 1950 - 1965 as a part of the regular consulting activities at the Swedish Geotechnical Institute. The piles at Gullbergsmotet were tested in 1962 - 1963 by the Geotechnical Department of the Sweden State Railways.

ULTIMATE BEARING CAPACITY OF PILES IN CLAY

The soil around a driven pile is disturbed during the driving. Measurements have shown that the undrained shear strength of cohesive soils is decreased appreciably immediately after the driving due to remolding to a distance of approximately one diameter from the pile surface. However, the shear strength of the soil and the pile bearing capacity increase with time. The increase of the bearing capacity which takes place later than one month after the driving is as a rule small for timber piles while for concrete and steel piles about three months are required to reach the final strength.

The ultimate bearing capacity of point bearing and skin friction piles are often calculated as the sum of the maximum skin friction resistance Q_{ult}^{skin} and the maximum point resistance Q_{ult}^{point} according to the equation

$$Q_{ult}^{pile} = Q_{ult}^{skin} + Q_{ult}^{point} \qquad (1)$$

It is thus assumed that the law of superposition is valid. However, only a very small axial deformation of the pile (a few tenths of an inch) is required to develop the maximum skin friction resistance while a relative large deformation (0.1 to 0.2 pile diameters) is required to develop the maximum point resistance.

At the maximum point resistance, the skin friction resistance may be equal to or considerably less than the maximum (peak) skin friction resistance as shown in Figs. 1a and 1b, respectively. The pile shown in Fig. 1a will have a "ductile" behaviour and its ultimate bearing capacity can be calculated from Eq(1). The pile which corresponds to Fig. 1b exhibits a "brittle" behaviour and the ultimate bearing capacity will be less than that indicated by Eg. (1). The difference can be large especially if the piles are subjected to cyclic loading.

The maximum skin friction resistance Q_{ult}^{skin} of piles which have been driven into a cohesive soil is except for very short piles considerably larger than the maximum point resistance Q_{ult}^{point}. The skin friction resistance is generally assumed to be approximately proportional to the contact area A_{skin} of the pile with the surrounding soil. It should be pointed out that the elastic compression of the pile may affect the mobilization of the skin friction resistance. The skin friction resistance is generally calculated from the expression

$$Q_{ult}^{skin} = c_a \cdot A_{skin} \qquad (2)$$

where c_a is the average unit skin friction resistance (adhesion) along the pile.

Test result reported by Bjerrum (1953), Fellenius

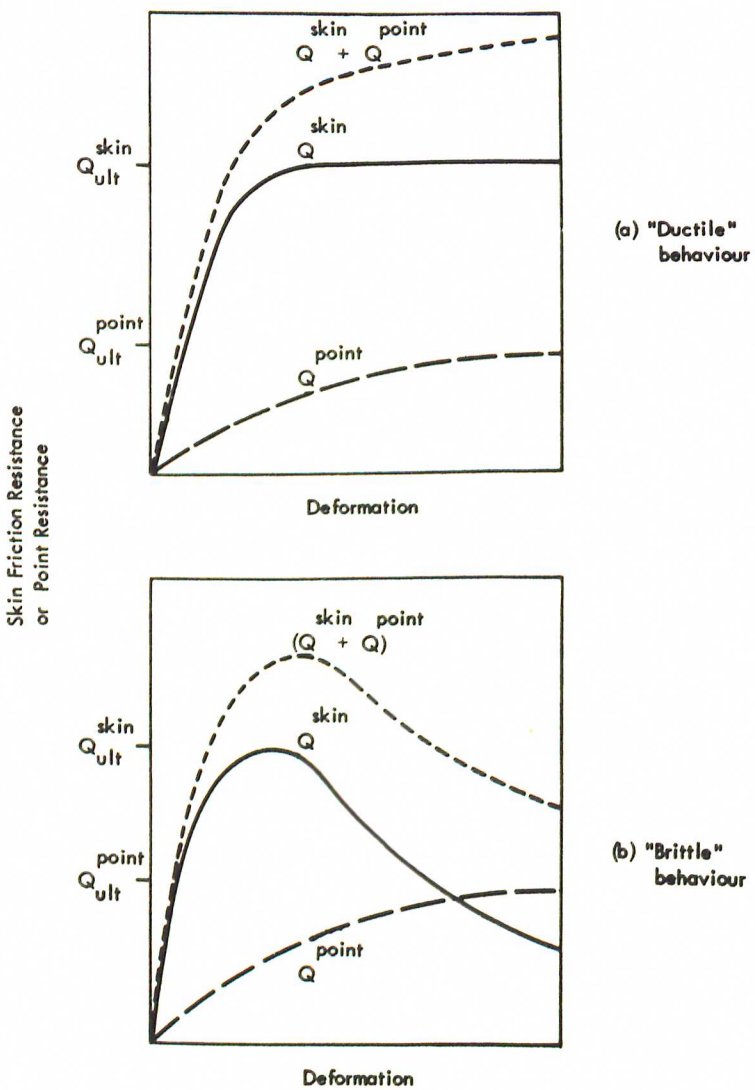

FIG. 1. Ductile and Brittle Behaviour.

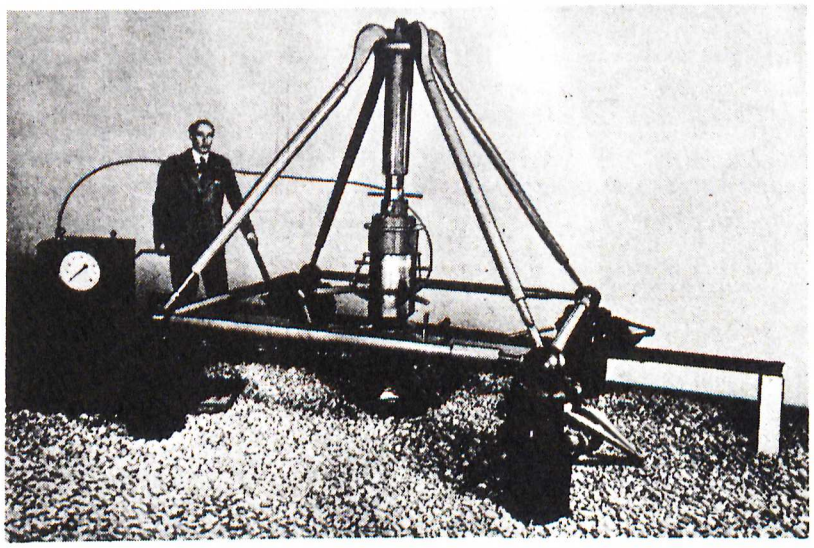

FIG. 2. Loading Arrangement.

(1955), Seed & Reese (1957), Tomlinson (1957), Bergfelt (1957), Peck (1959, 1961), Mohan & Jain (1961) and by Woodward, Lundgren & Boitano (1961) and others indicate that the adhesion c_a when a pile is loaded the first time is approximately equal to the undrained shear strength c_u [1] of the soil when c_u is less than about 1 000 lb/ft^2. When c_u is larger than this value, the adhesion can frequently be considerably smaller than the undrained shear strength of the soil. The adhesion for wood and concrete piles is often larger than that of steel piles. No information is available about the skin friction resistance of piles which are loaded cyclically.

The following safe values of the unit skin friction resistance are frequently used in Sweden to calculate the ultimate bearing capacity of piles which have been driven into cohesive soils.

Table 1. Evaluation of adhesion c_a for piles driven into cohesive soils.

(a) $c_u < 1\,000$ lb/ft^2	Adhesion c_a
Steel piles	0.5 c_u
Concrete piles	0.8 c_u
Wood piles	1.0 c_u

(b) $c_u > 1\,000$ lb/ft^2	Adhesion c_a
Steel piles	200 lb/ft^2
Concrete piles	600 lb/ft^2
Wood piles	1 000 lb/ft^2

The maximum point resistance Q_{ult}^{point} is assumed to be dependent of the unrained shear strength of the soil. This resistance can be calculated when the pile point is located at a depth below the ground surface which exceeds four pile diameters from the following equation (Meyerhof, 1951; Skempton, 1951):

$$Q_{ult}^{point} = 9\, c_u \cdot A_{point} \qquad (3)$$

where A_{point} is the area of the pile point. In general the point resistance corresponds to approximately 10-20 % of the total pile bearing capacity. Thus, the point resistance as a rule will not have a larger influence on the total bearing capacity of a pile in clay.

TEST ARRANGEMENT

The test arrangement shown in Fig. 2 which was used for the cyclic load tests at Uppsala I, Uppsala II and Björktorp consists of a light weight truss, a hydraulic jack with 80 tons capacity and various recording instruments. Three to five timber piles were used as reaction piles to resist the uplift forces which developed

1) Experience in Sweden indicates that the undrained shear strength of a clay is often overestimated by the standard test methods (e.g. fall-cone tests, vane tests or unconfined compression test) when the liquid limit or the fineness number exceeds 80. (The liquid limit is approximately equal to the fineness number, Karlsson, 1961.)

The undrained shear strength for a clay is generally reduced in Sweden as follows.

Fineness number (approx. equal to the liquid limit)	Reduction coefficient
80 - 100	0.9
100 - 120	0.8
120 - 150	0.7
150 - 180	0.6
> 180	0.5

during the load tests.

The deflection of the test pile was measured by dial indicators with respect to a reference beam which was supported on two short wooden piles. The piles were driven about 10 ft from the test pile. This distance is generally sufficient to prevent the test pile from influencing the test results.

The light weight truss can generally be assembled within two to three hours by a crew consisting of one experienced foreman and two crew members. Each part of the truss system can be handled conveniently without lifting devices.

A conventional loading frame was used for the load tests at Gullbergsmotet. The reaction force was in this case resisted by six tension piles.

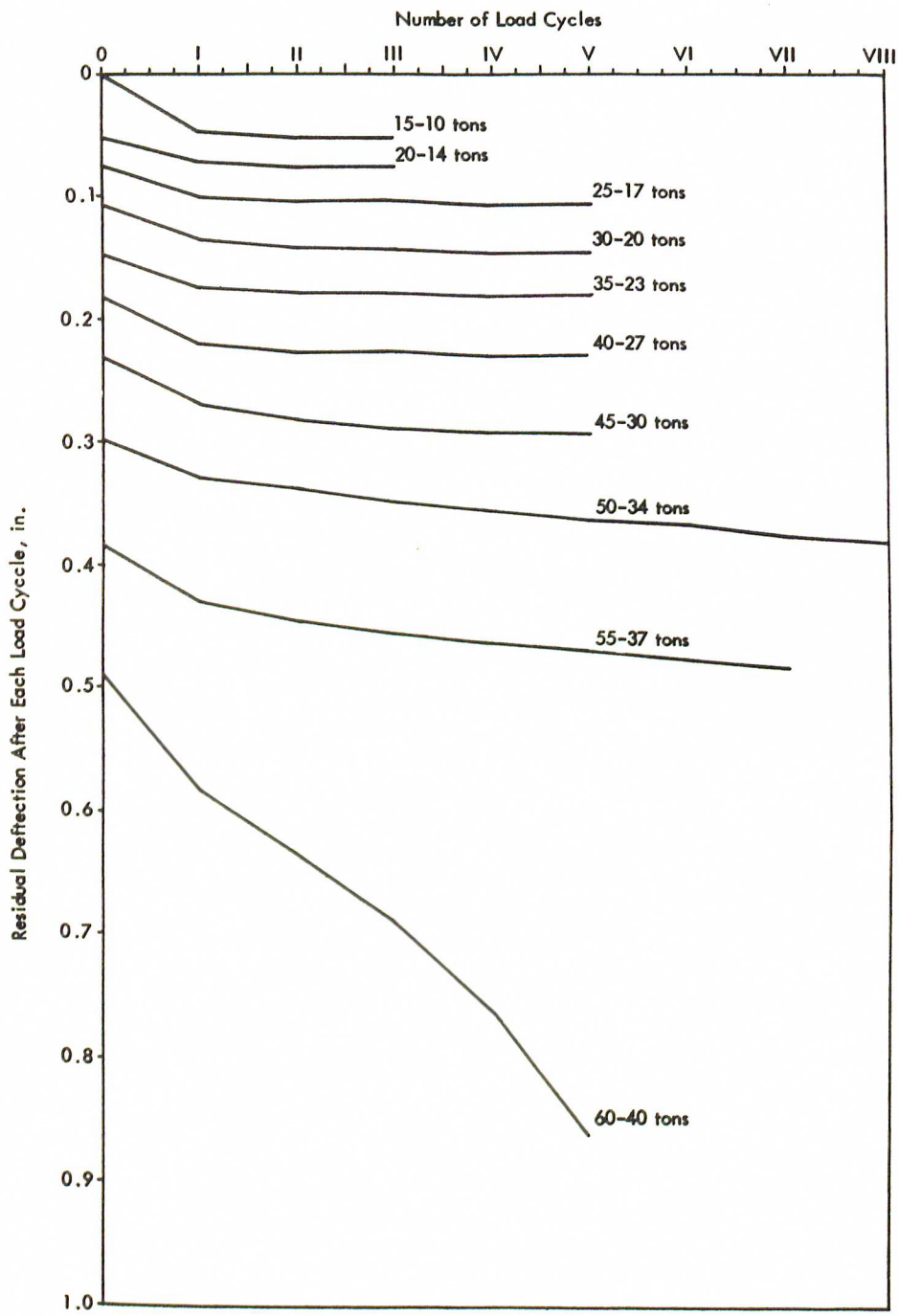

FIG. 3. Relationship between Residual Deflection, Applied Load and Number of Load Cycles.

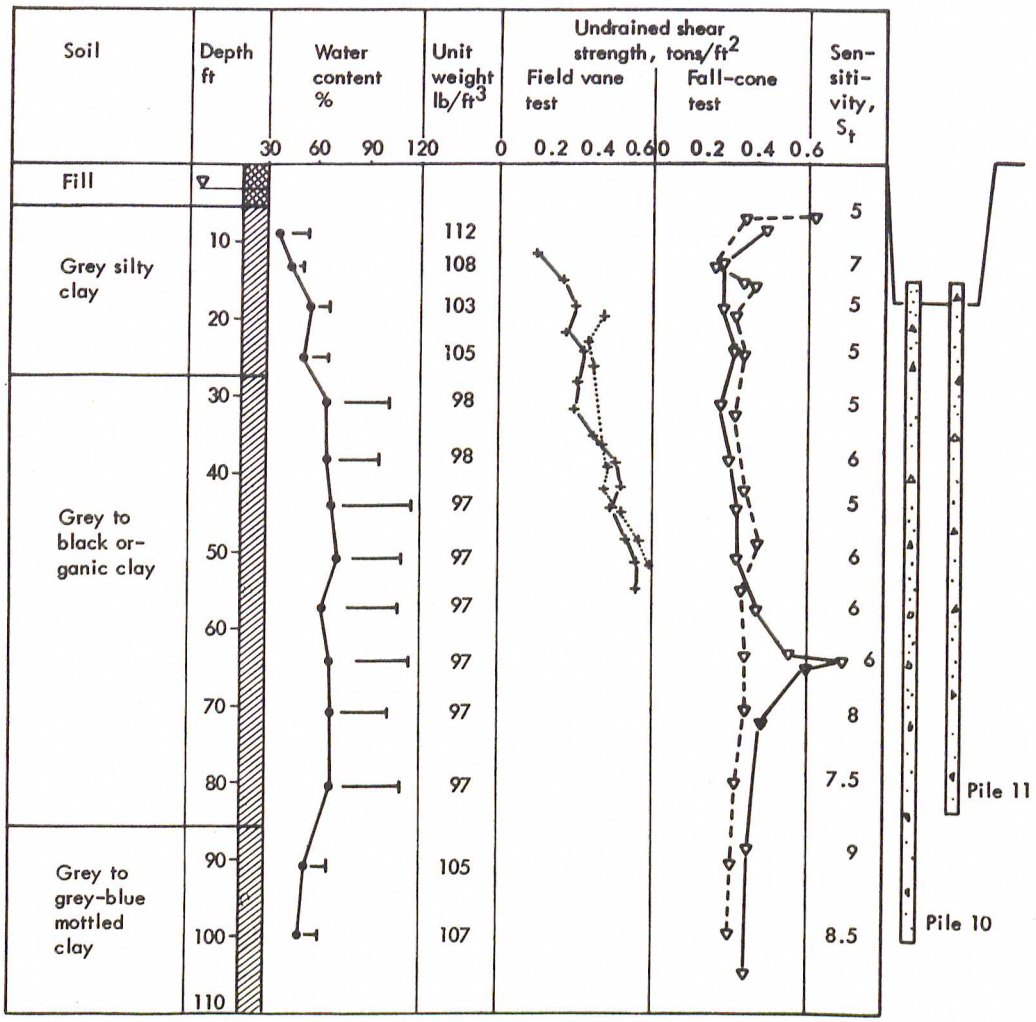

FIG. 4. Soil Conditions at Uppsala 1.

LOADING PROCEDURE

The purpuse of the load tests was to determine the critical load level below which cyclic loads will not cause failure. The critical load was determined by measuring the increase of the pile deflection after each load cycle. At loads, less than the critical load, the increase of the pile deflection during each load cycle decreases or becomes constant. The increase of the pile deflection is generally small after a large number of load cycles. The number of load cycles required to reach a steady state increases as a rule with increasing applied load.

Approximately 5 to 10 load cycles are required at low load levels, while up to 100 load cycles may be required when the critical load is approached. The maximum applied load during each load cycle is normally 25, 50, 70, 80, 85, 90, 95 and 100 per cent of the estimated critical load while the minimum load for each load cycle is dependent of the type of structure to be supported as discussed previously. If, for example, the critical load has been estimated as 60 tons, the test pile is first loaded to 15 tons (25 per cent of the estimated critical load). This load is maintained for three to five minutes whereafter the load is decreased to, for example, 10 tons. (The time interval between each cycle was kept constant during the whole test.) After an additional three to five minutes, the pile load was increased to 15 tons. This procedure is repeated until the deflection increase for each load cycle is small or becomes constant. The load is then increased to 30 tons (50 per cent of the estimated critical load). The pile is subjected to the number of load cycles until the deflection increase becomes small after each load cycle. The procedure is repeated at successively higher load levels until the critical load is reached.

The relationship between pile deflection, load and number of load cycles which was obtained from a typ-

ical load test on a timber pile driven into a normally consolidated clay is shown in Fig. 3. It can be seen that the deflection of the pile did not increase after three load cycles when the applied load was 15 or 20 tons. No increase was observed after five load cycles at a load of 25, 30, 35, 40 or 45 tons. At 50 and 55 tons the increase was constant after three cycles. When the maximum load reached 60 tons, the increase of the pile deflection gradually increased after two load cycles. The critical load has in this case been estimated as 60 tons.

LOAD TEST AT UPPSALA I

Two square reinforced concrete piles (Piles Nos. 10 and 11) with 10 x 10 in. cross-section were tested at Uppsala I. The test site was located within the town of Uppsala and the test results were used for the design of the eastern abutment of a bridge (Järnbron) over the river Fyrisån.

Soil conditions. The soil at the test site consists of fill (silty sand and bricks) to a depth of 6 ft below the ground surface as shown in Fig. 4. The fill is underlain by a deep layer of clay which extends to a least 130 ft below the ground surface.

The clay is silty to a depth of about 28 ft. The fineness number of the clay is about 70. (The fineness number is approximately equal to the liquid limit of soil.) Below this depth the clay is organic with a fineness number of 110. The fineness number decreased, however, to about 70 at a depth of 85 ft below the ground surface. Also the organic content was low at this level.

The undrained shear strength was measured by field vane and by the Swedish fall-cone test (Hansbo, 1957). It can be seen from Fig. 4 that the vane shear strength increased with increasing depth. The measured average shear strength of the silty clay was 0.328 tons/ft^2. The shear strength of the organic clay located between 28 and 85 ft below the ground surface was 0.488 tons/ft^2. The shear strength measured by the Swedish fall-cone test was approximately constant. The average shear strength was 0.342 tons/ft^2, 0.403 tons/ft^2 and 0.383 tons/ft^2 for the silty clay, the organic clay and the mottled clay, respectively.

The sensivity of the soil as measured by the Swedish fall-cone test varied between 5 and 9. Approximately the same sensivity was obtained with the vane test. This means that the soil is classified as a clay with normal sensivity according to the classification system used in Sweden.

Load test. The fill and the upper part of the silty clay were excavated before the driving of the two test piles as shown to the right in Fig. 4 to a depth of 10 ft above the organic clay layer. The piles were driven about 3 1/2 months before the load tests. The embedded pile length was 82.0 ft for Pile 10 and 65.1 ft for Pile 11. The light steel truss described previously was used during the load tests. The piles were loaded in cycles at successively higher load levels and the minimum load during each cycle was half the maximum applied load. Up to 35 cycles were used at each load level and the total time for each load cycle was about 5 minutes.

The measured residual axial deformation after each load cycle is shown in Fig. 5. The critical loads of Piles 10 and 11 were 149.6 kips and 132.0 kips, respectively. It can be seen that the deflection after each load cycle increased at the critical load after about 20 cycles for Pile 10 and after about 10 cycles for Pile 11.

Analysis of Test Results. The ultimate bearing capacity of the test piles has been calculated assuming that the adhesion along the piles is 80 % of the undrained shear strength of the clay as shown in Table 1.

When the fineness number of the soil exceeds 80, the shear strength is generally reduced as mentioned above. The reduction factor which corresponds to a fineness number of 110 is 0.8. The average shear strength as measured by field vane tests 0.328 tons/ft^2 (1.0 x 0.328) for the silty clay and 0.391 tons/ft^2 (0.8 x 0.488) for the organic clay. These shear strengths correspond to a calculated ultimate bearing capacity of 171.4 kips for Pile 10 and of 133.2 kips for Pile 11 as shown in Table 2.

The reduced average shear strength as determined by the Swedish fall-cone test is 0.342 tons/ft^2 (1.0 x 0.342) for the silty clay, 0.323 tons/ft^2 (0.8 x 0.403) for the organic clay and 0.383 tons/ft^2 (1.0 x 0.383) for the mottled clay. These shear strength values correspond to a calculated ultimate bearing capacity of 155.6 kips for Pile 10 and 116.6 kips for Pile 11.

With respect to the field vane test the values of the ratio Q_{crit}/Q_{calc} are 0.87 and 0.99 for Piles 10 and 11, respectively. With respect to the Swedish fall-cone test the corresponding values for Piles 10 and 11 are 0.96 and 1.13, respectively. It can be seen that the critical strength is approximately equal to the calculated ultimate strength.

LOAD TEST AT UPPSALA II

Four timber piles (Piles I, II, V and 2) were tested at Uppsala II. The test site is located at Kallbadhusbron at the river Fyrisån in Uppsala. The piles were driven

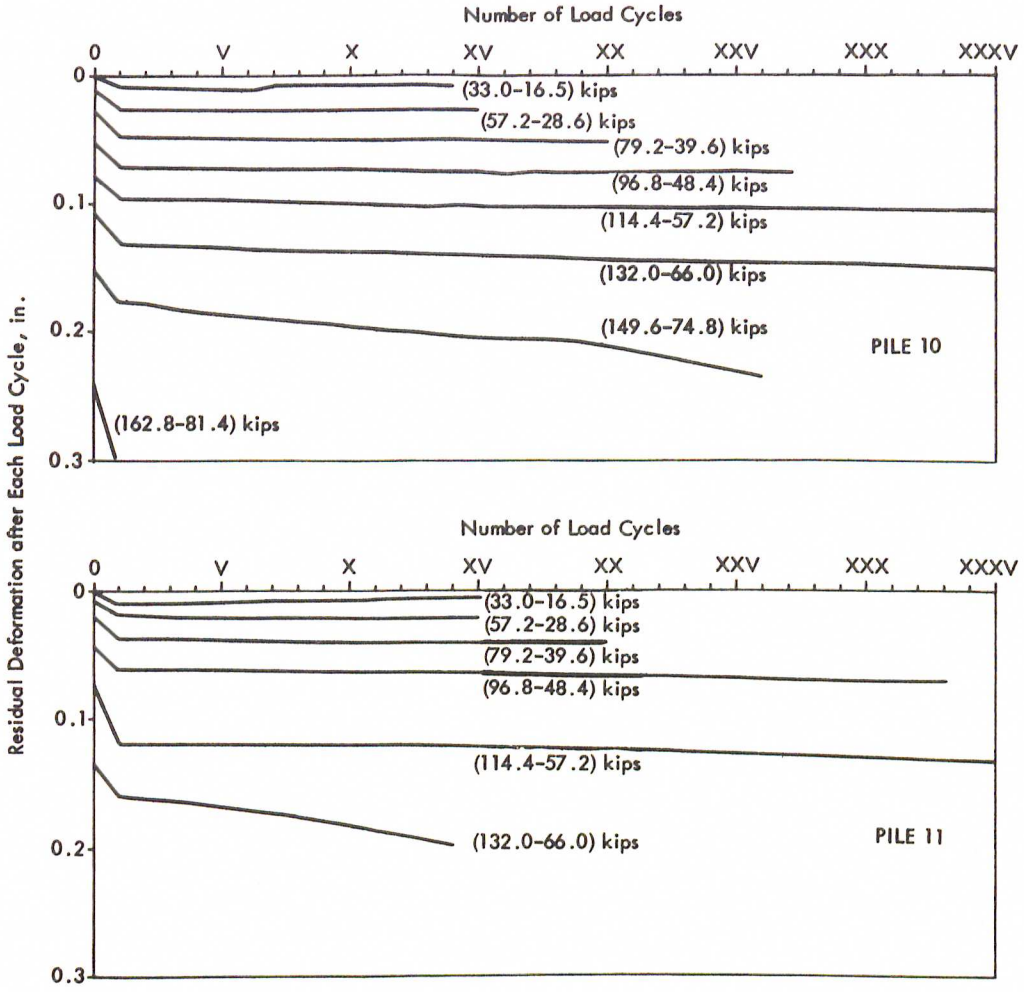

FIG. 5. Test Results from Piles 10 and 11.

Table 2. Summary of Test Results, Uppsala I.

Pile No.	Pile length L, ft	Calculated ultimate capacity, Q_{ult}, kips		Critical bearing capacity Q_{crit}, kips	Ratio Q_{crit}/Q_{ult}	
		Field vane test	Fall-cone test		Field vane test	Fall-cone test
10	82.0	171.4	155.6	149.6	0.87	0.96
11	65.1	133.2	116.6	132.0	0.99	1.13

into a deep layer of soft to very soft clay.

Soil Conditions. The soil consists, as shown in Fig. 6, of a grey silty clay to a depth of about 13 ft below the ground surface. Between 13 ft and 35 ft a layer of dark-grey organic clay was found. Below is a deep layer of grey mottled clay. Ram sounding tests indicated that this layer extended beyond the tip of the test piles.

The undrained shear strength was measured by the unconfined compression test and the Swedish fall-cone test. The measured shear strengths were approximately constant except at the interface between the organic clay layer and the underlaying mottled clay. The average undrained shear strength as determined by the unconfined compression test and by the Swedish fall-cone test was 0.164 tons/ft^2 and 0.221 tons/ft^2, res-

pectively.

Load Tests. Piles I and II were driven on the eastern bank of the river Fyrisån, Pile V in the middle of the river and Pile 2 at the western bank.

Piles I, II, V and 2 were tested 23, 22, 25 and 33 days, respectively, after the driving. Thus, Piles I, II and V have probably not reached their final strengths at the time of the load tests. It is estimated that the final strengths of these piles are 20 per cent higher than the measured values.

The truss system described previously was used for the load tests. Four vertical timber piles were used as reaction piles. The test piles were loaded cyclically and the minimum applied load during each load cycle was half the maximum applied load. The time for each load was about six minutes. Piles II and V were loaded to failure.

The deformation measured after each load cycle is shown in Fig. 7. The critical strengths of Pile I, V and 2 were 44.0, 39.6 and 61.6 kips, respectively. It can be seen that the deformation of Pile II increased with increasing rate when the pile was loaded statically by 44.0 kips. This load has been taken as the critical strength of this pile.

Analysis of Test results. The critical strengths of Piles I, II and IV have been increased by 20 % because these piles have, as mentioned above, probably not reached the final strength at the time of the load test.

The ultimate strength of the piles shown in Table 3 has been calculated from Table 1 assuming that the adhesion is equal to the undrained shear strength of the soil.

It can be seen in Table 3 that the measured critical strength exceeded the calculated values when the shear strength of the caly was evaluated by the unconfined compression test. The agreement was satisfactory when the shear strength of the clay was determined by the Swedish fall-cone test.

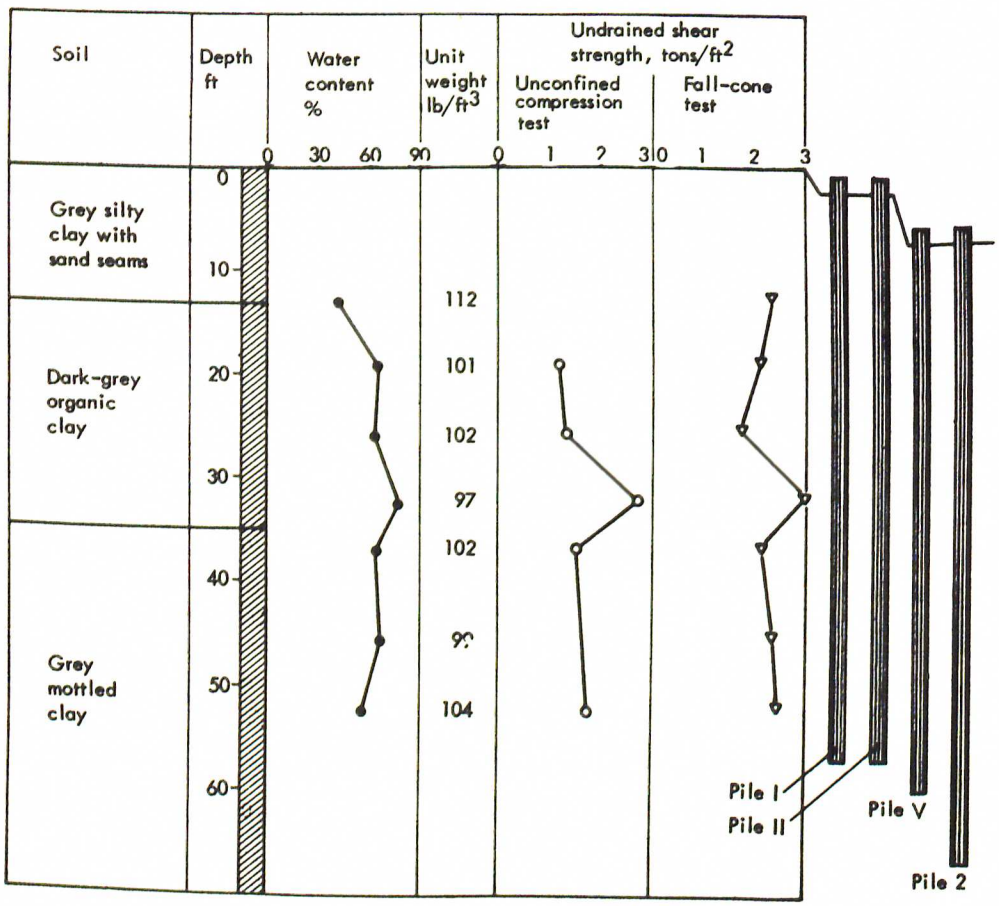

FIG. 6. Soil Conditions at Uppsala II.

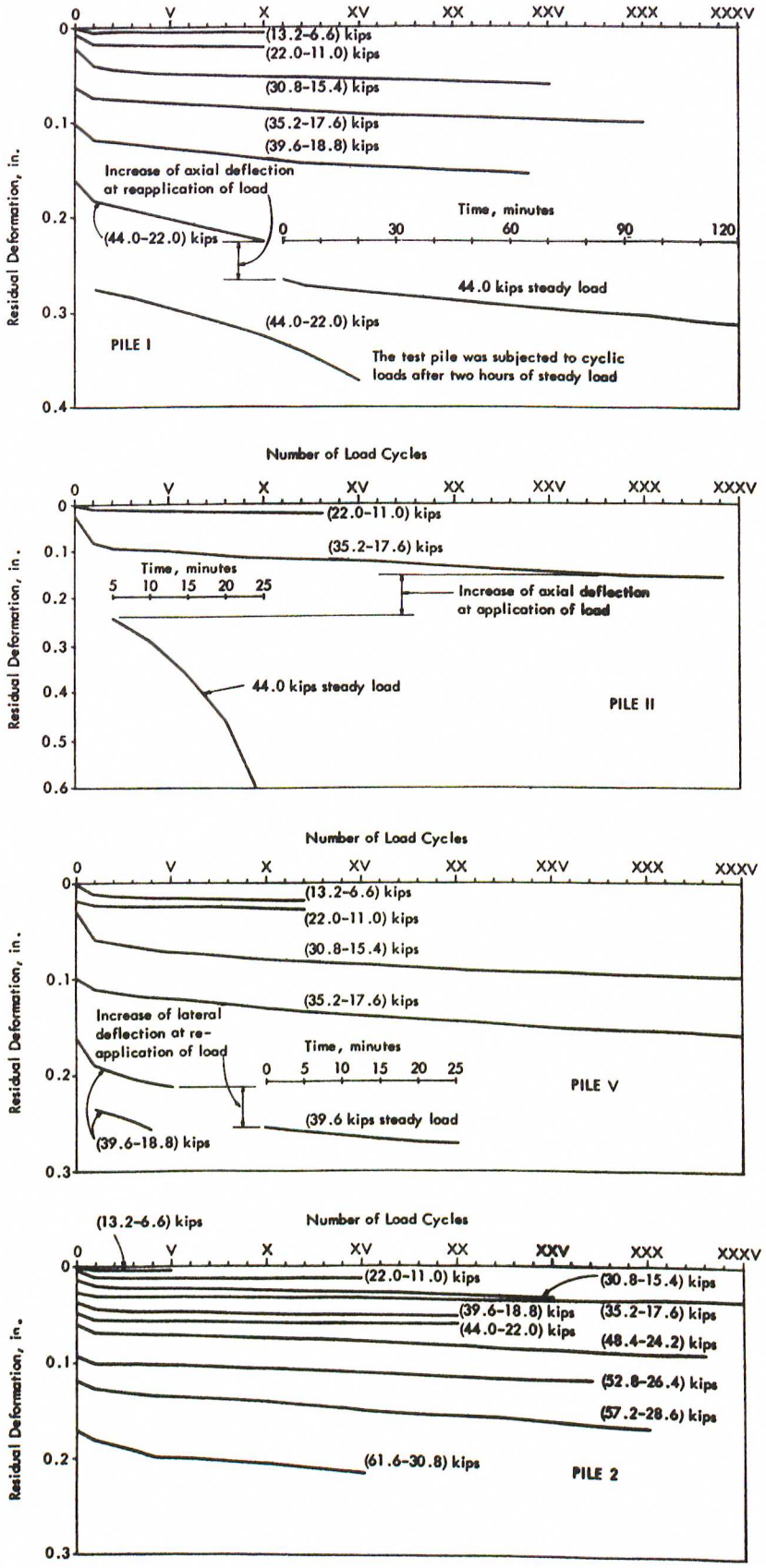

FIG. 7. Load Test on Piles I, II, V and 2. (Uppsala II)

Table 3. Summary of Test Results, Uppsala II.

Pile No.	Pile length L, ft	Diameter, in.		Average undrained shear strength, tons/ft^2		Calculated ultimate capacity, Q_{calc}, kips		Critical strength Q_{crit}, kips	Ratio Q_{crit}/Q_{calc}	
		Top	Bottom	Unconf. compr. test	Fall-cone test	Unconf. compr. test	Fall-cone test		Unconf. compr. test	Fall-cone test
I	54.3	13.8	4.9	0.164	0.221	43.8	59.2	52.8 [1)]	1.20	0.89
II	54.3	12.6	4.9	0.164	0.221	40.6	54.7	52.8 [1)]	1.30	0.97
V	52.3	14.6	4.9	0.164	0.221	44.2	59.5	47.5 [1)]	1.07	0.80
2	57.8	13.8	4.9	0.164	0.221	46.7	63.0	61.6	1.32	0.98

1) The values have been increased by 20 %, because the load tests were carried out 22 to 25 days after driving.

LOAD TEST AT BJÖRKTORP

Five square reinforced concrete piles (Piles 2, 3, 4, 5 and 6) with a cross-section of 10 x 10 in. were tested at Björktorp. The test site was located close to the railroad station at Björktorp in the southwestern part of Sweden. The results from the load tests were used in the design of the abutments for a highway bridge over the river Viskan. The piles were driven by a drop hammer through a shallow surface layer of sand into a deep layer of normally consolidated clay.

Soil conditions. Piles 2 and 3 were driven at the northwestern bank of the river Viskan to a depth of 59.5 and 47.5 ft, respectively. The soil conditions (Boreholes 2 and 4) are shown in Fig. 8. The soil consists to a depth at 11 ft below the ground surface of brown sand with low to medium relative density as indicated by the Swedish weight and the Swedish ram sounding methods. Below this depth there is a deep layer of grey varved

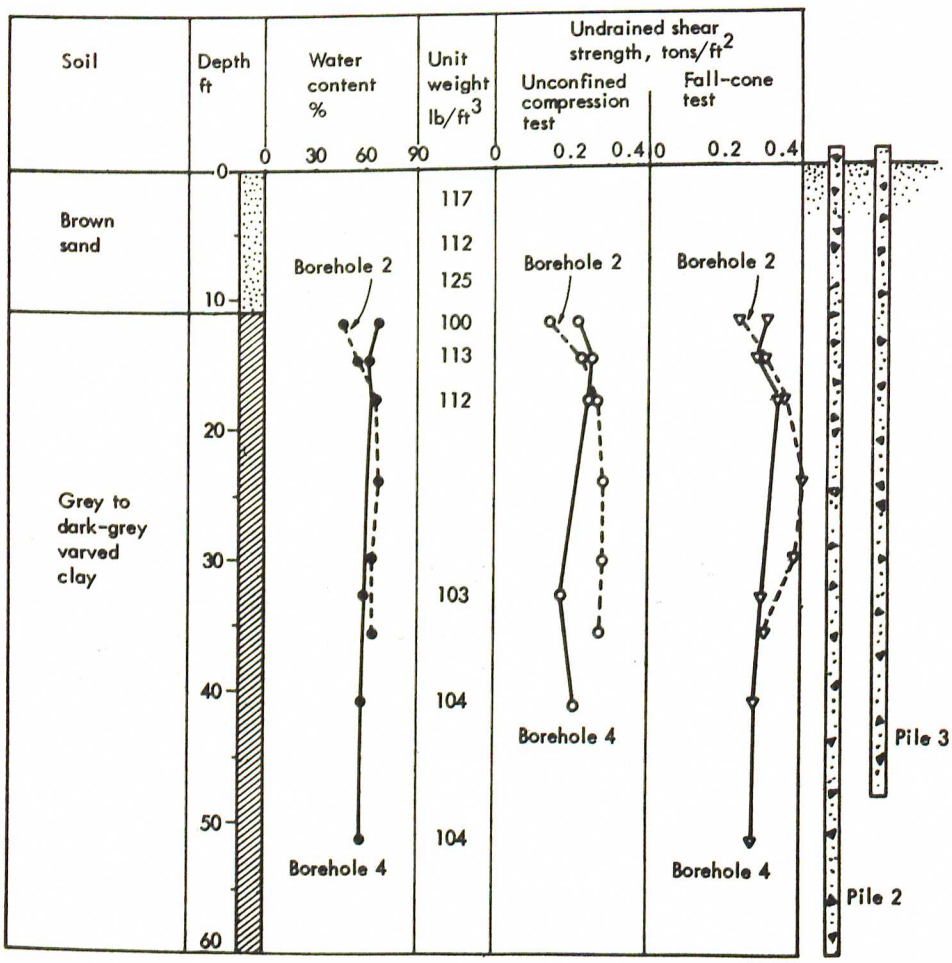

FIG. 8. Soil Conditions at Test Site of Piles 2 and 3.

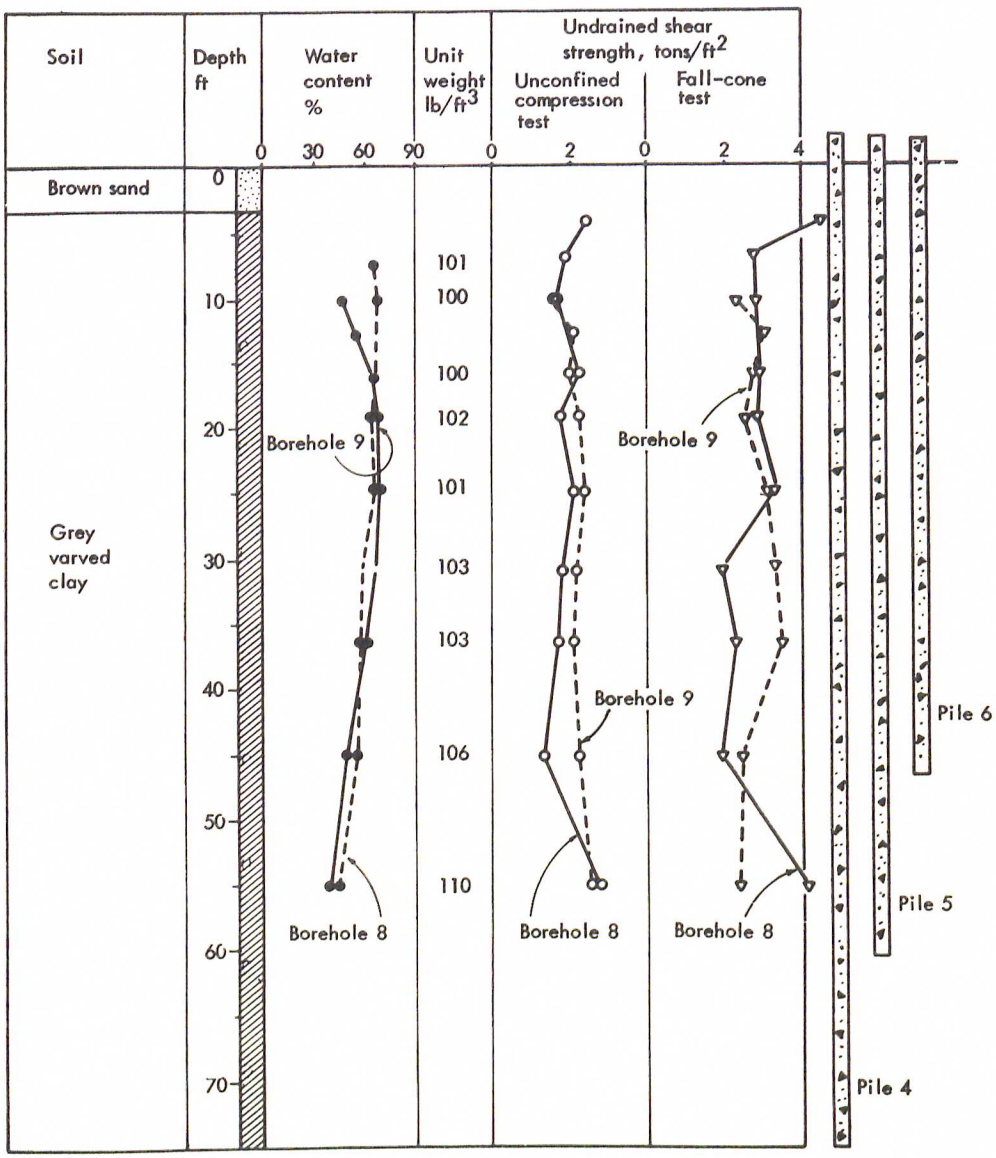

FIG. 9. Soil Conditions at Test Site of Piles 4, 5 and 6.

clay which extends below the tip of Pile 2. The undrained shear strength was measured by the unconfined compression and Swedish fall-cone tests. The average shear strength was 0.235 tons/ft^2 as determined by the unconfined compression test ($q_u/2$) and 0.305 tons/ft^2 by the Swedish fall-cone test. Thus, the shear strength as measured by the fall-cone test was 30 % larger than the unconfined compression test values.

Piles 4, 5 and 6 were driven at the southeastern bank of the river to a depth of 74.8, 59.2 and 47.0 ft, respectively, below the ground surface. The soil conditions are shown in Fig. 9. The soil consists of a loose to medium dense sand to a depth of 3 ft below the ground surface. The sand is underlain by a deep layer of soft grey varved clay to a depth of at least 75 ft below the surface. The shear strength of the varved clay was approximately constant. The average undrained shear strength as determined by undrained compression tests was 0.203 tons/ft^2. The corresponding average shear strength as determined by the Swedish fall-cone test was 0.286 tons/ft^2. The average shear strength from the fall-cone tests was thus about 40 % higher than the unconfined compression values.

Load Tests. The loading frame described previously was used with four vertical timber piles as reaction piles. The test piles were loaded cyclically 2 to 2 1/2 months after the driving. The minimum load during each load cycle was half the maximum applied load and the time for each load cycle was six minutes. The residual axial deformation after each load cycle has been plotted in Figs. 10 and 11 as a function of the number of load cycles. The critical load could be reached for

all the piles except for Pile 4. When this pile had been subjected to two load cycles as 140.8 tons, one of the connections with the reaction piles slipped. The critical loads for Piles 2, 3, 5 and 6 were 114.6, 88.0, 101.2 and 88.0 kips, respectively. It can be seen from Fig. 10 that the axial deflection of Pile 2 suddenly increased when the applied load reached 48.4 kips. The reason for this behaviour was probably separation of the test pile at one of the pile joints.

Analysis of Test Results. The ultimate bearing capacity of the test piles has been calculated assuming that the unit skin-friction resistance within the sand layer is $0.4\ \bar{p}_v$, where $\bar{p}_v$ is the effective overburden pressure. (The coefficient of lateral earth pressure and the friction angle of the pile surface has been assumed equal to 1.0 and 22 degrees, respectively.)

It has been assumed furthermore that the adhesion with-

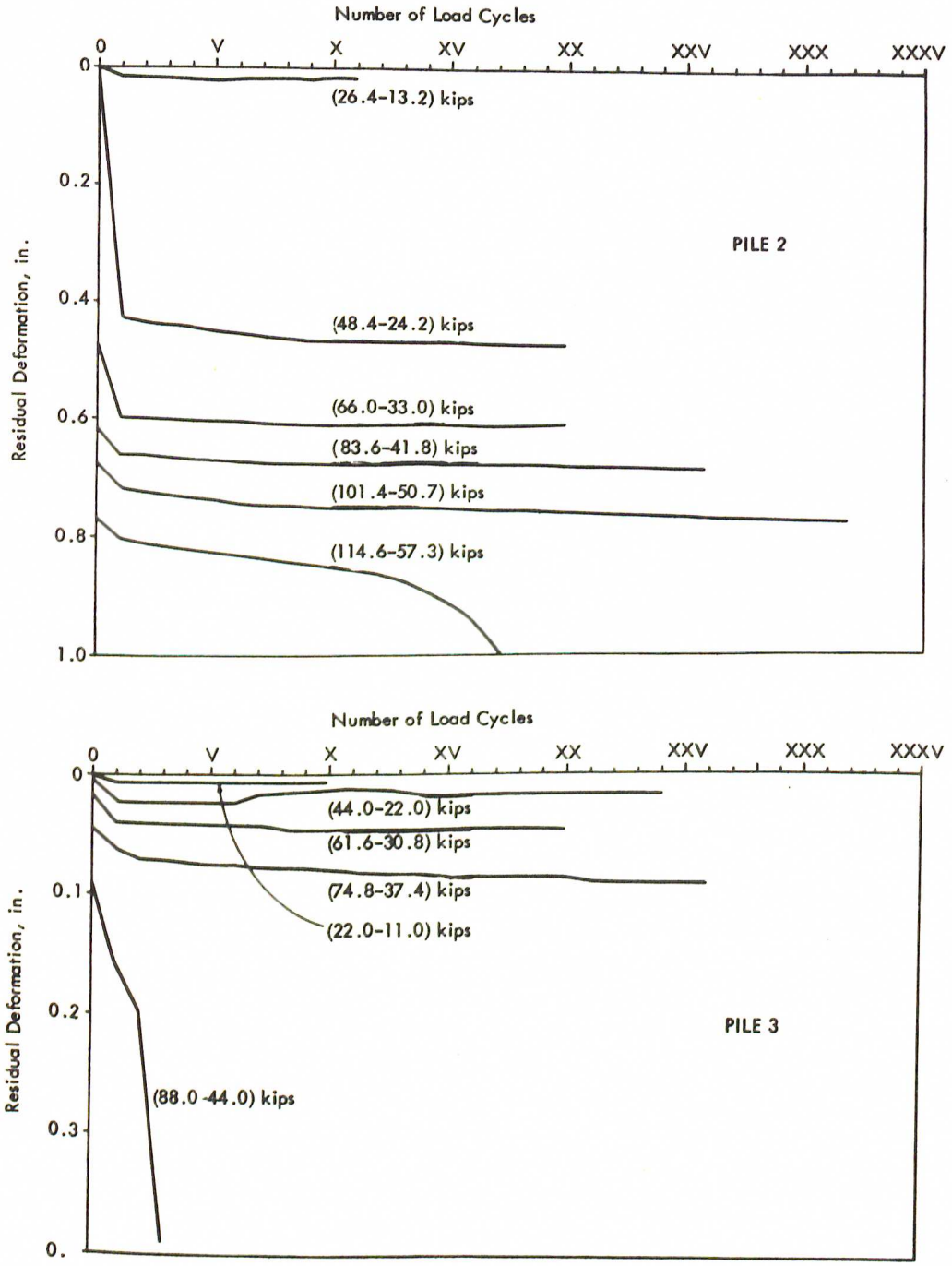

FIG. 10. Load Tests on Piles 2 and 3.

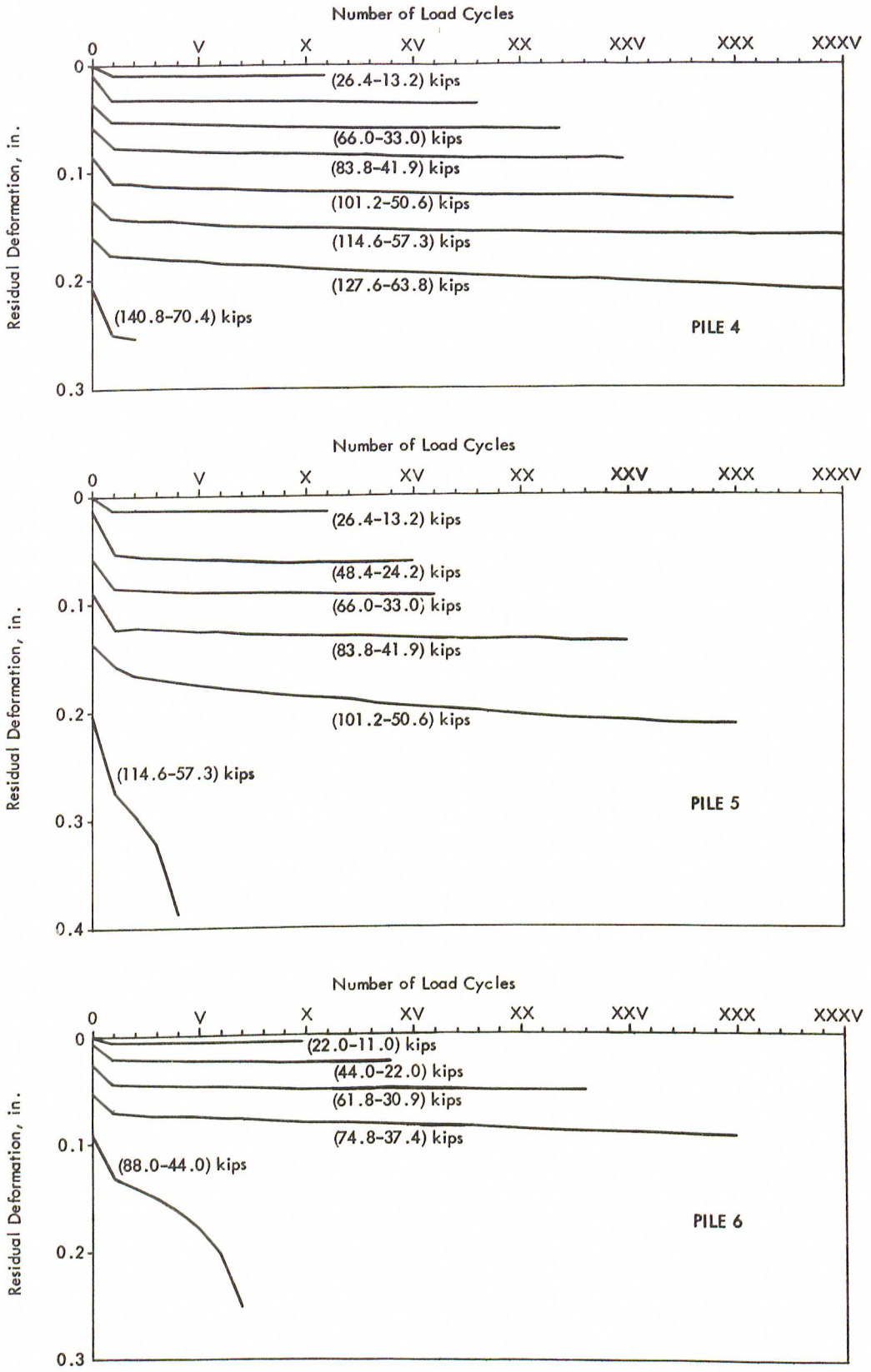

FIG. 11. Load Tests on Piles 4, 5 and 6.

Table 4. Summary of Test Results, Björktorp.

Pile No	Pile length L, ft	Average undrained shear strength, c_u, tons/ft^2		Calculated ultimate capacity, Q_{calc}, kips		Critical strength, Q_{crit}, kips	Ratio Q_{crit}/Q_{calc}	
		Unconf. compr. test	Fall-cone test	Unconf. compr. test	Fall-cone test		Unconf. compr. test	Fall-cone test
2	59.4	0.235	0.305	72.5	92.1	114.6	1.56	1.24
3	47.5	0.235	0.305	59.2	72.5	88.0	1.48	1.21
4	74.8	0.203	0.286	80.8	113.7	140.8	1.74	1.24
5	59.2	0.203	0.286	63.8	89.9	114.6	1.79	1.27
6	47.0	0.203	0.286	50.5	71.5	88.0	1.74	1.23

in the clay layer corresponds to 80 % of the average undrained shear strength as measured by the unconfined compression test or by the Swedish fall-cone test according to Table 1 and that the unit point resistance at failure is nine times the average shear strength of the soil.

The test results are summarized in Table 4.

It can be seen that bearing capacity as calculated from the Swedish fall-cone test is somewhat smaller than the measured critical loads while the ultimate capacity as calculated from unconfined compression tests was much smaller than the measured values.

LOAD TEST AT GULLBERGSMOTET

Two composite piles (Piles 4 and 5) were tested to failure at Gullbergsmotet in Gothenburg. Each pile consisted of one timber pile section and three precast hexagonal reinforced concrete pile sections. The tip diameter of the 65.7 ft long timber section of both piles was 5.4 in. The diameter at the joint with the concrete section was 12.5 in. and 11.9 for Piles 4 and 5, respectively. The circumference of the three hexagonal concrete elements with a total length of 91.8 ft was 37.4 in.

Soil conditions. The soil as shown in Fig. 12 consisted of approximately 2 ft of topsoil, 7 ft of sandy, silty clay, 21 ft of organic clay, 35 ft of uniform clay, 20 ft of clay with silt seams and at least 105 ft of uniform clay.

The water content of the clay layer located at a depth of 30 to 65 ft below the ground surface was approximately 80 %, while the clay layer at a depth of 85 to 180 ft had a water content of 70 %.

The fineness number of the shallow clay layer exceeded the natural water content, while the deep clay layer had a fineness number which was less than the natural water content of the soil. The undrained shear strength as measured by the Swedish fall-cone test increased with depth. It was approximately 0.18 tons/ft^2 at the ground surface and 0.68 tons/ft^2 at a depth of 179 ft below the ground surface. The clay had a normal sensivity according the Swedish classification system.

Pile Tests. The two test piles were driven with a drop hammer. Each pile was loaded cyclically two and six months after the driving. The two test piles were in addition loaded statically to failure after each cyclic load test.

Pile 4 was subjected to 10 to 60 load cycles at successively higher load levels (88, 110, 132, 143, 154 and 165 kips during the first cyclic load test and 88, 110, 132, 154 and 176 kips during the second cyclic load test). The minimum load during each load cycle was 33 kips. The time required for each load cycle was approximately 30 minutes.

During the two static load tests (carried out after each cyclic load test) load was applied in increments of 11 kips every five minutes until failure was reached. The ultimate loads for Pile 4 were 220 and 231 kips two and six months, respectively, after driving. The corresponding ultimate loads for Pile 5 were 231 and 264 kips, respectively.

After the second static load test (six months after driving) the two test piles were loaded at a constant deformation rate. The deformation rates were 0.02 in./min for Pile 4 and 0.01 in./min for Pile 5. The pile resistance reached a maximum at an axial deflection of about 0.6 in. whereafter the resistance decreased to about 90 % of its maximum capacity when the deflection was 3.0 in. The maximum resistance was 215 kips for Pile 4 and 251 kips for Pile 5. Thus, the ultimate bearing capacity had been decreased from 231

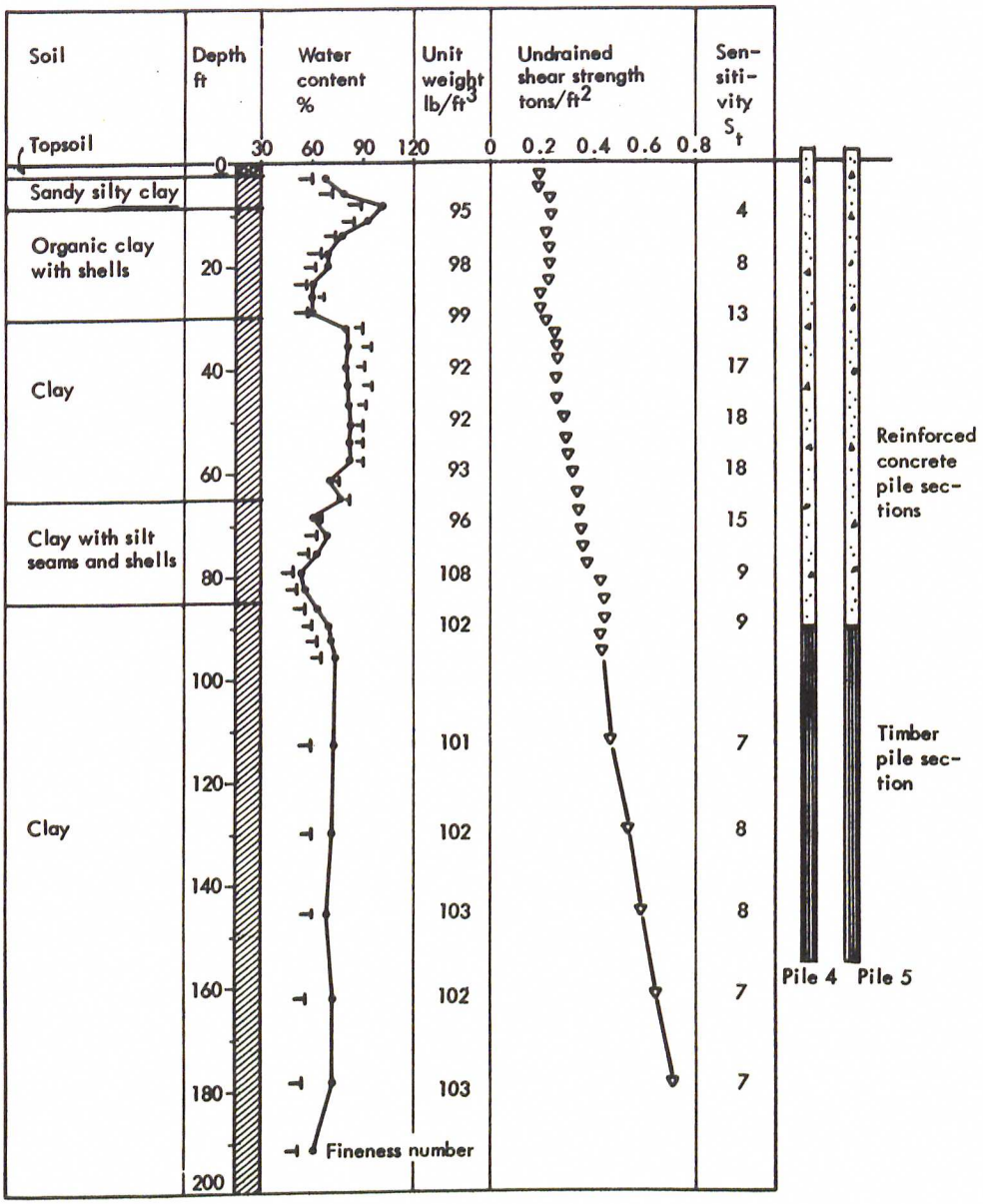

FIG. 12. Soil Conditions at Gullbergsmotet.

to 215 kips for Pile 4 and from 264 to 251 kips for Pile 5 when the piles were reloaded.

Analysis of Test Results. The calculated bearing capasity of Piles 4 and 5 is 255 and 246 kips, respectively, if it is assumed that the adhesion for the concrete sections is equal to 80 % of the undrained shear strength of the soil as measured by the Swedish fall-cone test. These calculated values are approximately equal to the measured ultimate capacities of 231 and 268 kips, respectively, for the two piles as can be seen from Table 5.

The test results indicate that cyclic loads do not appreciably affect the ultimate bearing capacity of piles which have been driven into a layer of normally consolidated clay.

SUMMARY

Test results from Uppsala I, Uppsala II and Björktorp indicate that the critical load of a cyclically loaded pile which has been driven into a normally consolidated clay is approcimately equal to the calculated static ultimate bearing capacity when the shear strength of the soil has been evaluated by the Swedish fall-cone test. If the undrained shear strength is determined by unconfined compression tests the critical load is underestimated. It has been assumed in the calculation that the average skin friction resistance is equal to the values shown in Table 1 and that the point resistance is

Table 5. Summary of Test Results, Gullberget

Pile No.	Pile length L, ft	Measured ultimate strength Q_{ult}, kips	Calculated ultimate strength Q_{calc}, kips	Ratio Q_{ult}/Q_{calc}
4	157.5	231	255	0.91
5	157.5	264	244	1.08

nine times the undrained shear strength of the soil.

The load tests carried out at Gullbergsmotet indicated that cyclic loading with a maximum intensity of approximately 75 % of the ultimate bearing capacity does not appreciably affect the static bearing capacity of a pile.

REFERENCES

BERGFELT, A., 1957. The axial and lateral load bearing capacity and failure by buckling of piles in soft clay. Proc. 4. Int. Conf. Soil Mech. a. Found. Engng. Vol. 2, pp. 8-13.

BJERRUM, L., 1953. Les pieux de fondation en Norvège. Ann. Inst. Techn. Bat. et Trav. Publ. 6:63:64, pp. 375-376, Sols et Fond. Nr. 13.

FELLENIUS, B., 1955. Resultat från pålprovningar vid Göteborg C. Kungl. Järnvägsstyrelsen, Geotekn. Avd. Medd. Nr. 5, Stockholm, 22 p. + 31 Pl.

HANSBO, S., 1957. A new approach to the determination of the shear strength of clay by the fall-cone test. Proc. R. Swed. Geotechn. Inst., No. 14, Stockholm, 46 pp.

KARLSSON, R., 1961. Suggested improvements in the liquid limit test with reference to flow properties of remoulded clays. Proc. 5. Int. Conf. Soil Mech. a. Found. Engng., Vol. 1, pp. 171-184.

MOHAN, D. & JAIN, G. S. 1961. Bearing capacity of bored piles in expansive soils. Proc. 5. Int. Conf. Soil. Mech. a. Found. Engng. Vol. 2, pp. 117-121.

PECK, R. B., 1959. A study of the comparative behavior of friction piles. Highw. Res. Board Spec. Rep. 36, 72 pp.

PECK, R.B., 1961. Records of load tests on friction piles. Highw. Res. Board Spec. Rep. 67, 412 pp.

SEED, H.B. & REESE, L.C. 1955. The action of soft clay along friction piles. Trans. Amer. Soc. Civ. Engrs., Vol. 122, pp. 731-764.

TOMLINSON, M.J. 1957. The adhesion of piles driven in clay soils. Proc. 4. Int. Conf. Soil. Mech. a. Found. Engng, Vol. 2, pp. 66-71.

WOODWARD, R.J., LUNDGREN, R. & BOITANO, J.D., 1961. Pile loading tests in stiff clays. Proc. 5. Int. Conf. Soil. Mech. a. Found. Engng., Vol. 2, pp. 177-184.

Bearing Capacity of End — Bearing Piles Driven to Rock

Portance de pieux résistant par la pointe battus dans la roche

Die Tragfähigkeit von in Gestein gerammten Spitzenbelastungspfählen

SVEN-ERIK REHNMAN, Civil Engineer, Swedish Geotechnical Institute, Banérgatan 16, S 115 26 Stockholm, Sweden.
BENGT B. BROMS, Director, Swedish Geotechnical Institute, Sweden.

Summary

Because of the very high loads which are often transferred through the pile point to the underlaying rock, an investigation was initiated at the Swedish Geotehnical Institute in order to evaluate some of the factors affecting the point bearing capacity of rock. The effects of repetitive loads, distance from existing open and closed cracks and the size of the loaded area were investigated. Test results indicate that the bearing capacity decreases rapidly with increasing number of load cycles. The fatigue strength after about 6,000 cycles is only 30 to 40% of the ultimate "static" strength. The open and closed vertical cracks affected the point bearing capacity appreciably. The ultimate strength is 25% of the point bearing capacity of the uncracked rock when the load is applied at an open vertical crack. The bearing capacity decreased with increasing size of the loaded area. The ultimate strength is reduced by 20% when the dowel diameter increases from 20 mm (0.79 in) to 60 mm (2.36 in).

Résumé

En raison des efforts très élevés qui sont souvent transmis par la pointe du pieu à la roche sous-jacente, une recherche fut effectuée à l'Institut National Suédois de Géotechnique afin d'étudier quelques uns des facteurs agissant sur la portance ponctuelle de la roche. Les effets d'efforts répétés, la distance entre l'effort appliqée et les fissures ouvertes et fermées existantes ainsi que la surface soumise aux efforts ont été décrits dans ce document. Les résultats des tests indiquent que la portance diminue rapidement avec l'augmentation du nombre de cycles d'efforts. La résistance à la fatique après environ 6000 cycles est seulment de 30—40% de la résistance "statique" finale. Les fissure verticales, ouvertes et fermées, ont une influence marquée sur la portance ponctuelle. La résistance finale est de 25% de la portance ponctuelle de la roche non fissurée quand les efforts sont appliqués sur une fissure verticale ouverte. La portance diminue quand la surface soumise aux efforts augmente. La résistance finale est réduite de 20% quand le diamètre de goujon est porté de 20 mm à 60 mm.

Zusammenfassung

Da oft sehr hohe Belastungen durch die Pfahlspitze auf das darunterliegende Gestein übertragen werden, wurde am Schwedischen Institut für Geotechnik eine Untersuchung vorgenommen, um einige der Faktoren zu untersuchen, die die Punkttragfähigkeit von Gestein beeinflussen. Die Wirkung wiederholter Belastungen, des Abstandes zwischen Belastungspunkt und etwaigen offenen und geschlossenen Rissen und der Grösse der belasteten Fläche sind in dieser Abhandlung beschrieben. Die Untersuchungsergebnisse zeigten, dass die Tragfähigkeit mit zunehmender Anzahl von Belastungswechseln (Belastungszyklen) rasch abnimmt. Nach ca. 6.000 Belastungswechseln betrug die Ermattungsfestigkeit nur 30 bis 40% der äussersten „statischen" Festigkeit. Die offenen und geschlossenen vertikalen Risse haben einen bedeutenden Einfluss auf die Punkttragfähigkeit. Die äusserste Festigkeit betrug 25% der Punkttragfähigkeit von nicht klüftigen Gestein, als die Belastung bei einer offenen vertikalen Kluft ausgeführt wurde. Die Tragfähigkeit nahm bei zunehmender Grösse der Belastungsfläche ab. Die äusserste Festigkeit reduzierte sich um 20%, als der Durchmesser des Dübels von 20 mm auf 60 mm vergrössert wurde.

Introduction

Over 75% of all the piles which were driven in Sweden during the year 1966 were precast concrete piles. These piles are generally provided with a point of high strength steel when they are driven to rock or through soils containing large stones or boulders as shown in Fig. 1. The diameter of the steel points (dowels) is generally 60 mm (2.36 in). Loads up to 60 Mp (132 kips) are often allowed on such piles. Even higher loads are permitted under favourable conditions. When the applied load is transferred to the underlying rock through the rock point, the contact stress below the steel point often exceeds 2,100 kp/cm^2 (30,000 psi). This is often the case when the piles have been driven into granite through a layer of very soft clay. A contact stress of 2,100 kp/cm^2 is of the same order of magnitude as the unconfined compressive strength of many rock materials in Sweden.

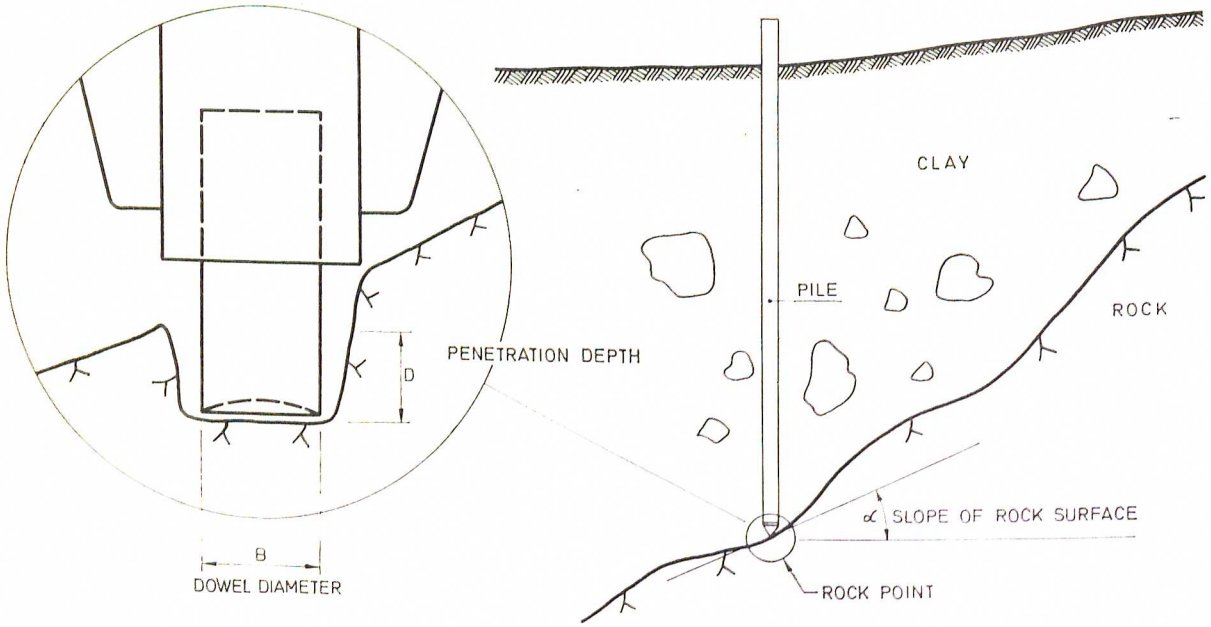

Fig. 1 — End bearing pile driven to rock. The pile point is provided with a steel dowel.

Fig. 1 — Pieu résistant par la pointe battu dans la roche. La pointe du pieu est pourvue d'un goujon an acier.

Bild 1 — In Gestein gerammter Spitzenbelastungspfahl. Die Pfahlspitze ist mit einem Stahlstift versehen.

Because of the very high loads which are often transferred through the pile point, an investigation was initiated at the Swedish Geotechnical Institute of the factors affecting the pointb earing capacity of piles which have been driven to rock. In this paper is described a part of a labaratory investigation of the point bearing capacity of granite. The effects of repetitive loads, distance of applied load from existing open and closed cracks and the size of the loaded area are reported herein. The total test program included approximately 90 load tests.

Testing Method

The load tests were carried out on rock cubes (13 x 13 x 10 cm or 20 x 20 x 10 cm) which were cast in concrete in a heavy steel pipe (cf. Fig. 4). The steel pipe prevented the rock samples from cracking during the load tests. A few tests were for comparison carried out directly on uncased rock cubes.

Load was applied perpendicular to the free rock surface by a steel dowel (pile point) through a hydraulic jack. Most of the load tests were carried out with 20 mm (0.79 in.) dowels. The applied load was read on a calibrated manometer and the penetration by two dial indicators which were rigidly attached to the dowel.

Rock Material

The load tests were made on granite which had been mined at Rixö located in the southwestern part of Sweden. The Rixö granite is massive and extremely uniform. The average size of the mineral grains (quartz, feldspar, mica, biotite and clorite) varies between 0.5 and 2 mm.

The compressive strength of the rock was evaluated from cylindrical samples with 50 mm (2 in.) diameter and 50 mm height. The average unconfined compressive strength was 2300 kp/cm² (32.700 psi). The spread of the individual test values was very small (less than 2%).

The shear strength τ_f was determined from cylindrical specimen with 50 mm (2 in.) legth at different normal pressures σ_f with the double direct shear apparatus illustrated in Fig. 2. The sample diameter was 15 mm (0.59 in). The test results are shown in Fig. 3. It can be seen that the measured (τ_f — σ_f) relationship is curved.

The tensile strength was evaluated by the Brazilian indirect tension test on samples with 40 mm (1.67 in) diameter and 40 mm length. The average tensile strength was 148 kp/cm² (2,100 psi).

Repetitive Load Tests

The fatigue strength of the rock was investigated in test series *A*. These load tests were carrird out on 20 x 20 x 10 cm granite cubes cast in concrete

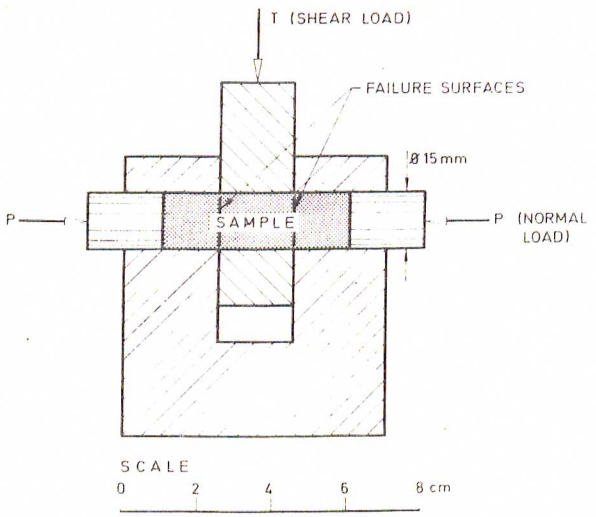

Fig. 2 — Double shear apparatus for rock (N. Lundborg 1965)

Fig. 2 — Appareil à double Cisaillement pour roche (N. Lundborg 1965).

Bild 2 — Zweifacher Schubapparat für Felsen (N. Lundborg 1965).

Fig. 4). The bottom surface of the 20 mm diameter dowel used in the experiments was plane. The applied pulsating load varied between 6 Mp (13.2 kips) and an upper value. The load frequency was between 5 to 25 cycles / min and the penetration was registered by a recorder.

The penetration of the dowel increased with increasing number of load cycles as shown in Fig. 5. In this test the applied load varied between 6 Mp and 18 Mp (40 kips). 18 Mp was about 40% of the failure load at first loadin«g (cfstatiailure› load).

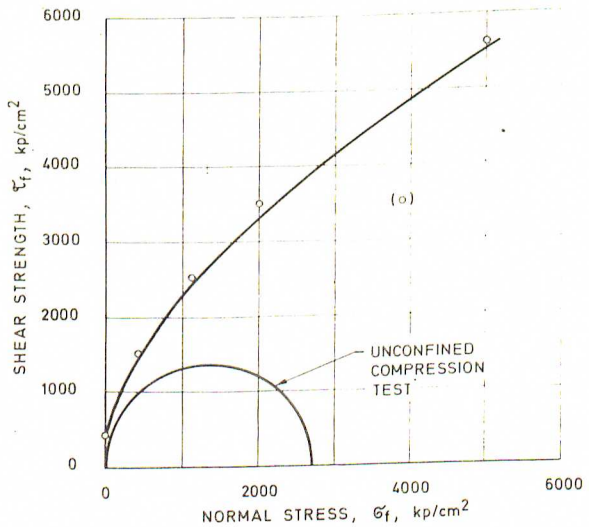

Fig. 3 — Shear strength of Rixö granite.

Fig. 3 — Résistance au cisaillement du granite Rixö.

Bild 3 — Schubfestigkeit des Rixö Granits.

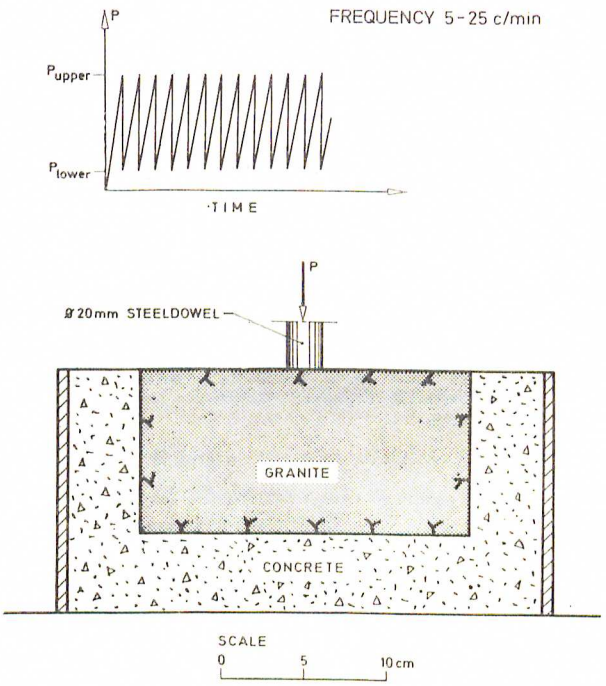

Fig. 4 — Cyclic load tests.

Fig. 4 — Essai cyclique de charge.

Bild 4 — Zyklischer Belastungsversuch.

It can also be seen in this figure that the penetration initially was small and that it increased relatively rapidly after 2,750 repetitions due to local failure under the dowel. The penetration increased rapidly during the following 1,000 cycles. Thereafter the increase was small. The test was interrupted after 8,000 cycles when total penetration of the dowel was 8 mm (0.3 in.).

The relationship between penetration and the number of load cycles for the case when the applied load varied between 6 Mp and 30Mp (70%of the »static« failure load) is shown in Fig. 6. The loading rate was 11 cycles/minute. Failure occurred after 248 load cycles when the dowel had penetrated about 2 mm (0.1 in.) into the rock. The test was interrupted after 374 cycles when the total penetration was 12 mm (0.5 in.).

The test results indicated that the fatigue strength of granite is considerably lower than the »static« strength q_{ult}^{stat}. The ultimate strength of a rock sample which previously has not been subjected to load (»static« strength) was 44 Mp (97 kips) or 14,000 kp/cm². (200 kpsi). This ultimate strength is six times higher then the compressive strength of the rock material (2,300 kp/cm²).

The measured relative point bearing capacity q_{ult}/q_{ult}^{stat} is shown in Fig. 7 as a function of the number of load cycles. It can be seen that the ultimate strength

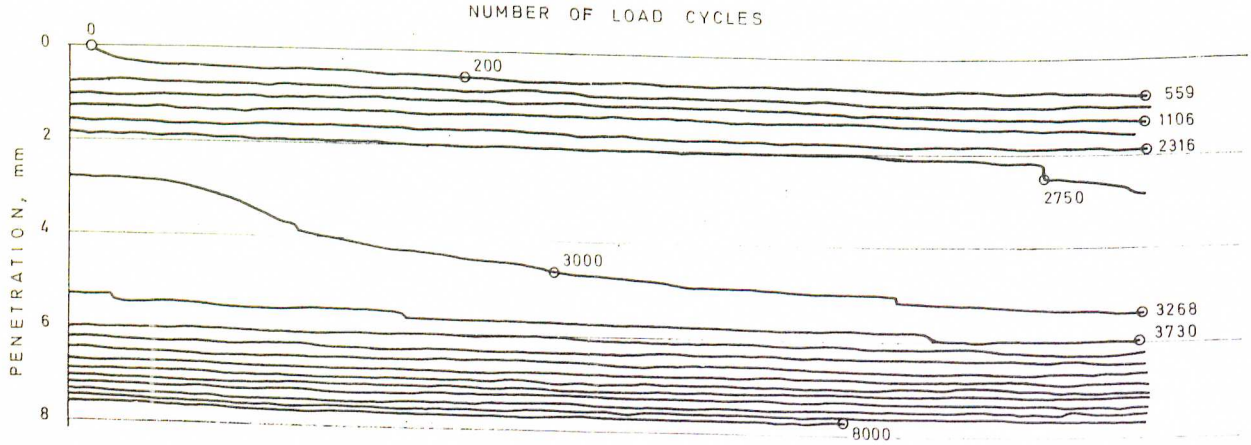

Fig. 5 — Cyclic load test on granite. Loade range: 6—18 Mp (13—40 kips) Loading rate: 22 cycles/minute.

Fig. 5 — Essai cyclique de charge sur granite. Gamme de charge: 6—18 Mp (13—40 pieux). Vélocité de chargement: 22 cycles/ minute.

Bild 5 — Zyklische Granitbelastungsversuche. Belastungsbereich: 6—18 Mp (13—40 Pfähle). Belastungsgeschwindigkeit: 22 Zyklen/Min.

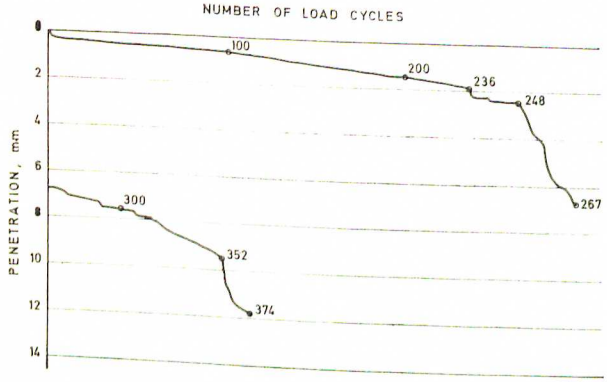

decreases by 20% after 30 load cycles and by 50% after approximately 1,000 cycles. The ultimate strength when the number of load cycles exceeded 6,000 corresponds to about 30 to 40% of the »static« strength. This »fatigue« strength is approximately twice the compressive strength of the rock material.

Fig. 6 — Cyclic load test on granite. Loade range: 6—30 Mp (13—66 kips). Loading rate: 11 cycles/minute.

Fig. 6 — Essai de chargement cyclique sur granite. Gamme de charge: 6—30 Mp (13—66 pieux). Vélocité de chargement: 11 cycles/minute.

Bild 6 — Zyklische Granitbelastungsversuche. Belastungsbereich 6—30 Mp (13 bis 66 Pfähle). Belastungsgeschwindigkeit: 11 Zyklen/Min.

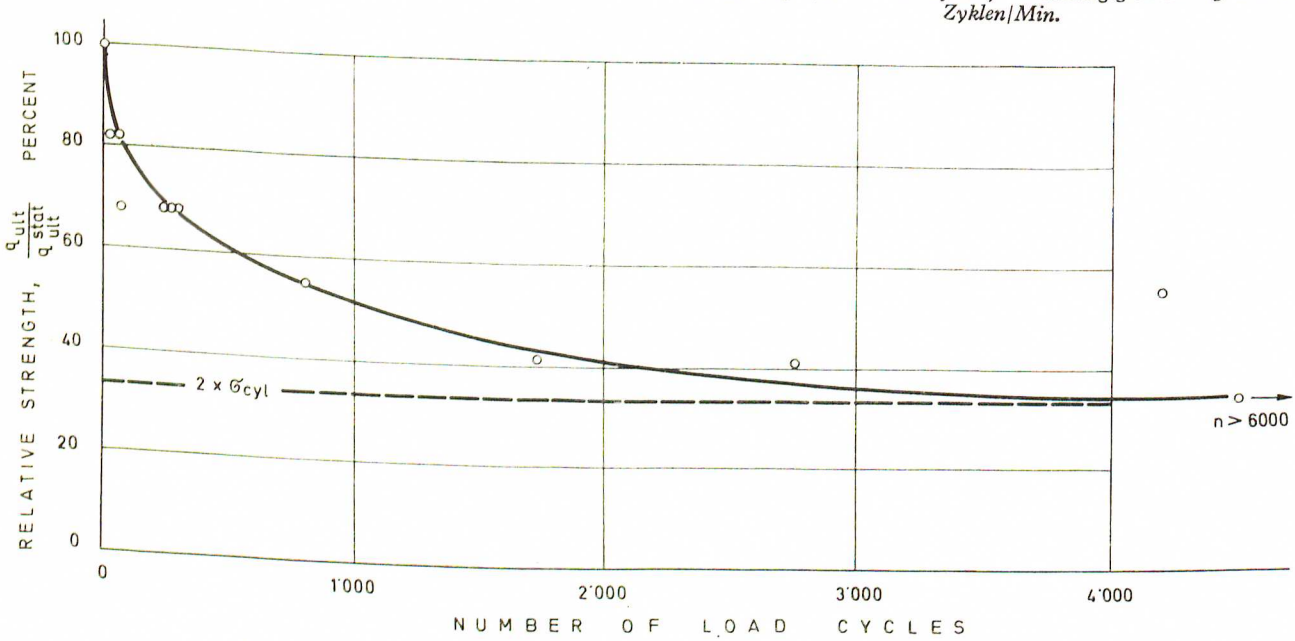

Fig. 7 — Relative point bearing capacity as a function of the number of load cycles.

Fig. 7 — Portance relative à la pointe comme fonction du nombre des cycles de chargement.

Bild 7 — Relative Tragfähigkeit an der Spitze als Funktion der Zahl der Ladunszyklen.

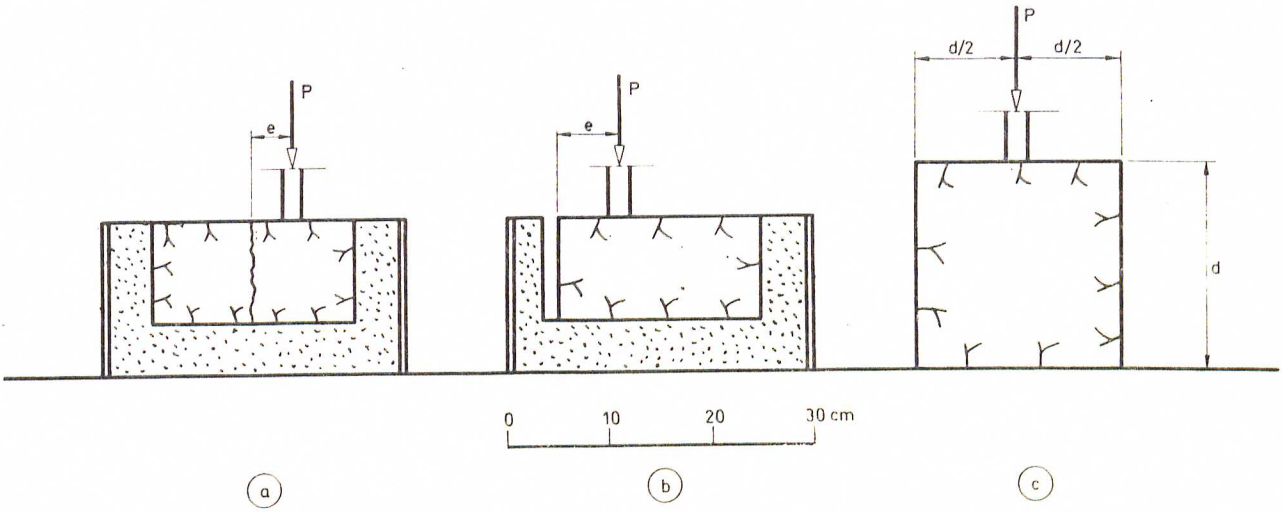

Fig. 8 — Effects of cracks on the ultimate bearing capacity of rock.

Fig. 8 — Effets de crevasses sur la portance de la roche à la rupture.

Bild 8 — Wirkung der Klüfte auf die Tragfähigkeit des Felsen beim Bruch.

Vertical and Horizontal Cracks

Cracks in the rock will affect the point bearing capacity if the cracks are unfavourably oriented with respect to the applied load. This effect was investigated in test series *B*. Rock samples with both open and closed cracks were tested (Fig. 8 a and 8 b). Load tests were also carried out on uncased rock specimen Fig. 8 c. The uncased specimen represent the case when the rock is intersected by a system of both vertical and horisontal cracks.

Closed Cracks

Load test were also carried out on 20 x 20 x 10cm 8 x 8 x 4 in granite blocks which were encased in concrete as illustrated in Fig. 8 a. Each block was split trought middle and the two halves were carefully fitted together before they were incased in concrete.

Load was applied perpendicular to the rock surface with a 20 mm steel dowel. The distance e from the crack to the applied load varied (Fig. 8 a).

In Fig. 9 is shown the ultimate relative strength of the rock as a function of the distance from the closed crack. The failure load was 30 Mp (66 kips) when the load was applied just above the crack ($e = 0$). This failure corresponds to 70% of the bearing capacity of the uncracked rock. At $e = 0.5\ B$ the bearing capacity was 80% of the ultimate strength of the uncracked rock. Extrapolation of the test results indicates that the ultimate strength is unaffected when the distance from a closed vertical crack exceeds about 1.5 times the diameter of the dowel.

Open Vertical Cracks

The influence of open vertical cracks was investigated with the test arrangement shown in Fig. 8 b. An open crack was simulated by placing cardboard along one side of the rock specimen during the ca-

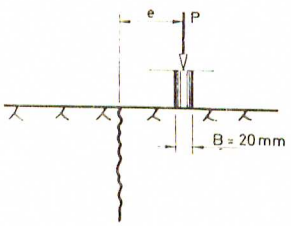

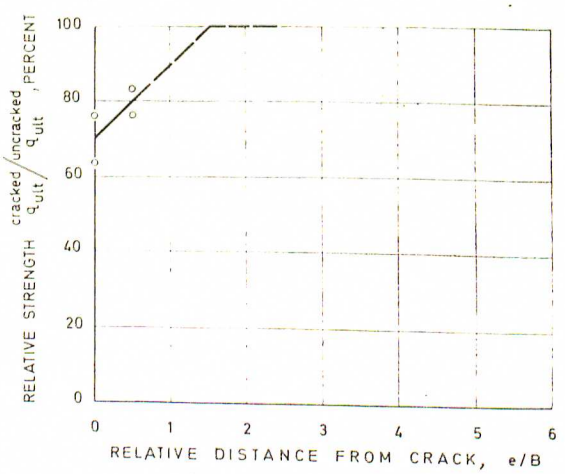

Fig. 9 — Effect of closed cracks on the ultimate bearing capacity.

Fig. 9 — Effets des crevasses closes sur la portance à la rupture.

Bild 9 — Wirkung ausgefüllter Klüfte auf die Tragfähigkeit beim Bruch.

sting. Load was applied with a 20 mm (0.79 in.) dowel. The distance of the load from the open crack was varied. The ultimate bearing capacity was low when the dowel was located at the crack (Fig. 10). The average failure load was 10 Mp (22 kips) for $e/B = 0.5$ which corresponds to 25% of the bearing capacity of the uncracked rock material. This bearing capactiy is approximately 50% larger than the unconfined compressive strength of the rock as determined on 50 mm (2.0 in) diameter samples. The failure load increased approximately linearly with increasing distance from the open cracks as shown in Fig. 10 and was equal to the ultimate strength of the uncracked rock when the distance exceeded about four dowel diameters.

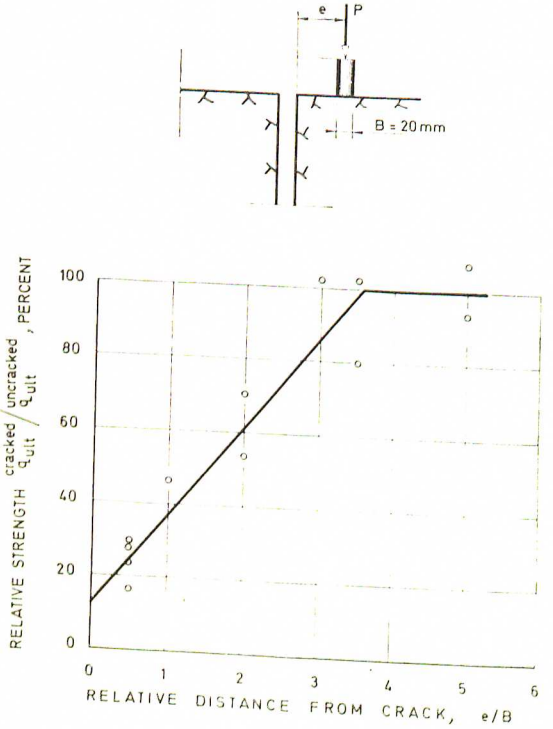

Fig. 10 — Effect of open cracks on the ultimate bearing capacity.

Fig. 10 — Effets des crevasses ouvertes sur la portance à la rupture.

Bild 10 — Wirkung offener Klüfte auf die Tragfähigkeit beim Bruch.

Open Vertical and Horizontal Cracks

A cube corresponds to a rock mass which is intersected by two sets of vertical cracks and one set of horizontal cracks when the angle between the three crack systems is 90°. The crack spacing corresponds to the side of the cube. The effects of vertical and horizontal cracks was investigated from load tests on uncased rock cubes. The testing arrangement is illustrated in Fig. 8 c. Dowels with 20 mm (0.79 in) diameter were used. Failure occurred either by splitting of the rock specimen as illustrated in Fig. 11

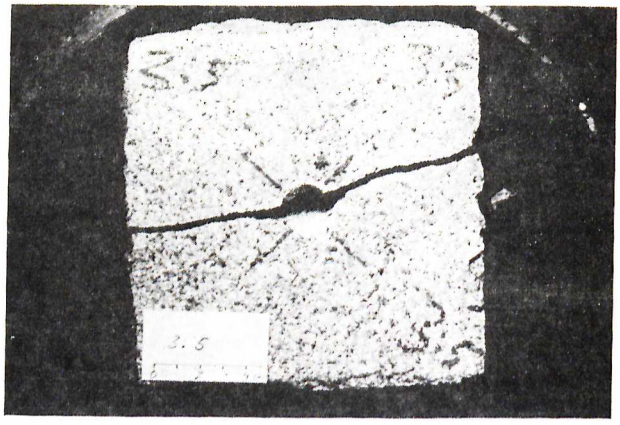

Fig. 11 — Failure in a 15 cm (6 in) cubic granite block.

Fig. 11 — Rupture dans un cube de granite de 15 cm (6").

Bild 11 — Bruch in einem 15 cm (6") Granitwürfel.

when the specimen was relatively small or by crushing of the rock below the dowel when the specimen size was relatively large.

The ultimate strength is shown in Fig. 12 as a function of the size of the test specimen. When the side exceded about 12 dowel diameters the ultimate strength corresponded to that of the uncracked rock.

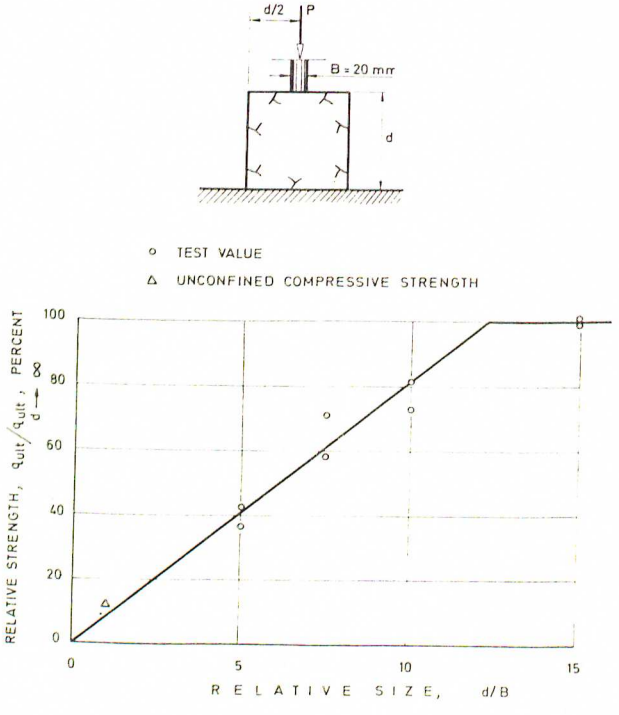

Fig. 12 — Effect of size of the granite block on the ultimate bearing capacity.

Fig. 12 — Effet de la dimension du block de granite sur la portance à la rupture.

Bild 12 — Wirkuug der Granitblockgrösse auf die Tragfähigkeit beim Bruch.

When the side was less than 12 dowel diameters the ultimate strength decreased approximately linearly with the side of the test specimen. A lower limit is reached when the side of the test specimen is equal to the diameter of the dowel. In this case the bearing capacity corresponds to the unconfined compressive strength of the rock as determined by test on samples with 20 mm (0.79 in) diameter and 20 mm height. The compressive strength is equal to 12% of the point bearing capacity of the uncracked rock.

Size of Loaded Area

The influence on the point bearing capacity of the diameter of the loaded area (dowel diameter) was investigated in two test series.

The first test series were carried out on unconfined 13 x 13 x 10 cm rock samples. The diameter of the dowel varied between 16 mm (0.64 in). and 21 mm (0.83 in.). The load was applied perpendicular to the free rock surface.

The ultimate strength decreased from 17,000 to 14,000 kp/cm² when the dowel diameter increased from 16 mm to 21 mm. The penetration at failure was about 1 mm (0.04 in.). A section of the rock sample after failure is shown in Fig. 13. The rock was crushed to a depth of about 10 mm (0.4 in) below the surface.

Rock cubes 30 x 30 x 30 cm were used in the second test series. The specimen were encased in concrete in a heavy steel pipe. The diameter of the dowels was 60 mm (2.36 in.). Four load tests were carried out in these test series. Failure occurred suddenly and the average failure load was 320 Mp

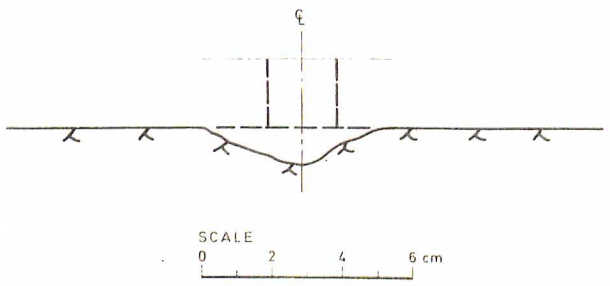

Fig. 13 — Shape of rupture surface in granite after a' oad test with 20 mm (0.79 in.) dowel.

Fig. 13 — Forme de la rupture à la surface du granite après un essai de chargement avec un goujon de 20 mm (0,79").

Bild 13 — Bruchform an der Oberfläche des Granits nach einem Belastungsversuch mit einem Stift von 20 mm (0,79").

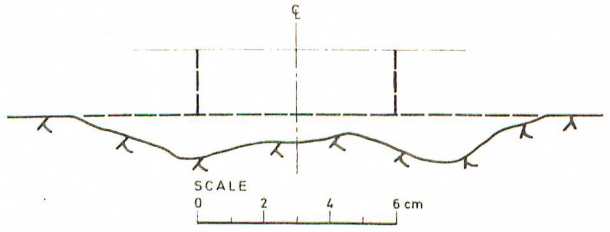

Fig. 14 — Shape of rupture surface on granite after a load test with 60 mm (2.36 in.) dowel.

Fig. 14 — Forme de rupture à la surface du granite après un essai de chargement avec un goujon de 60 mm (2,36").

Bild 14 — Bruchform an der Oberfläche des Granits nach einem Belastunsversuch mit einem Stift von 60 mm (2,36").

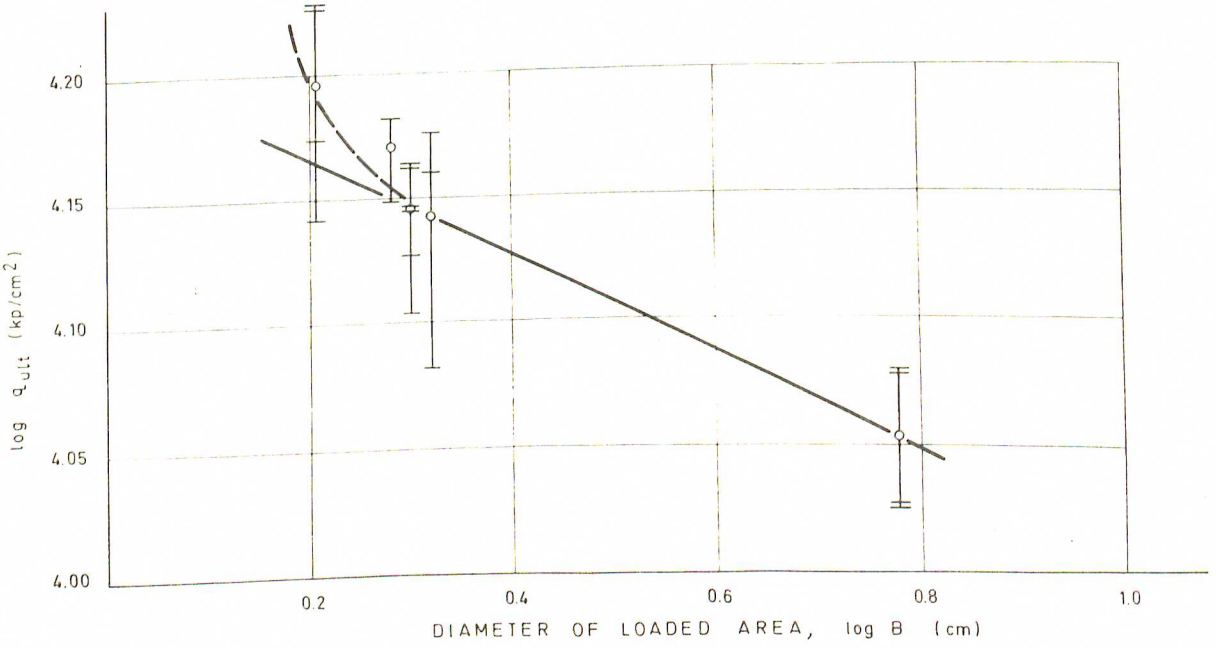

Fig. 15 — Effect of size of the loaded area on the ultimate point bearing capacity.

Fig. 15 — Effets de la dimension de la région chargée sur la portance à la pointe lors de la rupture.

Bild 15 — Wirkung der Grösse des Belastungsbereiches auf die Tragfähigkeit an der Spitze beim Bruch.

(70.5 kips) which corresponds to a contact stress of 11,300 kp/cm² (161 kpsi). This ultimate strength corresponds to 80% of that for the 20 mm dowel (14,000 kp/cm²).

The penetration of the dowel was at failure about 1.5 mm (0.06 in). A section of the specimen after failure is shown in Fig. 14. The rock was crused to a depth of 5 — 13 mm (0.2 — 0.5 in.) below the rock surface. The ratio of the depth of the crushed zone and the dowel diameter decreased with increasing dowel size as can be seen from a comparison with Fig. 13. Also the appearance of the failure surfaces was different. Extensive crushing and chipping occurred along the perimeter of the 60 mm dowel. The volume of crushed rock was relatively small just below the center of the dowel.

In Fig. 15 is shown the ultimate point bearing capacity q_{ult} as a function of the diameter B of the loaded area (diameter of dowel). It can be seen that the point bearing capacity increased rapidly with decreasing diameter when the dowel diameter was less than 20 mm (0.79 in.). However, the relatively large mineral particles in the granite probably effected the load tests with the small dowels.

Coates and Gyenge (1966) have derived the following relationship between ultimate strength, q_{ult}, the diameter of the loaded area B and the unconfined compressive strength σ_{cyl}.

$$q_{ult} = 7 \frac{\sigma_{cyl}\ (kp/cm^2)}{B^{0,2}\ (cm)}$$

or

$$q_{ult} = 5{,}8 \frac{\sigma_{cyl}\ (psi)}{B^{0,2}\ (in)}$$

which was found to sit the test results in fig. 15.

Acknowledgements

This paper is based on a thesis by the first author (Rehnman, 1968) for the degree of Teknologie Licentiat at the Royal Institute of Technology, Stockholm, Sweden. The investigation has been supported financially by the Committee on Pile Research of the Swedish Academy of Engineering Sciences (IVA).

References

[1] COATES, D. F. and GYENGE, M., — 1966, „*Plate-Load Testing on Rock for Deformation and Strength Properties*", Testing Techniques for Rock Mechanics, Am. Soc. Test. Mat., STP, pp. 19—35.

[2] LUNDBORG, N., — 1965, „*Triaxial Shear Strength of some Swedish Rocks and Ores*", Proc. First Congr. Int. Soc. Rock Mech. Lisbon, Vol. 1, pp. 251—255.

[3] REHNMAN, S. E., — 1968, „*Bärförmaga hos släntberg vid statisk belastning av bergspets. Resultat fran modellförsök*", Swed. Geot. Inst., Repr. a. Prel. Rep. No. 27,74 pp.

Utgivna handlingar

Meddelanden

1 Slagningsprov av pålskor med bergdubbar
Bror Fellenius
1963 10: —

2 Provpålning för broar inom blivande Olskroks- och Gullbergsmoten i samband med byggande av Europaväg 6 genom Göteborg
Bror Fellenius—Waldemar Pejrud 1964
1964 Slut

3 Jämförelse mellan moment, krökningsradie och sprickvidd i betongpålar slagna genom lös lera till sluttberg vid Tingstadsdelen, Göteborg
Bror Fellenius
1964 10: —

4 Pålprovning för järnvägsbro vid Vännäs
Bror Fellenius
1964 slut

5 Beräkningsmetoder för sidobelastade pålar
Bengt Broms
1965 slut

6 Brottlast för snett belastade pålar
Bengt Broms
1965 10: —

7 Beräkning av vertikala pålars bärförmåga
Bengt Broms
1965 10: —

8 Provpålning mot sluttberg vid Skansen Lejonet, Göteborg
Waldemar Pejrud
1965 25: —

9 Inverkan av armeringsmängd, förspänning och fallhöjd på sprickrisken hos betongpålar vid slagning
Sven Sahlin
1965 15: —

10 Bärförmågan hos armerade betongpålar slagna till fast bergbotten
Hjalmar Granholm
1967 20: —

11 Bärförmågan hos pålar slagna till sluttberg
Bengt Broms
1965 15: —

12 Dynamisk draghållfasthet hos modellpålar av oarmerad betong. Resultat av orienterande försök
Sven Sahlin—Lars Hellman
1966 15: —

13 Pålgruppers bärförmåga
Bengt Broms
1967 10: —

14 Påkänningar, sprickbildning och utmattning vid slagning av armerade modellpålar av betong
Bo Göran Hellers—Sven Sahlin
1971 30: —

15 Bärförmåga hos sluttberg vid statisk belastning av bergspets. Resultat av modellförsök
Resultat av modellförsök
Sven-Erik Rehnman
1968 15: —

16 Stålpålars bärförmåga. Resultat av fältförsök med lätta slagdon.
Gunnar Fjelkner
1970 30: —

17 Bergdubbens hållfasthet. Resultat från statiska belastningsförsök.
Sven-Erik Rehnman
1970 20: —

18 Negative skin friction on long piles in clay
I. Results of a full scale investigation.
II. General views and design recommendations.
Bengt H Fellenius
1971 30: —

Övrigt

Slagning och provbelastning av långa pålar. Försök i Gubbero, Göteborg. (Statens Råd för Byggnadsforskning, rapport 99) 35: —

Pålningsprotokoll. Blanketter upprättade enligt Särtryck och preliminära rapporter nr 11. Block om 50 blad
pris per block 10: —

Pålkommissionens handlingar kan rekvireras från Ingenjörsvetenskapsakademien, Biblioteket, Box 5073, 101 42 Stockholm.

Vänd
/